

University of Pavia

FACULTY OF ENGINEERING

Department of Electrical Engineering

Laurea Degree Course of Electrical Engineering

MASTER THESIS

Sliding Mode Traction Control Strategies for Vehicles Platooning

Strategie di Controllo Sliding Mode della Trazione
di Veicoli in Plotone

Advisor

Prof. Antonella Ferrara

Candidate

Alessio Mosca

Supervisor

Ph.D. Gian Paolo Incremona

Thesis submitted in 2016

ALESSIO MOSCA
Master Thesis
Sliding Mode Traction Control Strategies
for Vehicles Platooning
A.Y. 2012/13

COLOPHON
This thesis was typeset using the typographical language L^AT_EX.

alessio.mosca01@universitadipavia.it

“To my Grandparents and my friend Giovanni”

Contents

Introduction	1
1 Vehicle model	9
1.1 Vehicle model	9
1.2 Tire model	11
1.3 Drag coefficient model	13
1.4 Fuel consumption model	13
1.5 Conclusion	16
2 The Proposed Strategy	19
2.1 Historical Background	19
2.2 Basic Concepts in Sliding Mode Control	19
2.2.1 Second Order Sliding Mode	22
2.3 The Platooning Problem	24
2.3.1 The Outer Control-Longitudinal Loop	26
2.3.2 The Inner Slip Control Loop	28
2.4 String Stability	29
2.5 Conclusion	32
3 Comparison inner loop controllers	33
3.1 Introduction	33
3.2 Some Preliminaries on the Application of Sliding Mode Control to the Slip Control Problem	35
3.2.1 Problem Statement	36
3.3 The Considered Sliding Mode Control Strategies	36
3.3.1 FOSM Control	36
3.3.2 SSOSM Control	36
3.3.3 STSM Control	37
3.3.4 ISSOSM Control	37
3.3.5 ISM Control	38
3.4 Simulations	39
3.4.1 Test Setup	39
3.4.2 Results	39
3.4.3 Controllers Evaluation	45
3.5 Conclusions	47

4 Simulation results	49
4.1 Discussion	50
5 Conclusions	63
5.1 Future Work	64
Appendices	64
A Simulink Control Scheme	65
Bibliography	77

List of Figures

1	PID control scheme	4
2	Fuzzy control scheme	5
3	MPC control scheme	6
1.1	The vehicle model	9
1.2	Bakker Pacejka tire model, with $F_{z_1} < F_{z_2}$	12
1.3	Variation Drag coefficient for the case with one follower	13
1.4	Variation Drag coefficient for the case with two follower	14
1.5	Variation Drag coefficient for the case with three follower	14
1.6	Engine spread	17
1.7	Traction diagram	17
1.8	Hierarchical slip control scheme of the i th vehicle	18
2.1	Sliding Manifold	20
2.2	Chattering	22
2.3	Second order sliding mode	24
2.4	Bang Bang Second order sliding mode	25
2.5	Suboptimal Second order sliding mode	25
2.6	Control scheme	26
2.7	Tire model	28
3.1	Sliding Mode slip control schemes	34
3.2	Matched disturbance and parametric uncertainties affecting the vehicle model	40
3.3	Step response of the controllers when disturbances are not present (left), and detail of the step response of the SSOSM, STSM and ISSOSM algorithms (right)	41
3.4	Step response of the controllers when all the disturbances are present (left), and detail with only PI and ISM controllers (right)	42
3.5	Difference in the controller performance in presence of different disturbances combinations when ISM (left) and PI (right) controllers are used	43
3.6	Detail of the control signals corresponding to controllers in Figure 3.5. Note that in the tests with delay, the increase of the control action is considerably stronger with the ISM controller	44
3.7	Perfomance indices representation for controllers STSM, PI and ISM	46
4.1	Vehicles Platooning	50

4.2	Leader acceleration	50
4.3	Longitudinal acceleration	51
4.4	Longitudinal velocity	52
4.5	Run distance	52
4.6	Distance and safety distance	53
4.7	Front traction force	54
4.8	Rear traction force	54
4.9	Front angular velocity	55
4.10	Rear angular velocity	55
4.11	Front slip ratio	56
4.12	Rear slip ratio	56
4.13	Front sliding variables	57
4.14	Rear sliding variables	57
4.15	Front input torque	58
4.16	Rear input torque	58
4.17	Shaft torque	59
4.18	Brake torque	59
4.19	External sliding variables	60
4.20	External loop control	61
4.21	Fuel consumption vehicles	61
4.22	Drag coefficient for follower vehicles platoon	62
A.1	Slip Control for Vehicles Platooning	65
A.2	Platoon	66
A.3	i-th follower vehicle model	67
A.4	Vehicle longitudinal dynamics	68
A.5	Floss	69
A.6	Bakker-Pacejka models	70
A.7	Front wheel Bakker-Pacejka	71
A.8	Rear wheel Bakker-Pacejka model	72
A.9	Front wheel slip ratio	73
A.10	Else front wheel slip ratio	74
A.11	If front wheel slip ratio	74
A.12	Rear wheel slip ratio	75
A.13	Else rear wheel slip ratio	76
A.14	If rear wheel slip ratio	76

List of Tables

3.1	RMS Error $e_{\text{RMS},\nu}$, $\nu = \{f, r\}$	45
3.2	RMS value of Control Signal $E_{c,\nu}$, $\nu = \{f, r\}$	46
4.1	vehicle parameters	49
4.2	Control parameters for the first follower	49
4.3	Control parameters for the second follower	51
4.4	Control parameters for the third follower	51

Abstract

Sliding mode control approach is presented in this thesis for the vehicle platoon control through the wheel slip control of road vehicles. The major design requirement for the controllers is to maintain the safety distance between vehicles controlled and the preceding vehicle. To do this, The proposed control scheme is composed by two control loops. The outer made to solve the platooning problem, while the inner one acts on the wheel torques to reach the reference slip ratio generated by outer control loop. Furthermore, in the present thesis different algorithms of first and second order type and integral or non integral nature for inner loop are discussed, with the aim to find which of these algorithms are better suited to be used on real vehicles.

Abstract

In questa tesi é presentato uno schema di controllo avanzato di tipo sliding mode per il controllo di un plotone di veicoli mediante il controllo del rapporto di slip. Il principale obbiettivo dello schema di controllo proposto é quello di mantenere la distanza di sicurezza tra i veicoli controllati e il veicolo che precede. Lo schema di controllo proposto é composto da due anelli. L'anello esterno ha il compito di risolvere il problema di platooning, mentre quello interno, agendo sulle coppie alle ruote, ha il compito di raggiungere e mantenere il rapporto di slip di riferimento generato dall'anello esterno. Sono stati inoltre studiati diversi algoritmi di tipo sliding mode di primo e secondo ordine e algoritmi di tipo integrale e non integrale per l'anello interno, allo scopo di trovare quale di questi algoritmi si presta meglio ad essere applicato su veicoli reali.

Introduction

The Control Theory is the discipline which studies the ways in which a sequence of desired events occurs independently of the human intervention. The main components of an automatic system are the process, the actuators, the sensors and the controller. Processes and all the interconnected agents each others or with respect to the external environment can be of any nature. For instance, in mechanical field a motor vehicle can be considered as a system, while in an electric field even a simple electric RL circuit is a process. The actuators can be electric motors, switches or butterfly valves and their task is to actuate the system according to the desired dynamics. The sensors collect information on the system evolution, i.e., provide states to the controller to close the control loop. The controller is in some sense the “brain” which decides the actions that the actuators have to do to control the dynamics of the system. It can be manual if the control action is set by human operator and automatic if it is controlled by a specifically designed device.

Thanks to technological development and above all thanks to the rise of microcomputers, nowadays it is possible to control motors, active suspensions, transmissions and brakes which were previously difficult to control. Nowadays traffic management has a fundamental role and, in fact, the increase of population has brought to a consequent increase of the number of vehicles, which can eventually imply a greater probability of collisions among vehicles and a major pollutant emissions as well as the increase in traffic congestion. For these reasons, the research world, in recent years, is focused to study new control techniques to increase the degree of safety of the streets, while contemporarily reducing emissions and traffic.

In the following, the main technologies used in automotive field are presented.

Automotive Highway Systems (AHS)

The first idea was born in 1940s when General Motors offered its vision of traffic control in which vehicles were controlled by an automatic device. In 1950s the first automatic vehicle controlled by a mechanical system and radio waves was proposed. Only later, with the technological development of computers, sensors and microelectronics they realized the first truly automated highway, which was proposed in years 1980s. With the birth of the AHS, a new relationship between the car and the highway has been designed, where accelerator, steering, and braking are controlled automatically by a computer with the objective of maintaining speed and safety of the vehicle. This has as a result that the safety and road capacity increase. To achieve this, the AHS uses communication technologies, sensors, obstacle detection that can detect, recognize and respond to highway conditions. Vehicles and highway

must work together to coordinate the motion of all the agents involved in the process, avoiding obstacles and improving the traffic flow, safety and reducing congestion. Basically this technology can be classified into fully automated or partially automated approach: the difference lies in the fact that there are mainly partial notification and alarm systems and only in case of emergency the control of the vehicle will be carried out by the computer, excluding the human action. This technology has many advantages, in fact, it has been shown that it is able to increase the capacity of the motorway, the safety, while reducing the polluting emissions. Since the future development of AHS depends on operations and innovations that take place today, it is clear the importance of the so-called Intelligent Autonomous Vehicle (AIV) [1]

Autonomous Intelligent Vehicle (AIV)

This vehicle must be able to measure, by using specific sensors, and estimate the needed information of the dynamics of the vehicle which precedes it. The onboard computer processes the data and, depending on the situation, will generate appropriate acceleration and braking signals to adequately control the vehicle. These decisions are made as a function of spacing policy. The main strategies are analyzed and, of course, the commands must be generated as quickly as possible, fulfilling safety and passenger comfort. Substantially the longitudinal operation of these vehicles can be divided into three modes:

1. regulation mode;
2. velocity-command mode;
3. entrainment mode.

In the regulation mode, it is assumed that the vehicle is close enough to the speed and reference distance (or headway). In this case the control system will have to adjust the vehicle through the acceleration and braking system in order to follow the references. The second mode is the velocity-command mode in which the distance from the vehicle ahead is sufficiently large as to make unnecessary the precise control of the distance. The last mode is the entrainment mode which regulates the transition between the first and the second mode and vice versa, always fulfilling the constraints on safety and comfort [2]. These techniques are very important and play a strategic role, in addition to the advantages of increasing the capacity of roads, improvement of roads travel times and security. They also allow to use special control systems to reduce the consumption of gasoline or diesel and therefore to reduce pollutants [3].

Cruise Control (CC)

It is possible to distinguish two CC technologies:

1. standard CC;
2. Adaptive CC (ACC).

In standard CC, the driver sets the speed to be maintained and if he decides to overtake or slow down, he has to press the accelerator or the brake pedal so that he has again the control of the speed. The second category is the ACC, which was introduced in 1995 by Mitsubishi. It has spread over a number of medium to high-end models and, in fact, it represents a fundamental step towards autonomous driving vehicles. It uses a laser–radar sensor to measure the distance to the vehicle in front of it. In the case that the considered distance is below the reference distance of the controller, the latter will slow down the vehicle. When the way is empty, the vehicle will continue to travel at the speed set by the driver. The first ACC were designed to increase the driving comfort with some improvement in the safety. If one thinks to a futuristic scenario, one has to consider that the vehicles which will adopt this technology will increase and therefore traffic and security issue have to be taken in account. In the literature, there are various control policies for spacing policy (it defines the space between the vehicle equipped with the ACC and the vehicle in front of it). In general, the desired distance is a function of the speed of the controlled vehicle, but it could also be a constant distance or a function of other variables such as the related speed between the controlled vehicle and the one preceding it. The spacing policy is very important in the ACC system. In fact, it has a great influence on vehicle safety and road capacity (number of vehicles).

The most commonly used spacing policies in automotive world is called Constant Time Gap (CTG) [4]. In this policy the desired distance is given by

$$S_d = hv + d_0 \quad (1)$$

where d_0 has to be at least equal to the length in meter of the preceding vehicle. However, it has been shown that if all vehicles of a particular stretch of motorway used this spacing policy, the flow would be unstable, because a perturbation would be propagated preventing to reach the stability [5]. In the literature it is proposed a variant of the CTG, i.e., a spacing policy which has as objective to maintain a fixed distance between the two vehicles regardless of the speed. This policy has as advantage to increase the capacity of the road and to decrease the emissions of pollutants, thanks to the fact that if a distance of 1 meter is maintained among the vehicles, the air force is at the minimum. This technique takes the name of Constant Spacing Headway [6]. However, this technique leads to instability of the line of cars. To solve this problem and ensure the stability [7] one must provide the information to the leaders of each vehicle in the queue control system. This is done by exchanging information among vehicles, by means of a special protocol. It has been discovered that using CTG implies two main problems: the system might be unstable and the ACC system might not work efficiently in high-traffic density area. A possible solution is to adopt Safety Spacing Policy. This policy acts like a human being. It takes into account the speed, distance and the braking system capacity. This results in an improvement compared to the CTG, both from the safety viewpoint and from an efficiency viewpoint. The desired distance will be

$$S_d = \gamma d + vt + d_0 \quad (2)$$

where t is the delay time due to the control system, γ is the safety coefficient which depends on the conditions of the asphalt and can be set by the user, d is the braking

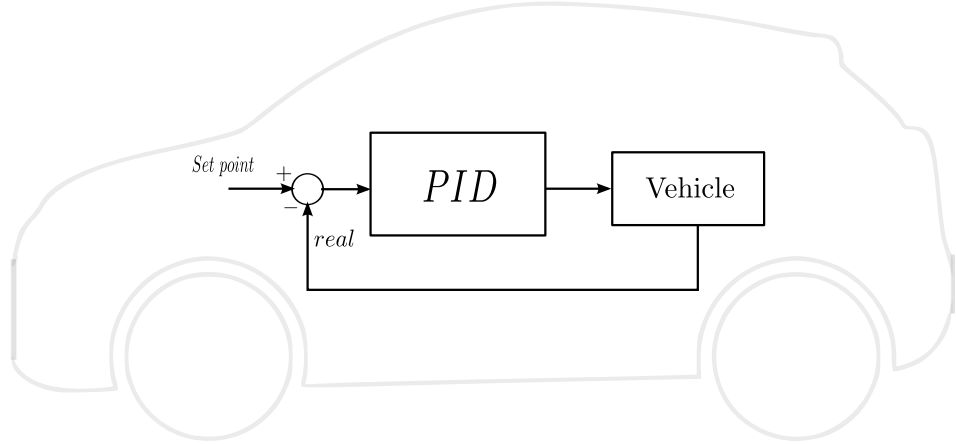


Figure 1: PID control scheme

distance or the distance in order to slow down to the speed v with the maximum braking power.

The Main Control Algorithms

In the following the main control algorithms used in automotive field will be recalled.

PID Control

It is based on the definition of the error signal, its first time derivative and its integral. The error is typically obtained as the difference between the desired reference value and the feedback output of the process. They are widely used in industrial environments. Their use allows one to control a wide range of processes. There are several techniques for automatic calibration, and it can be used even without a precise model of the system being monitored. They were introduced in the automotive industry in 1960s for the lateral control of the automatic guidance system [8] [9] [10]. The classic form of PID can be described as

$$u_{PID} = K_P e + K_I \int_{t_0}^t e + K_D \dot{e} \quad (3)$$

where u_{PID} is the control action and e is the error, while K_P , K_D and K_I are suitably designed function. This control system, however, suffers from problems due to the presence of the integral and derivative action. In fact, the integral action causes the so-called saturation phenomenon, which causes a non-linear effect that can significantly deteriorate the control performance. This problem is solved by using the so-called anti wind-up scheme. As for the problem caused by the derivative, the solution is the soft insertion of the automatic regulation.

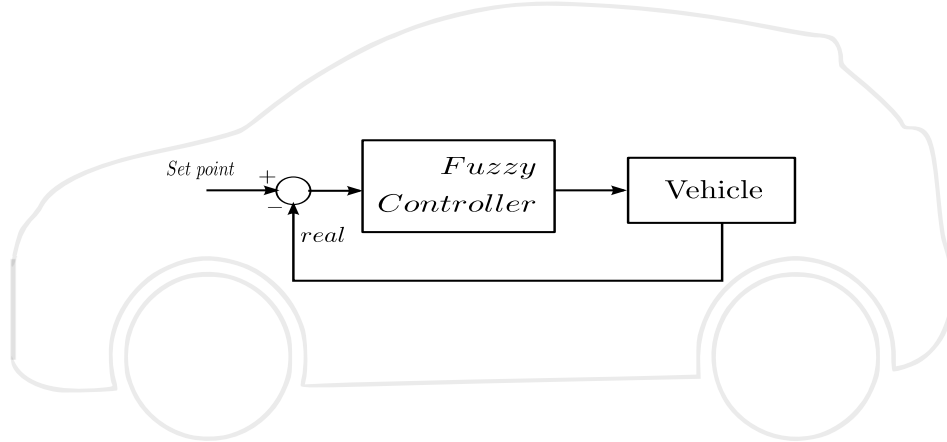


Figure 2: Fuzzy control scheme

Fuzzy Control

Technique that was introduced in 1965 by L. A. Zadeh, but it is having more and more popularity in recent decades, thanks to the wide variety of commercial applications and for use in the automotive industry. It is particularly appreciated in the automotive industry since it is able to reproduce the human behavior: this means that it has a particular use for the design of ACC. The fuzzy control is a control system based on the so-called fuzzy logic and is conceptually very simple. It is based of several cycles of the type if–then–else. The fuzzy logic, through a deterministic method, allows one to make control systems more versatile and easier to adapt to the interferences, the non-linearity of the system and the parametric variations. For all these reasons they are used in traffic control. Vehicle models are highly nonlinear and affected by large uncertainties. Furthermore, by exploiting the theorem of approximation, you can approximate all linear control laws through a fuzzy logic algorithms (for instance fuzzy PID control). One of the main problem of this techniques is the lack of rigorous tool in order to make an analytical study of stabilities and robustness features of the fuzzy algorithms [11] [12].

Model Predictive Control

Model Predictive Control (MPC) is an appropriate choice to solve constrained control problem for even complex MIMO systems, providing an optimal control strategy [13]. In MPC these constraints are explicitly taken into account by solving a constrained optimization problem in real-time to determine the optimal predicted inputs. Typically the optimization problem and the control law are defined in the discrete-time domain and the knowledge of the model of the plant is a crucial point in MPC algorithms. It needs three main elements:

- model-based prediction;
- cost function and optimization;
- receding horizon.

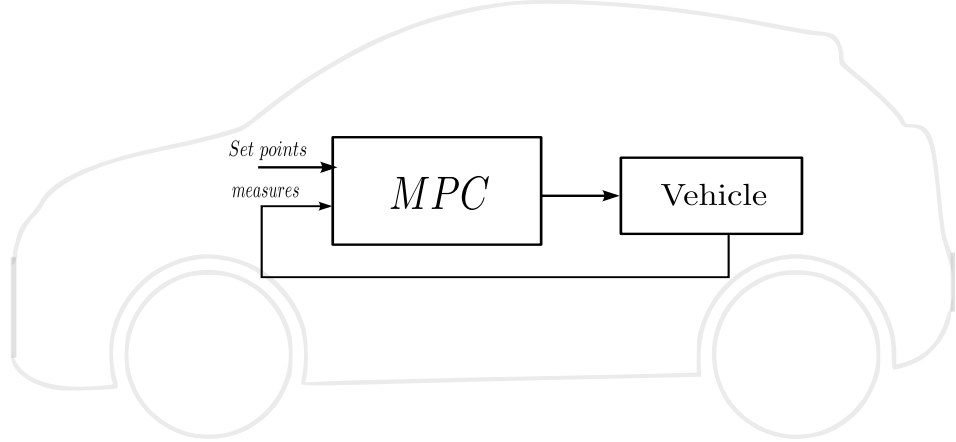


Figure 3: MPC control scheme

Typically the system is of the following

$$x(k+1) = Ax(k) + Bu(k) \quad (4)$$

where $x(k) \in \mathbb{R}^n$ is the state vector, $u(k) \in \mathbb{R}^m$ is the input vector, both at the k -th sampling time instant. It is based on the definition of a number N which denotes the prediction horizon. Given an input sequence, i.e., $u(k) = [u^T(k|k), u^T(k+1|k), \dots, u^T(k+N-1|k)]^T$, the time evolution of the state is generated by simulating the model forward for N sampling intervals with initial condition $x(k|k) = x(k)$.

The predicted input fed into the plant is generated by solving an optimization problem, i.e., by minimizing a pre-specified cost function, which is defined in terms of the state and on the input

$$J(x(k), u(k), N) = \sum_{i=0}^N \|x(k+i|k)\|_Q^2 + \|u(k+i|k)\|_R^2 \quad (5)$$

where Q and R are positive definite matrices. The aim is to find the optimal control sequence and according to the so-called receding horizon (RH) approach, only the first element of the optimal control sequence is applied into the plant, i.e.,

$$u(k) = u^o(k|k) \quad (6)$$

This value is repeated at each sampling time instant k and the prediction horizon is of the same length despite the repetition of the optimization at future time instants.

This technique is also applied in traffic control. It turns out to be also effective in the control of autonomous vehicles [14], as well as for the optimization in the emission of CO₂ through the use of ACC [15].

Sliding Mode Control (SMC)

Variable Structure Control Systems (VSCS) theory was developed for the first time in the early 1960s by Emel'yanov and Barbashin, in Russia and then by Itkis and

Utkin in England. In these systems the control law is changed during the control process depending on the real state of the system and according to some defined rules.

This kind of controller allows to force the system states to reach and then to remain on a surface, which is the so-called sliding surface $\Sigma = 0$ or manifold, within the state space. When the system is confined to this surface through an infinity frequency discontinuous control law, this is defined as an ideal sliding motion whose the two main properties are the followings:

- there is a reduction in order of the system;
- it is invariant towards the so-called matched uncertainty and it makes controlled system robust.

We can distinguish two phases in the dynamical behavior of the system, that are the reaching phase during which the states are being driven towards the sliding surface and then the sliding phase during which the system is reduced in order and it is invariant towards the matched uncertainty.

One of the main problems of the SMC is related to the control law which is discontinuous. When one applies this kind of signal to a mechanical system, we do not have got an ideal sliding motion but delays and hysteresis contribute to induce an high frequency motion known as chattering [16], that is the repeatedly crossing rather than remaining on the sliding surface. As this effect stresses the actuator components, the discontinuous control action is modified so that the states are forced to remain within an arbitrarily small boundary layer about the surface. In this case one has a pseudo-sliding motion in which the invariance properties are lost [17].

Second Order Sliding Mode (SOSM) Control

In order to reduce the all problems related to the implementation of the control algorithms to actual dynamical systems, the control theory has developed several sophisticated control techniques to solve this kind of problem for some classes of uncertain systems.

SMC, as explained in the previous section, represents a very interesting approach to control some classes of uncertain system but it implies the chatter effect which causes an unpredictable oscillatory behaviors of the dynamical systems. The main methods to reduce this phenomena are the followings: the so called pseudo-sliding mode control, as explained in [18], then the technique based on the use of an observer, as explained in [19], or a third approach based on embedding the original system into a higher-order system with the explicit use of time derivative of control which implies the solution of a differential inequality.

According to the recent theory of the Higher-Order Sliding Mode (HOSM), a second-order Sliding Mode (2-SM) control represents an effective approach to avoid chattering without using observer. According to [20], it consists in a sliding motion on a surface $\sigma(x(t)) = 0$ in the state space, with its first time-derivative $\dot{\sigma}(x(t)) = 0$, with the control signal depending on $\sigma(x(t))$, but directly acting only on $\dot{\sigma}(x(t))$.

Sliding Mode Control in Automotive Systems

Sliding Mode Control is also widely used in the automotive world. In fact, in the context of control of motor vehicles there are heavy uncertainties and a wide ranges of operative mode. For these reasons the control for this technique must be robust. If one is using SMC of the first order, the output that the control system generates will be a discontinuous signal to infinite frequency and in case of longitudinal dynamic control of the vehicle, the output of SMC will be the torque input. It is easy to understand that using SMC of first order implies several problems for the actuators and consequently for comfort. This is the reason why it is preferred to adopt the SOSM. The discontinuous control signal will be made continuous by the integrator action, thus preventing the occurrence of the so-called chattering phenomenon [21].

Thesis Organization

The thesis is organized as follows. In chapter 1 we have analyzed the model of the vehicle. In chapter 2 brief introduction on the basic concepts of second order sliding mode control and also the design of the second order sliding mode controller. In chapter 3 we have compared different control algorithms to the inner loop. In chapter 4 simulation results for a platoon composed by four vehicles while in chapter 5 conclusions are gathered in the last section.

Chapter 1

Vehicle model

1.1 Vehicle model

In order to simulate the dynamics and behavior of the vehicle in the most realistic case we should adopt a model of the vehicle very complex. Adopting the appropriate simplifications we can derive a simplified single track model of the vehicle. The model adopted considers the vehicle as a rigid body, and we consider only the longitudinal dynamics [22]. It is assumed that there are no differences between the left wheel against to the right wheel of the same axle (front, rear) i.e., we adopt a model that is the so-called bicycle model [23]. We do not take into account the lateral, pitch and roll, yawing dynamics. The resulting equations of motion under this simplifications

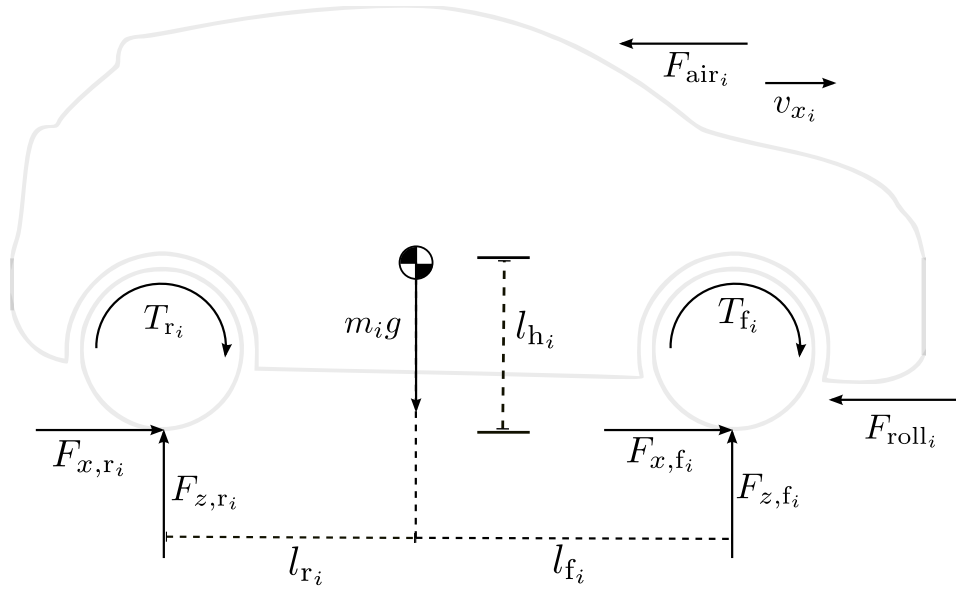


Figure 1.1: The vehicle model

for the i -th vehicle that composes the platoon are:

$$m_i \dot{v}_{x_i} = 2[F_{xf_i}(\lambda_{f_i}) + F_{xr_i}(\lambda_{r_i})] - F_{\text{loss}_i} \quad (1.1)$$

$$J_{f_i} \dot{\omega}_{f_i} = T_{f_i} - r_{f_i} F_{xf_i} \quad (1.2)$$

$$J_{r_i} \dot{\omega}_{r_i} = T_{r_i} - r_{r_i} F_{xr_i} \quad (1.3)$$

$$F_{\text{loss}_i}(v_{x_i}) = F_{\text{air}}(v_{x_i}) + F_{\text{roll}} = c_x v_{x_i}^2 \text{sign}(v_{x_i}) + f_{\text{roll}} m_i g \quad (1.4)$$

$$F_{zf_i} = \frac{l_{r_i} m_i g - l_{h_i} \dot{v}_{x_i}}{2(l_{r_i} + l_{r_i})} \quad (1.5)$$

$$F_{zf_i} = \frac{l_{r_i} m_i g + l_{h_i} \dot{v}_{x_i}}{2(l_{r_i} + l_{r_i})} \quad (1.6)$$

where v_{x_i} is the longitudinal velocity of the vehicle centre of gravity, ω_i is the wheel angular velocity(front or rear), T_i is the input torque, F_{x_i} is the traction force on a wheel (rear or front), F_{z_i} is the normal force on a wheel, approximated in this work as a static value, ignoring the influence of the suspension, F_{air} is the air drag resistance, and, F_{roll} is the rolling resistance, λ_i is the slip ratio on a wheel. Subscripts f and r denote “front tire” and “rear tire”, respectively. As for the vehicle parameters are the following: m_i is the vehicle mass, c_x is the longitudinal wind drag coefficient, f_{roll} is the rolling resistance coefficient, J_i is the wheel moment of inertia, r_i is the wheel radius, l_{f_i} is the distance from the front axle to the center of gravity (c.g.), l_{r_i} is the distance from the c.g. to the rear axle, and , l_{h_i} is the vertical distance to the c.g.

As can be noted, all of the equations are expressed as a function of the slip ratio, while the control variables for traction are assumed to be the front and rear torques. We can see what we have just said, by studying the dynamics of the slip ratio. More specifically, one has

$$\lambda_{f_i} = \frac{\omega_{f_i} r_{f_i} - v_{x_i}}{\max(\omega_{f_i} r_{f_i}, v_{x_i})} \quad (1.7)$$

and in case of acceleration

$$\lambda_i = \frac{\omega_i R_i - v_x}{\omega_i R_i} \quad (1.8)$$

with $\omega_i R_i > v_x$ and $\omega_i \neq 0$, $i \in \{f, r\}$. Thus the wheel slip dynamics during acceleration can be described by differentiating with respect to time, as

$$\dot{\lambda}_{acc_i} = -\frac{\dot{v}_x}{\omega_i r_i} - \frac{\dot{\omega}_i v_x r_i}{(\omega_i r_i)^2} \quad (1.9)$$

$$\dot{\lambda}_{acc_i} = f_{acc_i} + h_{acc_i} T_i \quad (1.10)$$

where

$$f_{acc_i} = -\frac{\dot{v}_x}{R_i \omega_i} - \frac{v_x F_{x_i}}{J_i \omega_i^2} \quad (1.11)$$

$$h_{acc_i} = \frac{v_x}{J_i R_i \omega_i^2} \quad (1.12)$$

In order to describe the dynamics during braking we need to use

$$\lambda_i = \frac{\omega_i R_i - v_x}{v_x} \quad (1.13)$$

with $\omega_i R_i < v_x$ and $v_x \neq 0$, $i \in \{f, r\}$. Analogously we obtain

$$\dot{\lambda}_{i_{decc}} = \frac{\dot{\omega}_i r_i}{v_x^2} - \frac{\omega_i \dot{v}_x r_i}{v_x^2} \quad (1.14)$$

$$\dot{\lambda}_{i_{decc}} = f_{decc_i} + h_{decc_i} T_i \quad (1.15)$$

where

$$f_{decc_i} = -\frac{R_i \omega_i \dot{v}_x}{v_x^2} - \frac{R_i^2 F_{x_i}}{J_i v_x} \quad (1.16)$$

$$h_{acc_i} = \frac{R_i}{J_i v_x \omega_i^2} \quad (1.17)$$

1.2 Tire model

For the tire model, the well-known Bakker-Pacejka model [24] is considered, which is a very good approximation of longitudinal force F_x as a function of the longitudinal slip λ_i , of the normal force applied at the tire F_z , and of the road adhesion coefficient μ_p . Thus, the traction force can be obtained through the empirical equation introduced by Pacejka and known as "magic formula". The equation is the follower:

$$F_x = D \sin(C \arctan \{B(l - E)(\lambda + S_h) + E \arctan [B(\lambda + S_h)]\}) + S_v \quad (1.18)$$

where

$$C = b_0 \quad (1.19)$$

$$D = \mu_p F_z \quad (1.20)$$

$$BCD = (b_3 F_z^2 + b_4 F_z) e^{b_5 F_z} \quad (1.21)$$

$$E = b_6 F_z^2 + b_7 F_z + b_8 \quad (1.22)$$

$$S_h = b_9 F_z + b_{10} \quad (1.23)$$

$$S_v = 0 \quad (1.24)$$

Force F_z is in kN, longitudinal slip is expressed as a percentage and force F_x is in N. The values of the parameters are:

- $b_0=1.65$
- $b_1=-7.6118$
- $b_2=1122.6$
- $b_3=-7.3600e-3$
- $b_4=144.8200$

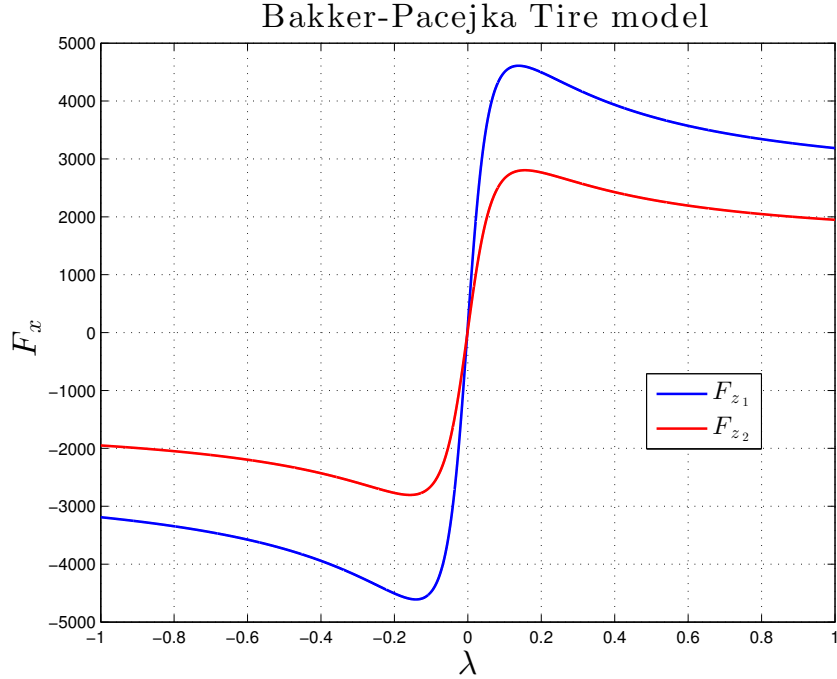


Figure 1.2: Bakker Pacejka tire model, with $F_{z_1} < F_{z_2}$

- $b_5 = -7.6614 \times 10^{-2}$
- $b_6 = -3.8600 \times 10^{-3}$
- $b_7 = 8.5055 \times 10^{-2}$
- $b_8 = 7.5719 \times 10^{-2}$
- $b_9 = 2.3655 \times 10^{-2}$
- $b_{10} = 2.3655 \times 10^{-2}$

where μ_p is the peak road/tire adhesion coefficient which depends on the road conditions. Typical value for μ_p are, for instance, 0.85, 0.6, and 0.3 which are associated with the case of dry asphalt, wet asphalt and snowy road, respectively [25] [26]. In our model it was chosen to adopt a simplification of Bakker-Pacejka [23] model, i.e.,

$$F_x = \mu_p \cdot f_t(\lambda, F_z) \quad (1.25)$$

It should be noted that the curve which is obtained has the same shape (will be scaled in depending on μ_p) when the surface changes to a fixed F_z .

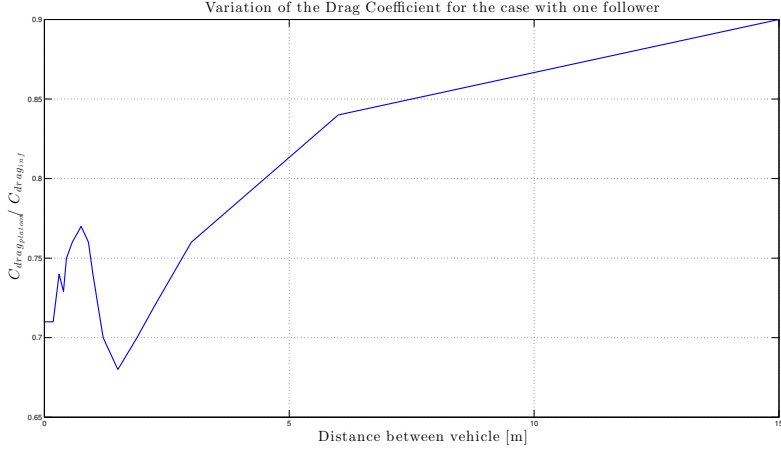


Figure 1.3: Variation Drag coefficient for the case with one follower

1.3 Drag coefficient model

In order to make the simulation more realistic and see how the controller reacts to this particular disturbance, we have implemented the possibility to change the c_x coefficient depending on the distance between the vehicles and by the number of vehicles constituting the platoon, while the rolling resistance coefficient f_{roll} depends on many factors, and thus, we have chosen to adopt a typical number for it.

The variation of the drag coefficient is obtained according to [27]. We have implemented an algorithm that as function of the number of vehicles in the the platoon (maximum four vehicles considering also the leader), the distances between the vehicles and the number of i -th vehicle, the algorithm finds the different value of the c_x for each vehicle. We can observe that the curves c_x assume different forms depending on the number of vehicles that make up the platoon, this we can note from Figure 1.3, 1.4, 1.5.

1.4 Fuel consumption model

Furthermore, we have taken into account the consumption of the i -th vehicle that composes the platoon. To obtain this we have used a simple method for estimating the consumption [28]. Fuel consumption can be obtained starting from the useful power delivered to engine P_b

$$P_b = P_{i_g} - P_f \quad (1.26)$$

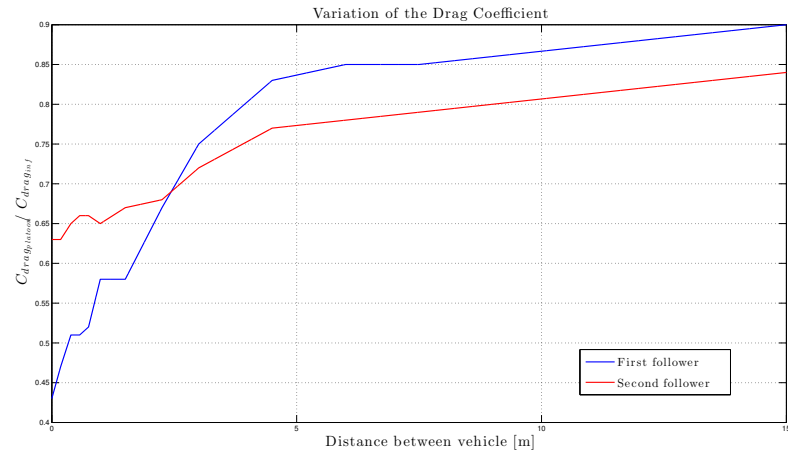


Figure 1.4: Variation Drag coefficient for the case with two follower

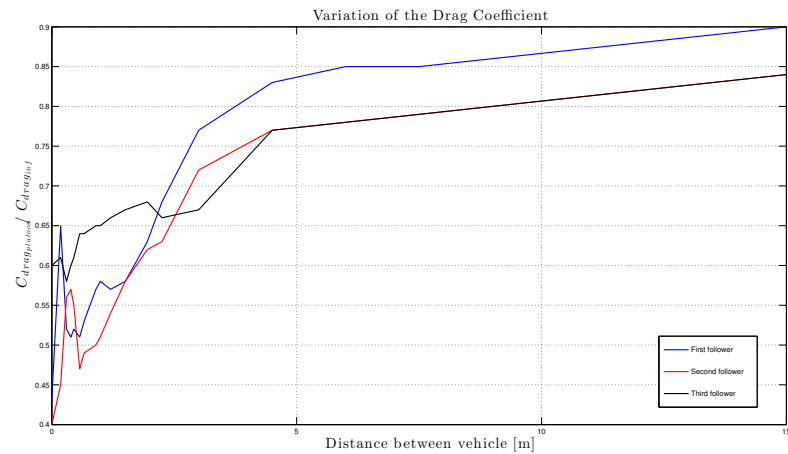


Figure 1.5: Variation Drag coefficient for the case with three follower

where P_{ig} is gross indicated power and P_f is the power losses due to friction from mechanical components,

$$P_{ig} = \eta_{f,i} \eta_c \dot{m}_f LHV \quad (1.27)$$

$$\eta_c = \eta_{c0} - \frac{A}{B + N} \quad (1.28)$$

$$P_f = \frac{FMEP V_d N}{R_c * 60} \quad (1.29)$$

$$FMEP = f + f_p N \quad (1.30)$$

where $\eta_{f,i}$ is the fuel efficiency, that compares the gross power with the power delivered by combustion of the fuel (in the first evaluation consider a value of 40 percent), η_c is the combustion efficiency that indicates a non-perfect combustion process, because the combustion depends also by the velocity of engine. This value is assumed to be 0.98, the value of A is 300 and B is 2000. FMEP is friction mean effective pressure, f is the constant of friction assumed to be 100 kPa and f_p is 20. R_c is 1 for 2 stroke engine and 2 for 4 stroke engine. In our case R_c is 2, LHV is the lower heating value in J/kg. Note that we added the term $\eta_{additional}$ to take into account additional losses. Therefore we can obtain the fuel mass flow as

$$\dot{m}_f = \frac{P_b + P_f}{\eta_{f,i} \eta_c LHV \eta_{additional}} \quad (1.31)$$

We note that the fuel consumption depends on engine speed N and useful power delivered to engine P_b , thus we need to find them. For the P_b value we can obtain it considering that it is the required power to the axis of the wheels, thus

$$P_b = \frac{T_{shaft_i} \omega_{f_i}}{\eta_{transmission}} \quad (1.32)$$

where T_{shaft_i} is the shaft torque for front rear of the i -th vehicle, ω_{f_i} is the angular velocity of the i -th vehicle and $\eta_{transmission}$ is the transmission efficiency, assumed to 0.91. It is necessary to remember that having assumed that the cars in the simulation are modeled by Front Wheel Driven, the shaft torque and brake torque to obtain the desired T_{f_i} and T_r are given by [22]:

$$T_f = 0.5 T_{shaft} - 0.3 T_{brake} \quad (1.33)$$

$$T_r = -0.2 T_{brake} \quad (1.34)$$

To find the number of revolutions of the engine, we have to start from the full load curve of the engine, that in our case described by the formula (1.35) [28], and taking into account the relationship of transmission (gear box) we can derive the curve of traction diagram [29]. The equation that describes the full load curve is the following

$$T = \frac{(-4.2e^{-6}N^2 + 0.032N + 105)T_{max}}{165} \quad (1.35)$$

and

$$T_{max} = 0.0879V_d \quad (1.36)$$

where the N is the velocity of the engine and V_d is the engine displacement, see the Figure 1.6. Obtaining the traction diagram we can associate to each speed in km h^{-1} a specific gear. Having these two values it is possible to derive the engine speed in rpm.

To derive traction diagram , see the Figure 1.7, we use the following equation [29]

$$v(\text{km/h}) = \frac{3.6\pi n_M r_{dyn}}{30i_i i_e} \quad (1.37)$$

$$T_{shaft_i} = T_{(n_M)} i_e i_i \eta_{transmission} \quad (1.38)$$

where n_M is the value of engine speed of the full load curve, r_{dyn} is the dynamic radius, i_e is a fixed value that depends on the type of transmission [29] and i_i is the transmission ratio value of i -th gear, $T_{(n_M)}$ is the torque of full load curve in n_M engine velocity. The Transmission value [25] are:

- $i_1 = 3.750$
- $i_2 = 2.235$
- $i_3 = 1.518$
- $i_4 = 1.132$
- $i_5 = 0.028$
- $i_e = 59/20$
- $\eta_{transmission} = 0.91$

Having found the relationship that exists between the two characteristic curves and knowing the gear it is possible to derive the consumption by formula (1.31).

1.5 Conclusion

in this chapter it is exposed and explained the model of the vehicle used to carry out simulations of a vehicle platoon control

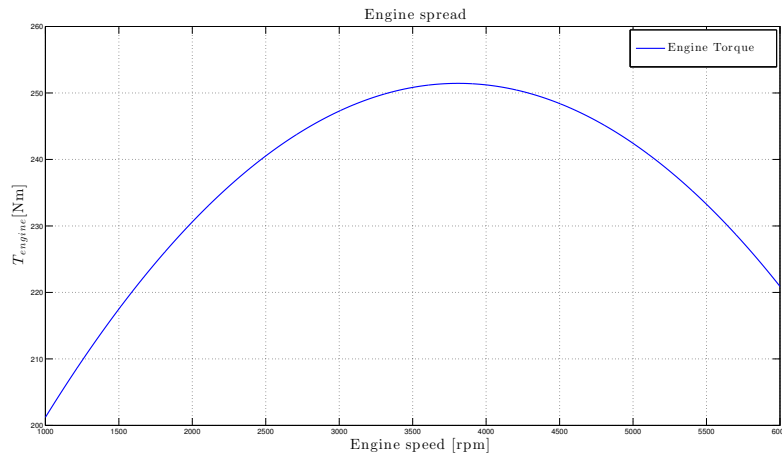


Figure 1.6: Engine spread

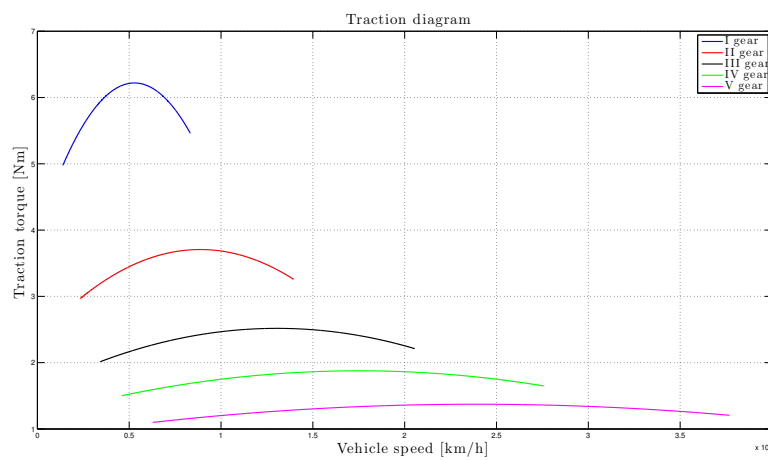
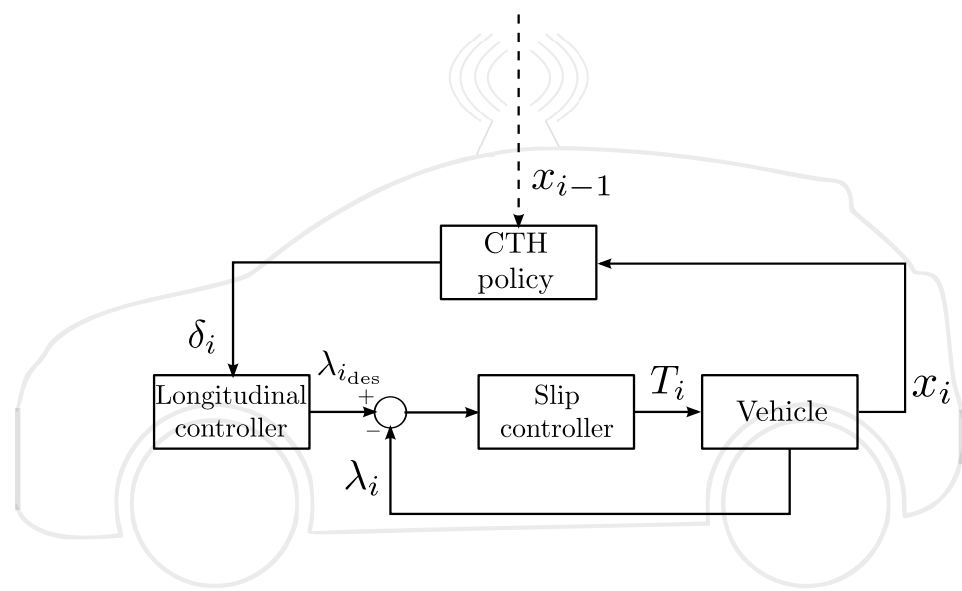


Figure 1.7: Traction diagram

Figure 1.8: Hierarchical slip control scheme of the i th vehicle

Chapter 2

The Proposed Strategy

2.1 Historical Background

It is possible to find a lot of evidence proving the existence of primordial feedback control systems used in ancient times with the advent of level control, water clocks, and pneumatics/hydraulics systems. Since the 17th century, the systems have been developed for temperature control in furnaces, the mechanical control of mills, and the regulation of steam engines. During the 17th and 18th century people began to use these systems but, It was only during the 19th century that it became clear that feedback systems were prone to instability or oscillatory behaviors and therefore they had to be improved.

This was particularly true for relay-based control systems, that is an electrically operated switch. The first relays were used in long distance telegraph circuits as amplifiers (a simple relay was included in the original 1840 telegraph patent of Samuel Morse). The relay systems were used intensively already from the beginning of the development of the control system to implement the so-called on-off control action: these can also be seen as primordial systems of the sliding mode control strategies. But people began to realize that they needed a basic theory. During World War II it was developed what is now the classical theory of automatic system controls. Then in the 50's and 60's the Soviets developed an alternative method of approach to dynamic modeling thanks to Lyapunov studies. But only after 70's we were able to best develop this theory through documents in English: all these documents will lead to the birth of the sliding mode control theory [1].

2.2 Basic Concepts in Sliding Mode Control

Consider a generic dynamical system S described by its state equation

$$\dot{x}(t) = f(x(t), u(t), t) \quad (2.1)$$

with $x(t_0)=x_0$, and $t, t_0 \in [0, \infty]$ where:

- $x(t) \in R^n$ is the system state
- $u(t) \in R^m$ is the system input, for example a system control action, so this is a variable by which we can influence the system.

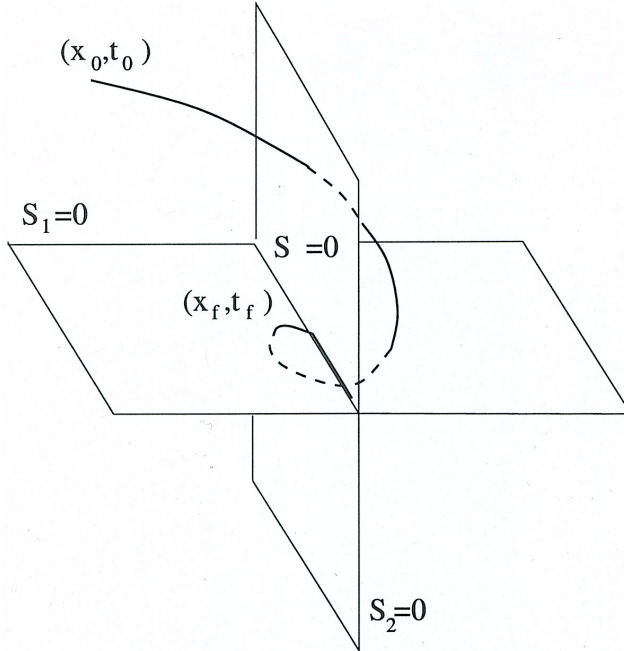


Figure 2.1: Sliding Manifold

Now consider the function of the system state $\sigma(x(t)) \in R^m$. it is a vector with the same dimension of the $u(t)$. Based on σ , also called sliding variable, we can define an associated sliding manifold or $\sigma(x(t)) = 0$ also $\in R^m$. The sliding manifold is nothing more than a subspace of the system state space having dimension $n - m$, where n is the dimension of the state, and m is the dimension of the input. What normally happens is that the sliding manifold may be a single surface or an intersection of more surfaces (see Figure 2.1).

The sliding mode is a system state sliding that occurs when the state of the system intersects the sliding manifold and pushes it against the sliding manifold, so when the state trajectory continuously crosses the sliding manifold, since in its vicinity the state motion is always directed towards the manifold, a sliding mode is enforced. To do this, we have to create a control that, each time that the system state crosses the manifold, inverts so that it continuously re-crossings to maintain the state. To create a controller that does this at the right frequency is necessary to design two elements, the sliding manifold and the control law. The sliding manifold is designed so that the system in sliding mode evolves in the desired way, the control law has to be chosen in order to enforce a sliding mode. An important design requirement is that the sliding mode needs to be enforced in a finite time.

When the system is in sliding mode we can note two interesting properties: the first is the order reduction, in fact, the system in sliding mode changes its order from n to $n - m$. The second is the invariance property: it is insensitive to matched uncertainties. These properties are given automatically when the system is in sliding mode. Typically the reduced order state equation describing the system in sliding mode is called equivalent system. Its dynamics can be assigned by suitably designing the sliding manifold.

In order to make a sliding manifold exist, it is necessary that the trajectories of the state are directed against the sliding manifold, from this we understand that the problem of existence is a system stability problem. We can demonstrate the existence of a sliding mode by the Lyapunov function. In case of single input system (we choose a single input case for the sake of simplicity) one has

$$V(x) = \frac{1}{2}\sigma^2(x) \quad (2.2)$$

Note that $\dot{\sigma}$ depends on the control variable (then it is discontinuous on $\sigma = 0$). The control variable has to be chosen so that in the attraction region, it holds

$$\dot{V}(x) = \sigma\dot{\sigma} < 0 \quad (2.3)$$

This condition is the so-called reachability condition [16]. It should be emphasized that the control law is a discontinuous law. This means that by using it in the equation (2.1) we do not get more than a differential equation but a differential inclusion. These differential equations can be solved through the Filippov method [30], or by the equivalent control developed by Utkin [16] [31]. Assume that a sliding mode is enforced, we have that $\forall t \geq t_r$, one has $\sigma(x) = 0, \dot{\sigma}(x)|_{eq} = 0$, thus if we can consider a sliding mode of a differential inclusion, one has

$$\dot{\sigma}(x)|_{eq} = \left[\frac{\delta\sigma}{\delta x} \dot{x}|_{eq} \right] = \left[\frac{\delta\sigma}{\delta x} \right] [A(x, t) + B(x, t)u_{eq}] = 0 \quad (2.4)$$

where u_{eq} is the so-called equivalent control and it is continuous. If we substitute u_{eq} in the equation of the system, we obtain a continuous differential equation that describes the evolution of the system state in the time, always in the Filippov sense, i.e.,

$$\dot{x} = A(x, t) + B(x, t)u_{eq} \quad (2.5)$$

The big problem of sliding mode control systems is the so-called chattering effect [21], Figure 2.2. An ideal sliding mode is enforced if the control variable is discontinuous on the sliding manifold. As we remember, every time the system crosses, changes direction and comes back (in an ideally infinite frequency): if this happens we can be sure that you never come off by sliding manifold. Clearly achieve something with infinite frequency is impossible. In the ideal case, after the step of reaching (achieving), the state reaches the sliding manifold and it slides on it. In the literature, the chattering is defined as the high frequency oscillation of the sliding variable (controlled variable) due to the discontinuity of the control variable [21].

Several methods have been proposed to alleviate the chattering effect and/or regularize the control signal. The classical methods are: the boundary layer control [18] and the filtered sliding mode control [32], while the modern methods are the use a second order sliding mode [20] or higher order sliding mode [33].

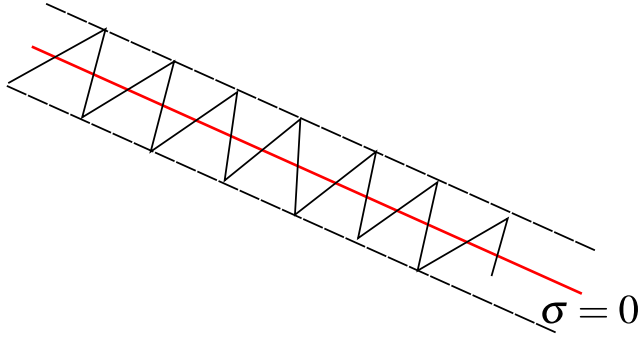


Figure 2.2: Chattering

2.2.1 Second Order Sliding Mode

In order to reduce the chattering problem, the control theory has been here developed for the second order sliding mode [20]. This consists in sliding motion on a surface $\sigma(x(t))=0$ in the state space, with its first time derivative $\dot{\sigma}(x(t))=0$, the control signal depending on $\sigma(x(t))$, but directly acting only on $\ddot{\sigma}(x(t))$.

Consider the system

$$\begin{cases} \dot{x}_i(t) = x_{i+1}(t) \\ \dot{x}_n(t) = f(x(t)) + g(x(t))u(t) \end{cases} \quad (2.6)$$

where $x(t) = [x_1, x_2, \dots, x_n]^T \in R^n$, and $f(\cdot)$ and $g(\cdot)$ are uncertain smooth functions such that

$$0 < G_1 \leq g(x(t)) \leq G_2 \quad |f(x(t))| \leq P_f + Q_f \|x(t)\| \quad (2.7)$$

$$\left\| \frac{\delta f(x(t))}{\delta x} \right\| \leq P_{df} + Q_{df} \|x(t)\| \quad (2.8)$$

$$\left\| \frac{\delta g(x(t))}{\delta x} \right\| \leq P_{dg} + Q_{dg} \|x(t)\| \quad (2.9)$$

with $G_1, G_2, P_f, Q_f, P_{df}, Q_{df}, P_{dg}, Q_{dg}$ known real positive constants. If we consider a sliding manifold expressed as

$$\sigma(x(t)) = x_n(t) + \sum_{i=1}^{n-1} c_i x_i(t) = 0 \quad (2.10)$$

where $c_i, i = 1, \dots, n-1$ are real positive constants we can obtain as first and

second-time derivative:

$$\dot{\sigma}(x(t)) = f(x(t)) + g(x(t))u(t) + \sum_{i=1}^{n-1} c_i x_{i+1}(t) \quad (2.11)$$

$$\ddot{\sigma}(x(t)) = \frac{d}{dt}f(x(t)) + \frac{d}{dt}g(x(t))u(t) + \\ + g(x(t))\dot{u}(t) + c_{n-1}[f(x(t)) + g(x(t))u(t)] + \sum_{i=1}^{n-2} c_i x_{i+2}(t) \quad (2.12)$$

We can see that if $\ddot{\sigma} = 0$ in finite time by the discontinuous control $\dot{u}(t)$, this means that even $\dot{\sigma} = 0$ and $\sigma = 0$ in finite time and that $u(t)$ is a continuous control, because it is a integral of the discontinuous control, and that undesired problem of the chattering is alleviated. Note that when we speak of the second order sliding mode we need to introduce an auxiliary system, because it is simpler to study than to that of departure. This system can be obtained using the sliding variable as a state variable and its first time derivative. Then define $\varepsilon_1 = \sigma(x(t))$ and $\varepsilon_2 = \dot{\sigma}(x(t))$, so the so-called auxiliary system can be written as:

$$\begin{cases} \dot{\varepsilon}_1 = \varepsilon_2 \\ \dot{\varepsilon}_2 = F(x(t), u(t)) + g(x(t))w(t) \end{cases} \quad (2.13)$$

where $\varepsilon_2(t)$ results in being unmeasurable, $w(t)$ is the auxiliary control and $F(\cdot)$ and $g(\cdot)$ are uncertain functions such that:

$$0 < G_1 \leq g(x(t)) \leq G_2 \quad |F(x(t), u(t))| < F \quad (2.14)$$

with G_1, G_2, F known positive constants.

This system is not easily solvable and we need to find $w(t)$ such that ε_1 and ε_2 are steered to zero in a finite time. In literature there are many algorithms, the more famous are: bang bang control [34] Figure 2.4, sub-optimal control [20] Figure 2.5 and Twisting and Super Twisting algorithms [35].

Now we consider the so-called sub-optimal control algorithm, proposed by Bartolini, Ferrara and Usai, because we have utilized it for our project. The control law is defined as:

$$w(t) = -\alpha U_{max} sgn(\varepsilon_1(t) - \frac{1}{2}\varepsilon_{max}) \quad (2.15)$$

$$\alpha(t) = \begin{cases} \alpha^* & if [\varepsilon_1(t) - \frac{1}{2}\varepsilon_{max}][\varepsilon_{max} - \varepsilon_1] > 0 \\ 1 & if [\varepsilon_1(t) - \frac{1}{2}\varepsilon_{max}][\varepsilon_{max} - \varepsilon_1] \leq 0 \end{cases} \quad (2.16)$$

where U_{max} is the control magnitude, ε_{max} is the last singular value of ε_1 , i.e., last local minimum, local maximum or horizontal flex point. The sufficient conditions to

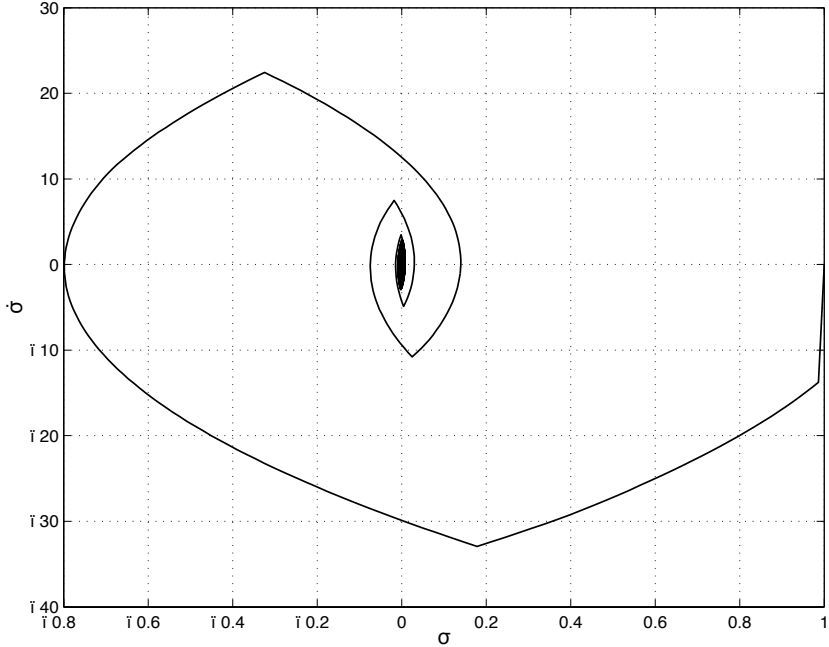


Figure 2.3: Second order sliding mode

guarantee the finite time convergence to the sliding manifold are:

$$U_{max} > \max\left(\frac{F}{\alpha^* G_1}, \frac{4F}{3G_1 - \alpha^* G_2}\right) \quad (2.17)$$

$$\alpha^* \in (0, 1] \cap (0, \frac{3G_1}{G_2}) \quad (2.18)$$

Thus a sequence of states with coordinates $(\varepsilon_{max}, 0)$ with the contraction property $|\varepsilon_{max_{i+1}}| < |\varepsilon_{max_i}|$, $i = 1, 2, \dots$ is generated and the convergence of the system trajectory to the origin of the plane proves to take place in finite time.

Therefore, since $\varepsilon_1(t)$ and $\varepsilon_2(t)$ are steered to zero in a finite time, a second order sliding mode is enforced with a control variable which is continuous. The chattering alleviation objective is contemporarily attained. In the figure 2.5,2.3,2.4 the are some behaviors of the auxiliary system.

2.3 The Platooning Problem

As we can see from the diagram 2.6, we need to design two controller to control the car's dynamics. The outer loop receives a position error due to the difference between the desired safety distance, and that which actually exists between the i -th car, and $(i - 1)$ -th car. The outer controller output is a desired value of slip ratio, that it used as reference for the inner loop. The inner loop receives a slip ratio error and generates a signal torque for the car.

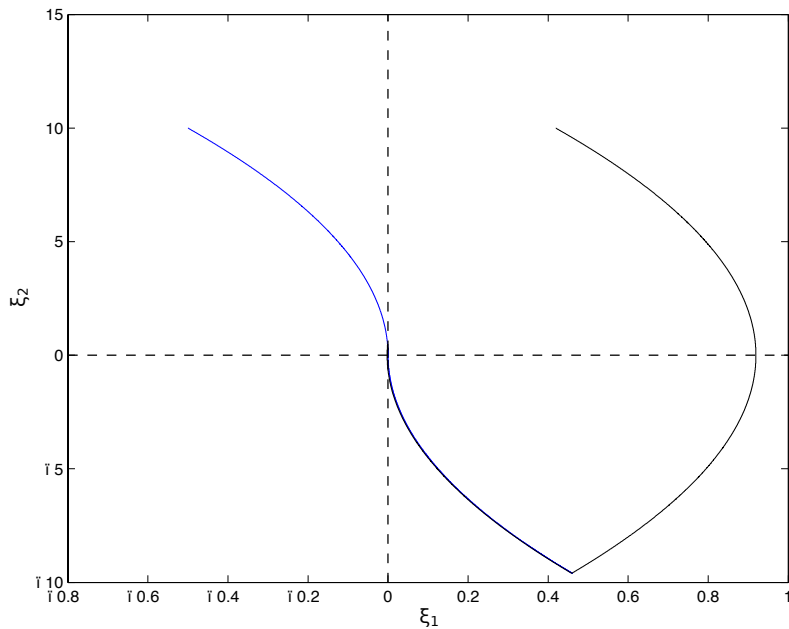


Figure 2.4: Bang Bang Second order sliding mode

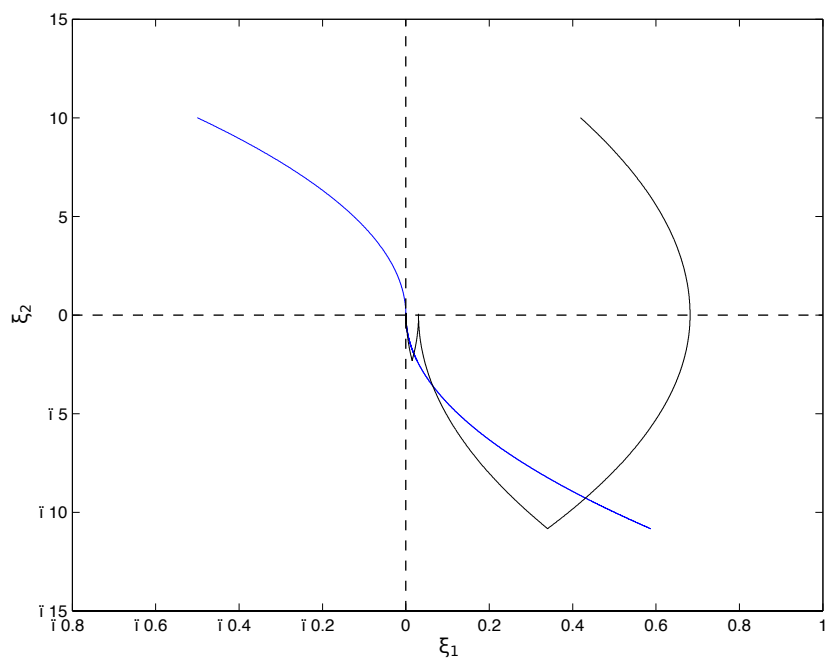


Figure 2.5: Suboptimal Second order sliding mode

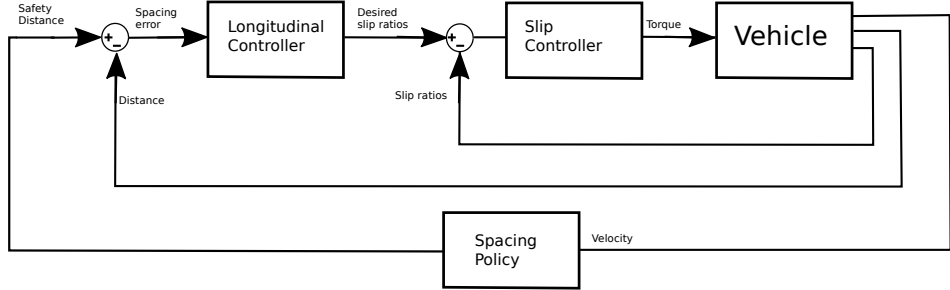


Figure 2.6: Control scheme

2.3.1 The Outer Control-Longitudinal Loop

Assuming that the acceleration and velocity for the leader (the 0-th vehicle, thus it has no preceding vehicle) are arbitrary, the control object of the i -th vehicle is to maintain the safety distance from the preceding vehicle, with $i = 1, 2, 3$. The reference of the distance between the machines, that is the desired safety distance, it is calculated by the policy of the Constant Time-Headway strategy [2]. It is as follows

$$S_{d_i}(v_{x_i}(t)) = S_{d_0} + hv_{x_i} \quad (2.19)$$

where S_{d_0} is the minimum value of the safety distance, h is headway time. Now considering the i -th vehicle, the spacing error is given by:

$$e_i(t) = S_{d_0} + hv_{x_i} - x_{i-1}(t) + x_i(t) \quad (2.20)$$

where x_i is the longitudinal position of the i -th vehicle. To apply the sliding mode we have to choose the sliding variable, and we choose as sliding variable the distance error as

$$S_i(t) = e_i(t) = S_{d_0} + hv_{x_i} - x_{i-1}(t) + x_i(t) \quad (2.21)$$

Now, to start to solve the control problem we need to find the auxiliary system. Because we want to use a sliding mode of second order to find the auxiliary system we need to time derive the sliding variable twice, thus we obtain

$$\begin{cases} \dot{S}_i(t) = \dot{e}_i(t) = v_{x_i}(t) - v_{x_{i-1}}(t) + h\dot{v}_{x_i}(t) \\ \ddot{S}_i(t) = \ddot{e}_i(t) = \ddot{v}_{x_i}(t) - \ddot{v}_{x_{i-1}}(t) + h\ddot{v}_{x_i}(t) \\ \quad = \varepsilon_i(t) + w_i(t) \end{cases} \quad (2.22)$$

where $\varepsilon_i(t) = \dot{v}_{x_i}(t) - \dot{v}_{x_{i-1}}(t)$ and $w_i(t) = h\ddot{v}_{x_i}(t)$ is the auxiliary control input. We can note that the therm $\varepsilon_i(t)$ is the difference between the longitudinal acceleration and thus is bounded by physical and mechanical limits [36].

$$|\varepsilon_i| \leq \Gamma_i \quad i = 1 \dots 3 \quad (2.23)$$

For resolving the auxiliary system we need to use the sub-optimal control, thus

$$w(t) = h\ddot{v}_{x_i}(t) = -\alpha W_{M_i} \operatorname{sgn}[S_i(t) - \frac{1}{2}S_{i_{Max}}] \quad \text{with} \quad W_{M_i} > 2\Gamma_I \quad (2.24)$$

The use of (2.24) allows to reach the origin of the state space plane in finite time. This means that the first and second time derivative of the sliding variable are steered to zero in finite time. It is necessary to highlight that the product of the multiplication $h\ddot{v}_{x_i}(t)$ results in an acceleration, and this means that $\dot{v}_{x_{desse_i}} = h\ddot{v}_{x_i}(t)$, from this can be seen that we do not need to integrate the control variable. Thus the auxiliary input control is discontinuous. This is not a problem because in our model there is not a real actuator, thus we have not a problem of saturation and stress of the actuator. Despite this we have used a low pass filter for making smooth the input of the system.

Obtained the auxiliary input control $w(t)$ we can find the sum of the desired traction force. We obtained this starting from the following equations

$$m_i \dot{v}_{x_i} = 2[F_{xf_i}(\lambda_{f_i}) + F_{xr_i}(\lambda_{r_i})] - F_{loss_i} \quad (2.25)$$

and

$$F_{xf_{desse_i}}(t) + F_{xr_{desse_i}}(t) = \frac{1}{2}[m_i \dot{v}_{x_{desse_i}} + F_{loss}(v_{x_i}(t))] \quad (2.26)$$

with $\dot{v}_{x_{desse_i}} = h\ddot{v}_{x_i}(t)$ and knowing that

$$F_{xf_i} < \mu_p F_{zf_i} \quad (2.27)$$

$$F_{xr_i} < \mu_p F_{zf_i} \quad (2.28)$$

Substituting in the previous ones

$$F_{zf_i} = \frac{l_{r_i} m_i g - l_{h_i} \dot{v}_{x_i}}{2(l_{r_i} + l_{h_i})} \quad (2.29)$$

$$F_{zf_i} = \frac{l_{r_i} m_i g + l_{h_i} \dot{v}_{x_i}}{2(l_{r_i} + l_{h_i})} \quad (2.30)$$

we obtain

$$F_{xf_i} < \mu_{p_i} \frac{l_{r_i} m_i g - 2l_{h_i} F_{xr_i} + l_{h_i} F_{loss_i}}{2(l_{f_i} + l_{r_i} + \mu_p l_{h_i})} \quad (2.31)$$

$$F_{xr_i} < \mu_{p_i} \frac{l_{r_i} m_i g + 2l_{h_i} F_{xf_i} + l_{h_i} F_{loss_i}}{2(l_{f_i} + l_{r_i} - \mu_p l_{h_i})} \quad (2.32)$$

$$(2.33)$$

and considering that the optimal tire force distribution to have the best acceleration response is given by

$$\frac{F_{xf_i}}{F_{xr_i}} = \frac{l_{r_i} + l_{h_i} \frac{F_{loss_i}}{m_i g} + \mu_{p_i} l_{h_i}}{l_{f_i} - l_{h_i} \frac{F_{loss_i}}{m_i g} - \mu_{p_i} l_{h_i}} \quad (2.34)$$

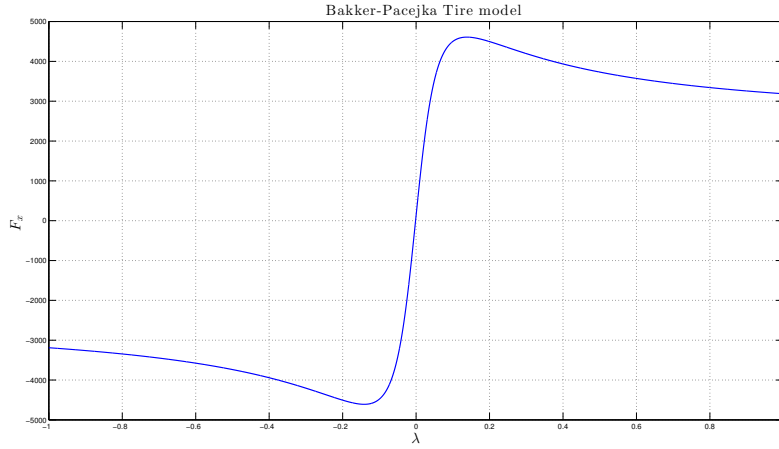


Figure 2.7: Tire model

that is the intersection point of the two boundary lines of (2.29). Combining (2.34) and (2.26) we obtain

$$F_{xr_{dessa_i}} = \frac{a}{b+1} \quad (2.35)$$

$$F_{xf_{dessa_i}} = b \frac{a}{b+1} \quad (2.36)$$

where: $a = \frac{1}{2}[m_i \dot{v}_{x_{dessa_i}} + F_{loss}(v_{x_i}(t))]$ and $b = \frac{l_{r_i} + l_{h_i} \frac{F_{loss_i}}{m_i g} + \mu_{p_i} l_{h_i}}{l_{f_i} - l_{h_i} \frac{F_{loss_i}}{m_i g} - \mu_{p_i} l_{h_i}}$.

Now through (2.35) and the $F_{x_i} = \mu_{p_i} f_{t_i}(\lambda_i, F_{z_i})$ we can find what values must has the slip ratio to have the desired traction force (2.35). The values of slip ratio $\lambda_{f_{dessa}}, \lambda_{r_{dessa}}$ are the output of the outer control loop and it is used as a reference signal for inner loop. In particular, the value that can take on the slip ratio was chosen to limit it between the maximum and the minimum of the curve, see the Figure 2.7, because it is the zone of stability, so doing you generate stable references

2.3.2 The Inner Slip Control Loop

The control object of the slip controller is to generate a torque signal, that is the input of our system (vehicle), such that it has the desired slip ratio. For this controller, the sliding variable is the error signal given by the difference between the desired slip ratio, which is that produced by outer control loop and the real slip ratio at the wheel.

$$\lambda_{je}(t) = \lambda_j - \lambda_{j_{des}} \quad j \in \{f, r\} \quad (2.37)$$

where f and r are for front and rear wheel. The sliding manifold are given by:

$$s_j(t) = \lambda_{je}(t) = 0 \quad j \in \{f, r\} \quad (2.38)$$

For obtaining the auxiliary system, we have to time derive the sliding variable twice, thus

$$\begin{cases} \dot{s}_j(t) = f_j(t) + h_j(t)T_j(t) - \dot{\lambda}_{j_{des}}(t) \\ \ddot{s}_j(t) = \dot{f}_j(t) + \dot{h}_j(t)T_j(t) + h_j(t)\dot{T}_j(t) - \ddot{\lambda}_{j_{des}}(t) \\ \quad = \varphi_j(t) + \gamma_j(t)\dot{T}_j(t) \quad j \in \{f, r\} \end{cases} \quad (2.39)$$

where $\varphi_j(t) = \dot{f}_j(t) + \dot{h}_j(t)T_j(t)$ and $\gamma_j(t) = h_j(t)$. Also in this case we know that the quantities $\varphi_f(t)$ and $\varphi_r(t)$ are bounded, thus we can find the upper limit by physical consideration through the formula. Thus

$$\phi_j \geq |\varphi_j(t)| \quad j \in \{f, r\} \quad (2.40)$$

The $\gamma_f(t)$ and $\gamma_r(t)$ are unknown bounded functions, and the bound are

$$0 < \Gamma_{j1} \leq \gamma_j(t) \leq \Gamma_{j2} \quad j \in f, r \quad (2.41)$$

As for the outer loop controller, it is used the sub-optimal control for solve the auxiliary system. This means that for this case we have to use the \dot{T}_j designed as

$$\dot{T}_j(t) = -\alpha_j(t)V_{jM}sgn(s_j(t) - \frac{1}{2}s_{jM}) \quad j \in \{f, r\} \quad (2.42)$$

$$\alpha_j(t) = \begin{cases} \alpha_j^* & if [s_j(t) - \frac{1}{2}s_{jM}][s_{jM} - s_j] > 0 \\ 1 & if [s_j(t) - \frac{1}{2}s_{jM}][s_{jM} - s_j] \leq 0 \\ j \in \{f, r\} & \end{cases} \quad (2.43)$$

with the constraints

$$V_{jM} > max(\frac{\phi_j}{\alpha_j^*\Gamma_{j1}}, \frac{4\phi_j}{3\Gamma_{j1} - \alpha_j^*\Gamma_{j2}}) \quad (2.44)$$

$$\alpha^* \in (0, 1] \cap (0, \frac{3\Gamma_{j1}}{\Gamma_{j2}}) \quad (2.45)$$

We note that the control is done on \dot{T}_j , and this means that the control variable T_j , that is the integral of \dot{T}_j is a continuos function, thus a chattering alleviation is obtained. The function s_{jM} is piece-wise constant function according to what was said before, thus this function describes a trajectory on the state space and the origin, that is $s_j = \dot{s}_j = 0$ is reached in a finite time, thus the control object is achieved.

2.4 String Stability

In this section the string stability of the considered vehicles platoon will be analyzed. The string stability of ACC vehicles platoon means that the spacing errors are not amplified as they propagate toward the tail of the string. Before moving to study the stability it is necessary to assume that the longitudinal dynamics of the i th vehicle

can be approximated [4] by the following a first order dynamics

$$\tau_a \ddot{v}_i + \dot{v}_i = v_{i_{des}} \quad (2.46)$$

where τ_a represents the actuator dynamics and a lag time, while $v_{i_{des}}$ is the desired value of acceleration to be designed in order to make the vehicle platoon string stable [4], i.e., steer to zero the spacing error in steady-state. Note that, in this thesis the control input $v_{i_{des}}$ will not require the presence of a physical actuator but it is necessary to find the force values fed into the vehicle, as shown in the hierarchical control scheme in 3.1.

For the sake of clarity, the formal definition of string stability is hereafter reported. Let $s := j\omega$ be the Laplace variable, j being the imaginary variable and ω the system bandwidth.

Definition 2.4.1. Given the spacing error (2.21), the transfer function relating the spacing errors of consecutive vehicles is given by

$$H(s) := \frac{\delta_i(s)}{\delta_{i-1}(s)} . \quad (2.47)$$

□

Note that, typically (2.47) is assumed such that the corresponding impulse response function does not change the sign [4].

Definition 2.4.2 (String Stability). Given the longitudinal vehicle dynamics (2.46), the ACC vehicle platoon is string stable if it holds

$$\|H(s)\|_\infty \leq 1 . \quad (2.48)$$

□

Note that, if condition (2.48) holds, the spacing error (2.21) is steered to zero. Moreover, assume that the ACC platoon is driving at a nominal velocity v_n with zero acceleration and the inter-vehicle spacing is equal to the desired one L , so that, for small velocity perturbations, it holds $v_i = v_n + \Delta v_i$, $\dot{v}_i = \Delta \dot{v}_i$, and the function (2.47) can be written as

$$H(s) = \frac{\Delta v_i(s)}{\Delta v_{i-1}(s)} . \quad (2.49)$$

Now, making reference to the inner loop in the control scheme, the following lemma can be proved.

Lemma 2.4.1. *Given the vehicle model (1.1), controlled by the SSOSM control law defined in (2.42) and (2.44), with sliding variable as in (2.37), then, the slip error is steered to zero in a finite time t_{r_λ} , $t_{r_\lambda} \geq t_0$.* □

Proof. The proof of this lemma directly follows from [4], where the contraction property of the auxiliary sliding variable in a finite time is proved. This implies that the sliding variable is steered to zero, i.e., the slip error is steered to zero in a finite time t_{r_λ} , $t_{r_\lambda} \geq t_0$. □

The previous lemma means that the vehicle is able always to follow the desired slip ratio $\lambda_{i_{\text{des}}}$. At this point it is possible to consider the longitudinal vehicle dynamics as in (2.46), in order to find an upper bound for the SSOSM control parameter of the longitudinal controller.

Lemma 2.4.2. *Given the longitudinal vehicle model (2.46), controlled by the SSOSM control law defined in (2.24), with sliding variable as in (2.21), then, the ACC vehicle platoon is string stable if*

$$W_{i_{\max}} < \frac{h}{2} (1 + \tau_a^2 \omega^4 - 2\tau_a \omega^2 + \omega^2) .$$

□

Proof. According to the definition of string stability, we need to find the explicit expression of the transfer function $H(s)$ in (2.47). Since it is assumed that $H(s)$ can be written as in (2.49), one has that the spacing error is almost equal to zero, so that $\xi_{i_{\max}}$ is negligible and the sign function can approximated with an hyperbolic tangent function such that the control law can be written as

$$\dot{v}_{i_{\text{des}}} \approx -\frac{1}{h} W_{i_{\max}} (\varepsilon_i(t) + L + h v_i(t)) \quad (2.50)$$

Substituting the control law (2.50) into (2.46) one has

$$\tau \dot{a}_{x_i} + a_{x_i} = -\frac{1}{h} W_{i_{\max}} (\varepsilon_i(t) + L + h v_i(t))$$

Computing the time derivative one obtains

$$\begin{aligned} h \tau_a \ddot{a}_{x_i} + h \dot{a}_{x_i} &= -W_{i_{\max}} (\dot{\varepsilon}_i(t) + h \dot{v}_i(t)) \\ h \tau_a \Delta \ddot{v}_i + h \Delta \dot{v}_i &= -W_{i_{\max}} (\dot{\varepsilon}_i(t) + h \Delta \dot{v}_i(t)) \\ h \tau_a \Delta \ddot{v}_i + h \Delta \dot{v}_i &= -W_{i_{\max}} (\Delta v_i - \Delta v_{i-1} + h \Delta \dot{v}_i(t)) \\ h \tau_a \Delta \ddot{v}_i + h \Delta \dot{v}_i + h \Delta \dot{v}_i(t) + W_{i_{\max}} \Delta v_i &= W_{i_{\max}} \Delta v_{i-1} \end{aligned} \quad (2.51)$$

Compute now the Laplace transformation of (2.51) such that

$$(h \tau_a s^3 + h s^2 + h s(t) + W_{i_{\max}}) \Delta v_i = W_{i_{\max}} \Delta v_{i-1}$$

and the transfer function (2.49) is

$$H(s) = \frac{\Delta v_i}{\Delta v_{i-1}} = \frac{W_{i_{\max}}}{(h \tau_a s^3 + h s^2 + h v_i s(t) + W_{i_{\max}})}$$

Applying the definition of string stability one has that

$$\frac{W_{i_{\max}}^2}{(\omega^2 h^2 (1 + \tau_a^2 \omega^4 - 2\tau_a \omega^2)) + (W_{i_{\max}}^2 + h^2 \omega^4 - 2W_{i_{\max}} h \omega^2)} \leq 1 .$$

After some computation it is possible to find the following upper bound for the

SSOSM control gain, i.e.,

$$W_{i_{\max}} < \frac{h}{2} (1 + \tau_a^2 \omega^4 - 2\tau_a \omega^2 + \omega^2) \quad (2.52)$$

which concludes the proof. \square

Finally, by virtue of Lemma 2.4.1 and Lemma 2.4.2 the string stability of the vehicles platoon controlled via the proposed SSOSM control scheme is proved.

Theorem 2.4.1. *Given the longitudinal vehicle model (2.46), controlled by the SSOSM control law defined in (2.24), with sliding variable as in (2.21) and control constraint in (2.52), then, the spacing error is steered to zero in a finite time t_{r_δ} , $t_{r_\delta} \geq t_0$.* \square

Proof. The proof of the theorem relies on the proof of finite time convergence reported in [1]. It can be proved that, with the constraints (2.52), the SSOSM control law (2.24) implies a sequence of states with coordinates featuring a contraction property expressed by

$$|\xi_{i_{\max_{k+1}}}| < |\xi_{i_{\max_k}}| \quad (2.53)$$

where $\xi_{i_{\max_k}}$ is the k -th extremal value of variable ξ_{1_i} . This motion implies that the sequence $\{t_{\max_k}\}$, which denotes the sequence of the time instants when an extremal value occurs, is such that

$$\lim_{k \rightarrow \infty} t_{\max_k} < \frac{\beta}{1 - \gamma} + t_{\max_1} \quad (2.54)$$

where $\gamma < 1$, and

$$\beta = \sqrt{|\xi_{i_{\max_1}}|} \frac{2W_{i_{\max}}}{(W_{i_{\max}} - \Phi_i)\sqrt{W_{i_{\max}} + \Phi_i}}. \quad (2.55)$$

Hence, one has that spacing error is steered to zero in a finite time t_{r_δ} , $t_{r_\delta} \geq t_0$, which concludes the proof. \square

2.5 Conclusion

In this chapter we have designed the controllers, the control scheme consists of two control loops, the outer one with the task of solving the problem of platooning and the inner loop with the purpose of the longitudinal dynamic control. It was also verified the stability of the platoon.

Chapter 3

Comparison inner loop controllers

3.1 Introduction

The problem of controlling the longitudinal dynamics in road vehicles has been studied in depth in the past few decades. Control theory has been widely used to pursue the objective of maximum tire-road adherence during acceleration phases, i.e., Traction Control (TC), and braking phases with the so-called Anti-Lock Brake System (ABS). With the new available technologies, like multi-actuated vehicles with electric motors for each wheel, it is now possible to merge the problems of TC and ABS control in a unique Fastest Acceleration/Deceleration Control (FADC) problem [37]. In all critical situations, where maximum tire/road adherence is needed, the designed controller should track a target slip-ratio, selected on the base of suitable tire friction models [24, 25].

The implementation of a feedback control requires several quantities to be known (vehicle velocity, wheel-slip, tire-road friction coefficient), so that the states of the adopted model can be estimated. The problem of estimation of these values has been studied in recent years, also by means of sliding mode observers [38, 39, 40, 41]. Sliding Mode Control (SMC) theory has been a popular choice for the design of the feedback controller, thanks to its robustness properties, in particular against matched disturbances. Early researches on the adoption of SMC in ABS date back to the early 90's. In [42], for instance, an adaptive sliding-mode vehicle traction control strategy is proposed, whereas in [43] the optimum friction is reached without a-priori knowledge of the friction curve.

Most of the research on wheel-slip control with SMC techniques has involved First Order Sliding Mode (FOSM) control, with the focus being placed on the observation of necessary signals [44] or with different approaches to chattering reduction [45, 46]. More recently, Higher Order Sliding Mode (HOSM) control techniques have been implemented. In [36], based on a bicycle model, torques on front and rear axles are controlled so that a target wheel-slip value is tracked on each axle.

In [47], the so called Suboptimal Second Order Sliding Mode (SSOSM) technique is used for the Traction Control in a motorcycle. In [48] a Super-Twisting Sliding Mode (STSM) control is coupled with linear observers for traction forces, with the focus being on robustness against parameter uncertainties. Evaluation is done through simulation and single-wheel test rig, and shows good results in comparison with Model Predictive Control (MPC).

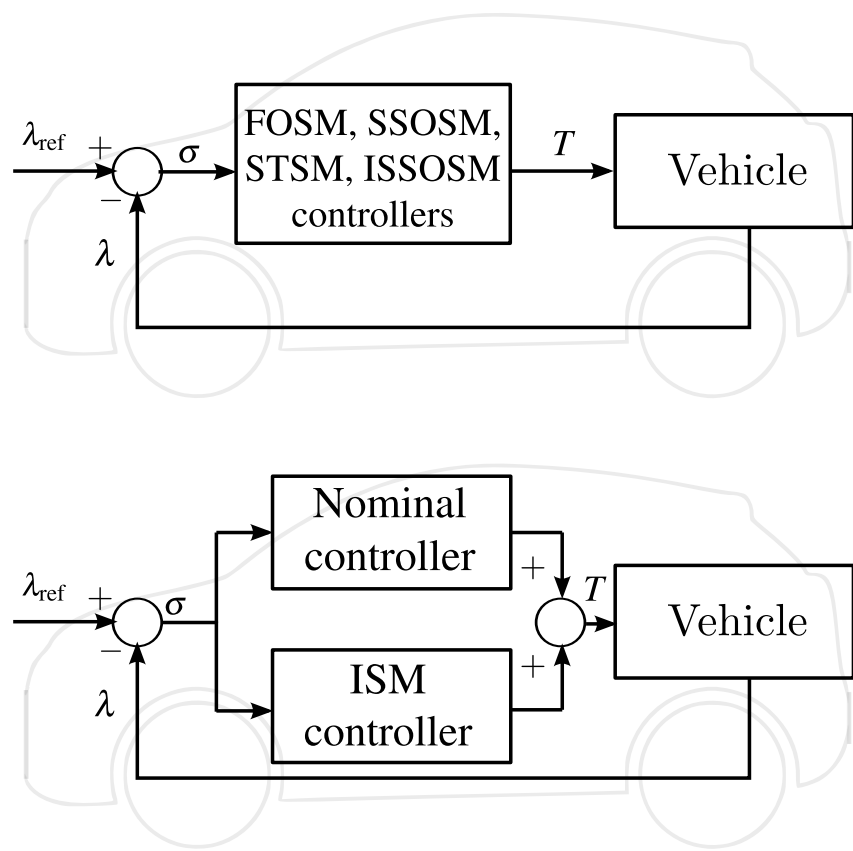


Figure 3.1: Sliding Mode slip control schemes

A sliding mode controller with conditional integrator is tested on a prototype vehicle in [49]: an integral component is added to the sliding variable, so that a PI-like effect is obtained inside a boundary layer.

The aim of this chapter is to assess the different SMC techniques proposed in recent years to solve the wheel-slip control problem, and compare their performances in different uncertainty conditions (see Figure 3.1). This work is a preliminary step in determining which SMC technique is more suitable for implementation on a vehicle, with the final goal of successfully run the most suitable algorithms on a real multi-actuated electric vehicle.

3.2 Some Preliminaries on the Application of Sliding Mode Control to the Slip Control Problem

In order to apply the sliding mode control methodology to solve the considered control problem, the so-called sliding variable needs to be defined. In this case we select $\sigma = [\sigma_f, \sigma_r]^T$ as

$$\sigma_\nu = \lambda_{\text{ref},\nu} - \lambda_\nu, \quad \nu = \{f, r\} \quad (3.1)$$

where $\lambda_{\text{ref},\nu}$ is the desired value of the slip ratio. Let ρ be the relative degree of the system, i.e., the minimum order of the time derivative of the sliding variable, $\sigma_\nu^{(\rho)}$, in which the control input T_ν explicitly appears. Now, compute the first and the second time derivative of the sliding variable, so that by posing $\xi_{1,\nu} = \sigma_\nu$ and $\xi_{2,\nu} = \dot{\sigma}_\nu$, the so-called auxiliary system can be written as

$$\begin{aligned} \dot{\xi}_{1,\nu}(t) &= \xi_{2,\nu}(t) \\ \dot{\xi}_{2,\nu}(t) &= f_{\pi,\nu}(t) + g_{\pi,\nu}(t)w(t), \quad \pi = \{a, b\}, \nu = \{f, r\} \end{aligned} \quad (3.2)$$

where $w(t) = \dot{T}_\nu$ is the auxiliary control variable, while the function $f_{\pi,\nu}(\cdot)$ and $g_{\pi,\nu}(\cdot)$ are

$$\begin{aligned} f_{a,\nu}(t) &= \ddot{\lambda}_{\text{ref},\nu} + \frac{\ddot{v}_x}{r_\nu \omega_\nu} - \frac{\dot{v}_x \dot{\omega}_\nu}{r_\nu \omega_\nu^2} + \frac{\dot{v}_x F_{x,\nu}}{J_\nu \omega_\nu^3} + \frac{\dot{v}_x \dot{F}_{x,\nu}}{J_\nu \omega_\nu^2} + \\ &\quad - \frac{2v_x F_{x,\nu} \dot{\omega}_\nu}{J_\nu^2 \omega_\nu^3} - \frac{v_x T_\nu \dot{\omega}_\nu}{J_\nu^2 r_\nu \omega_\nu^3} - \frac{\dot{v}_x T_\nu}{J_\nu^2 r_\nu \omega_\nu^2} \\ f_{b,\nu}(t) &= \ddot{\lambda}_{\text{ref},\nu} + \frac{r_\nu \dot{\omega}_\nu}{v_x} + \frac{r_\nu \omega_\nu \dot{v}_x}{v_x^2} + \frac{r_\nu^2 \dot{F}_{x,\nu}}{J_\nu v_x} - \frac{r_\nu^2 F_{x,\nu} \dot{v}_x}{J_\nu v_x^2} + \\ &\quad - \frac{2r_\nu \omega_\nu \dot{v}_x}{J_\nu v_x^2} - \frac{v_x T_\nu \dot{\omega}_\nu}{J_\nu^2 r_\nu \omega_\nu^3} - \frac{\dot{v}_x T_\nu}{J_\nu^2 r_\nu \omega_\nu^2} \\ g_{\pi,\nu}(t) &= -\frac{v_x^2}{J_\nu r_\nu \omega_\nu^2} \end{aligned} \quad (3.3)$$

Since velocities are assumed to be always positive and physical limits exist such as the limit characteristic curves of the torques which the engine can transfer to the wheels, it is assumed that functions $f_{\pi,\nu}(\cdot)$ and $g_{\pi,\nu}(\cdot)$ are bounded, with, in particular

$$|f_{\pi,\nu}(t)| \leq F \quad (3.4)$$

$$-G_{\max} \leq g_{\pi,\nu}(t) \leq -G_{\min} < 0 \quad (3.5)$$

$$|w(t)| \leq W \quad (3.6)$$

where F , G_{\min} , G_{\max} and W are positive constants, which in practical cases can be estimated and are therefore assumed known.

3.2.1 Problem Statement

On the basis of the vehicle model (1.1)-(1.16) the following control problem can be stated: *Given a slip reference value λ_{ref} , find a bounded control law such that the slip error is steered to zero in a finite time in spite of matched and unmatched uncertainties affecting the system, as well as transmission delays in both the feedback and actuation path..*

3.3 The Considered Sliding Mode Control Strategies

The proposed slip control schemes are illustrated in Figure 3.1. In this chapter different sliding mode control strategies are discussed. More specifically, in the following subsections a FOSM control [50], a SSOSM control [20], a STSM control [51], an Integral Sliding Mode (ISM) control [52] and the recently published Integral SSOSM (ISSOSM) control algorithm [53] are considered. Consider now the first control scheme of Figure 3.1.

3.3.1 FOSM Control

The first strategy discussed in this chapter is the classical FOSM control [50]. Given the choice of the sliding variable (3.1), the relative degree is $\rho = 1$ so that a FOSM naturally applies. The control law in this case is

$$T_{\nu}(t) = -U_{\nu,\max} \operatorname{sgn}(\sigma_{\nu}(t)) \quad (3.7)$$

where the control parameter $U_{\nu,\max}$ is a positive constant chosen so as to enforce a sliding mode [50]. The main difficulty with applying of this approach to solve the slip control problem is the discontinuity of the control variable which can cause chattering phenomenon [21] which is hardly acceptable.

3.3.2 SSOSM Control

SSOSM control is a particular case of HOSM control (see, for instance, [54] and [33] for other second order sliding mode algorithms). Given the auxiliary system (3.2), in which the relative degree is artificially increased by introducing the auxiliary control

variable w , the control law can be expressed as

$$T_\nu(t) = - \int_{t_0}^t \alpha_\nu W_{\nu,\max} \operatorname{sgn}(\xi_{1,\nu}(\zeta) - \frac{1}{2}\xi_{\max}) d\zeta \quad (3.8)$$

where ξ_{\max} is the local minimum or maximum of the sliding variable, while the control parameters $\alpha_\nu = \alpha_\nu^*$ and $W_{\nu,\max}$ are chosen such that

$$W_{\nu,\max} > \max\left(\frac{F}{\alpha_\nu^* G_{\min}}, \frac{4F}{3G_{\min} - \alpha_\nu^* G_{\max}}\right) \quad (3.9)$$

$$\alpha_\nu^* \in (0, 1] \cap \left(0, \frac{3G_{\min}}{G_{\max}}\right) \quad (3.10)$$

Note that the SSOSM algorithm requires the control $w(t) = \dot{T}_\nu(t)$ to be discontinuous. Yet, the control actually fed into the plant is continuous, which is highly appreciable in case of mechanical plants. Moreover, in [20] it has been proved that, under constraints (3.9), the convergence of the auxiliary system trajectory to the origin takes place in a finite time. More specifically, the control law (3.8) implies a contraction property of the extremal values of the sliding variable so that the slip error and its first time derivative are steered to zero in a finite time. Moreover, an important advantage of the SSOSM control is that the knowledge of the first time derivative of the sliding variable is not required, but only the computation of its extremal values, for instance through the methods described in [20].

3.3.3 STSM Control

STSM control is another particular case of second order sliding mode control in which, similarly to the SSOSM algorithm, the knowledge of the first time derivative of the sliding variable is not required [51]. The STSM control law can be expressed as

$$\begin{aligned} T_\nu(t) &= \int_{t_0}^t (v_\nu(\zeta) - W_{\nu,\max} \sqrt{|\xi_{1,\nu}(\zeta)|} \operatorname{sgn}(\xi_{1,\nu}(\zeta))) d\zeta \\ v_\nu(t) &= -V_{\nu,\max} \operatorname{sgn}(\xi_{1,\nu}(t)) \end{aligned} \quad (3.11)$$

where $W_{\nu,\max}$ and $V_{\nu,\max}$ are suitably chosen in order to ensure the sliding mode [51].

3.3.4 ISSOSM Control

In this subsection, the recently introduced ISSOSM control methodology is recalled [53]. This represents an extension of the SSOSM control algorithm with improved robustness properties against the uncertainties affecting the system. The idea is to reduce to a minimum the so-called reaching phase [50], during which the controlled system is not insensitive to the disturbances. Consider the auxiliary system (3.2) and define a *transient function* as

$$\begin{cases} \varphi_\nu(t) = (t - t_r)^2(c_0 + c_1(t - t_0)), & \forall t, t_0 \leq t \leq t_r \\ \varphi_\nu(t) = 0, & \forall t > t_r \end{cases} \quad (3.12)$$

where c_0 and c_1 are

$$c_0 = \sigma_\nu(t_0)T^{-2} \quad (3.13)$$

$$c_1 = \dot{\sigma}_\nu(t_0)T^{-2} + 2\sigma_\nu(t_0)T^{-3} \quad (3.14)$$

while $T = t_r - t_0$ is the so-called “prescribed time”, which allows one to steer the sliding variable σ_ν to zero at the time t_r . Note that, from (3.13) and (3.14), the transient function is realized such that the initial conditions are

$$\sigma_\nu(t_0) = \varphi_\nu(t_0) \quad (3.15)$$

$$\dot{\sigma}_\nu(t_0) = \dot{\varphi}_\nu(t_0) \quad (3.16)$$

Then, the auxiliary sliding manifold is defined as

$$\Sigma_\nu(t) = \sigma_\nu(t) - \varphi_\nu(t) = 0 \quad (3.17)$$

where Σ_ν is an auxiliary sliding variable such that $\xi_{1\nu} = \Sigma_\nu$ and $\xi_{2\nu} = \dot{\Sigma}_\nu$, while the control law is of the same form of (3.8) with constraints as in (3.9) and (3.10). The finite time convergence of the sliding variable in front of matched uncertainties can be proved relying on the results presented in [53].

3.3.5 ISM Control

Now, consider the second control scheme in Figure 3.1. ISM method enables to generate an ideal sliding mode of the controlled system starting from the initial time instant t_0 [52]. The ISM control variable is split into two parts

$$T_\nu(t) = T_{\nu,0}(t) + T_{\nu,1}(t) \quad (3.18)$$

where $T_{\nu,0}(t)$ is generated by any suitably designed high level controller, for instance a PI controller as in this thesis, and $T_{\nu,1}(t)$ is a discontinuous control action designed to compensate the uncertainties affecting the system. The so-called integral sliding manifold is defined as in (3.17), where the integral term φ_ν is

$$\varphi_\nu(t) = \sigma_\nu(t) + \int_{t_0}^t \frac{\partial \sigma_\nu}{\partial \lambda_\nu} \dot{\lambda}_\nu(\zeta) d\zeta \quad (3.19)$$

with the initial condition $\varphi_\nu(t_0) = \sigma_\nu(t_0)$. The ISM control law is then defined as

$$T_{\nu,1}(t) = -U_{\nu,\max} \operatorname{sgn}(\Sigma_\nu(t)) \quad (3.20)$$

with $U_{\nu,\max} > 0$ to enforce the sliding mode. By virtue of the choice of $\varphi_\nu(t)$ and $\varphi_\nu(t_0)$, it is apparent that the controlled system is in sliding mode on the manifold $\Sigma_\nu(t) = 0$ since the initial time instant. Moreover, under suitable assumptions on the auxiliary sliding variable, it is possible to show that the unmatched uncertainties are not amplified [52].

3.4 Simulations

In this section the sliding mode controllers are evaluated in a step response test, where the wheel-slip is regulated to a fixed value. A PI controller is also used in the same test for the sake of comparison. It is assumed that the maximum traction/braking force is obtained for $\lambda_{\text{ref},\nu} = \pm 0.2$ (the sign corresponds to the sign of the driver's torque demand, which is considered a matched disturbance in this work).

3.4.1 Test Setup

The presented controllers are evaluated in 4 different conditions:

1. matched uncertainties;
2. matched and parameters uncertainties;
3. matched uncertainties and delays;
4. matched, parameters uncertainties and delays.

Matched disturbances are always included, as their rejection is the main advantage of using SMC. They consist of sinusoidal torques which induce an acceleration or a braking phase on each axle, depending on the torque sign. With the purpose of showing the controllers robustness against unmatched disturbances, in Tests 2 and 4 time varying parameter uncertainties on vehicle mass, drag coefficient and road friction coefficient are included. The behavior of all disturbances is shown in Figure 3.2. Results on front and rear axles are almost identical, as the only parametric differences affecting the respective dynamics are the geometric ones introduced in equations (1.1). For this reason, in this section only results on the front axle are shown.

In Tests 3 and 4 delays are introduced on the acquired signals used for control (20 ms) and on the actuation (50 ms). Modeling of the actual delays found on a vehicle would require a far deeper analysis, including studies on sensors, CAN bus and actuators dynamics: nevertheless, assessing the response of the proposed controllers in the presence of a generic delay helps evaluating which SMC is more suitable to be implemented in a real test environment.

Please note that in the ISM design a nominal controller is required to be included, whereas it is not necessary in the other SMCs. The nominal control is the same PI algorithm used in the standalone experiment. All controllers parameters have been tuned in order to obtain an adequate response for each algorithm.

3.4.2 Results

In Figure 3.3 the step response of all considered controllers is shown, when no disturbances or delays are applied. It can be observed that FOSM and ISSOSM have strong oscillations, which vanish too slowly at steady state, or do not vanish at all in case of FOSM. The PI and ISM controllers show the highest overshoot and longest settling time, but nevertheless they converge to the reference value at steady state. It can be observed more in detail in the second graph of Figure 3.3, that the STSM algorithm has slightly higher settling time and lower steady state oscillations.

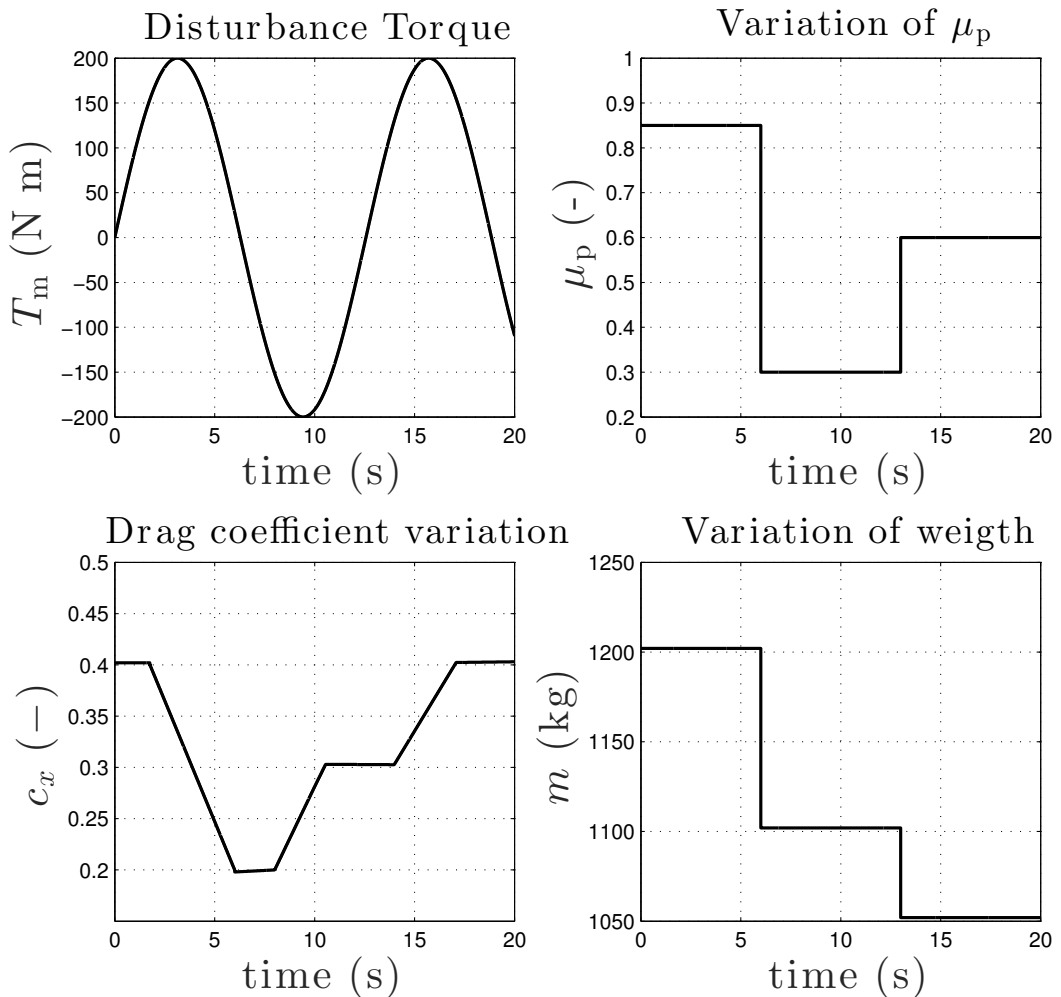


Figure 3.2: Matched disturbance and parametric uncertainties affecting the vehicle model

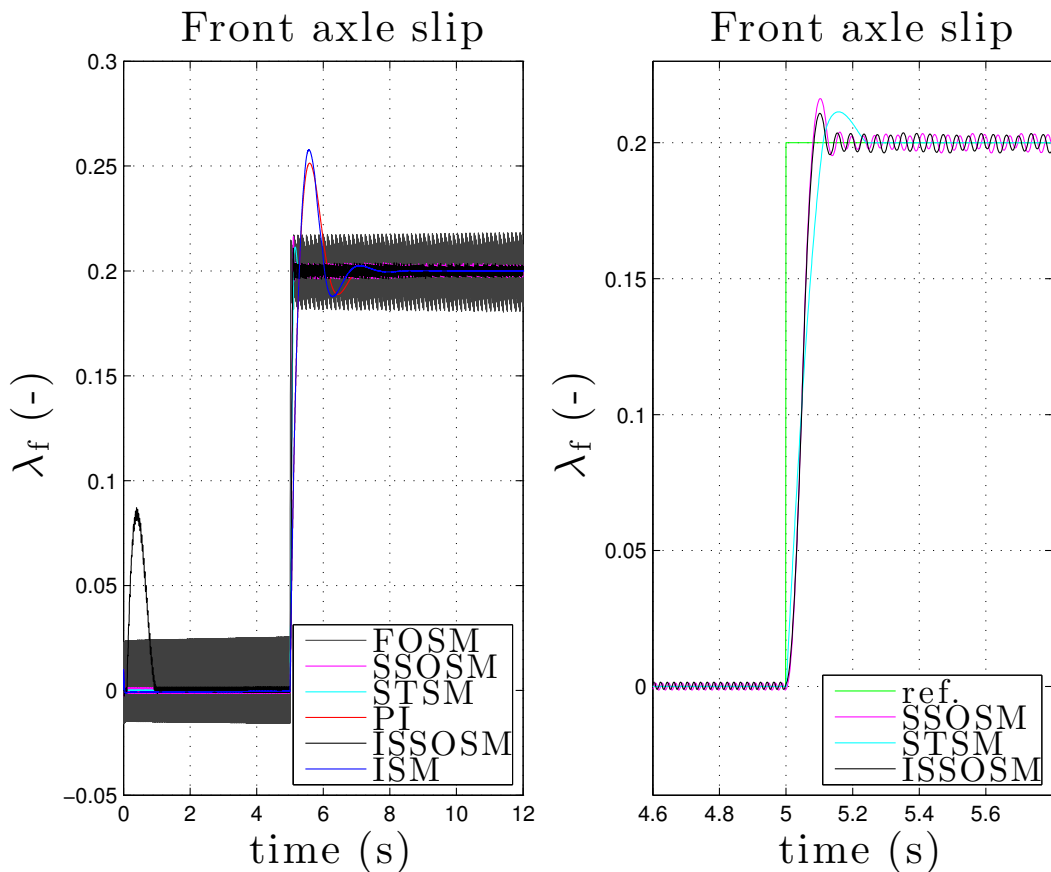


Figure 3.3: Step response of the controllers when disturbances are not present (left), and detail of the step response of the SSOSM, STSM and ISSOSM algorithms (right)

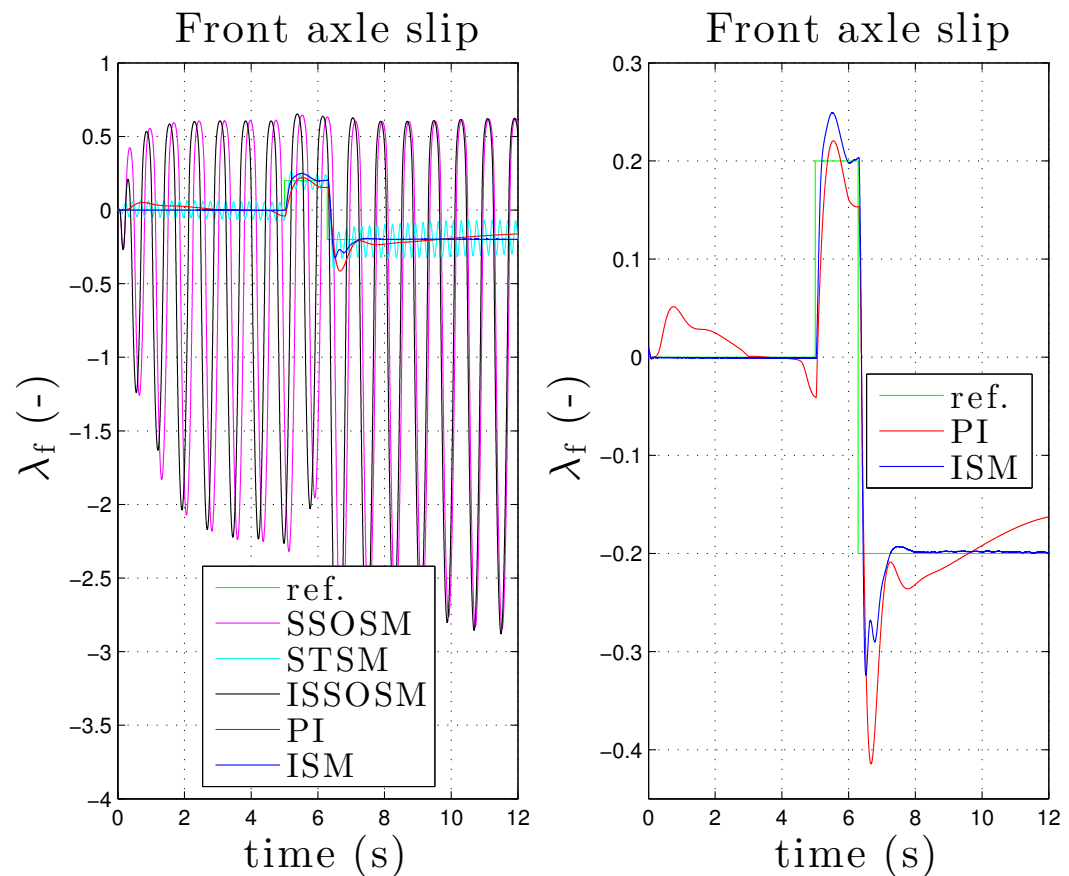


Figure 3.4: Step response of the controllers when all the disturbances are present (left), and detail with only PI and ISM controllers (right)

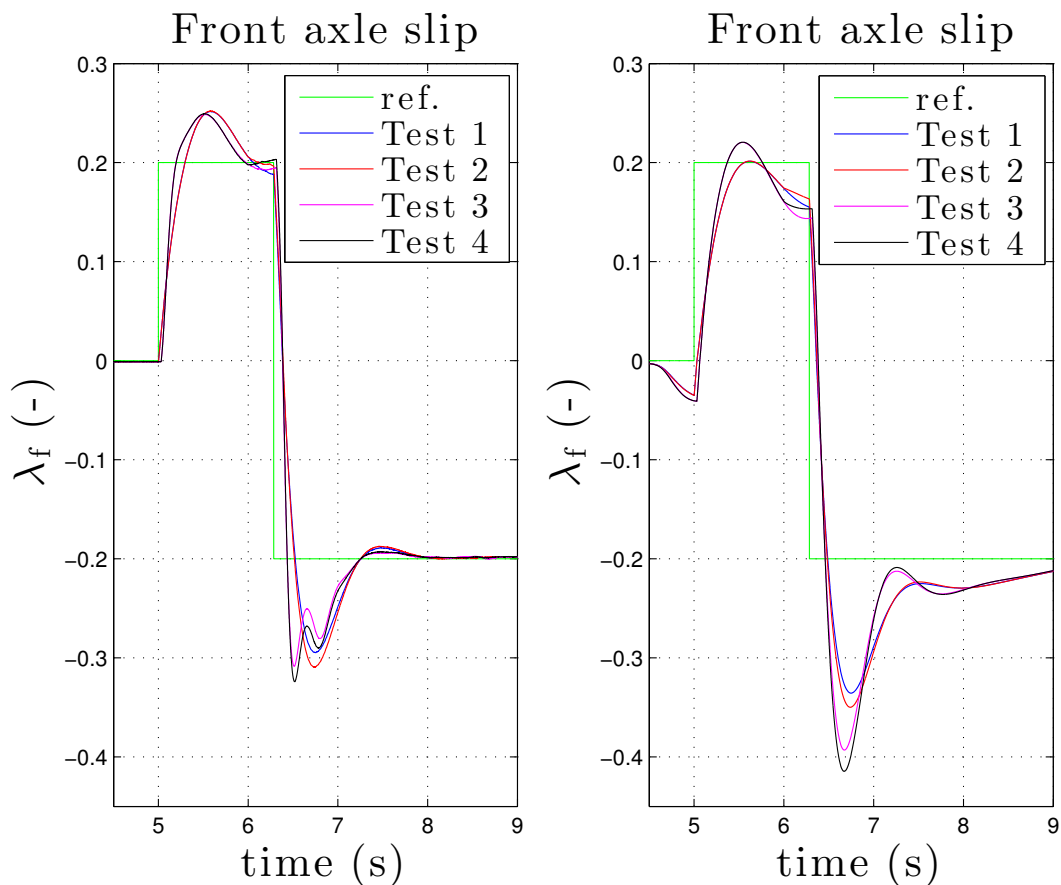


Figure 3.5: Difference in the controller performance in presence of different disturbances combinations when ISM (left) and PI (right) controllers are used

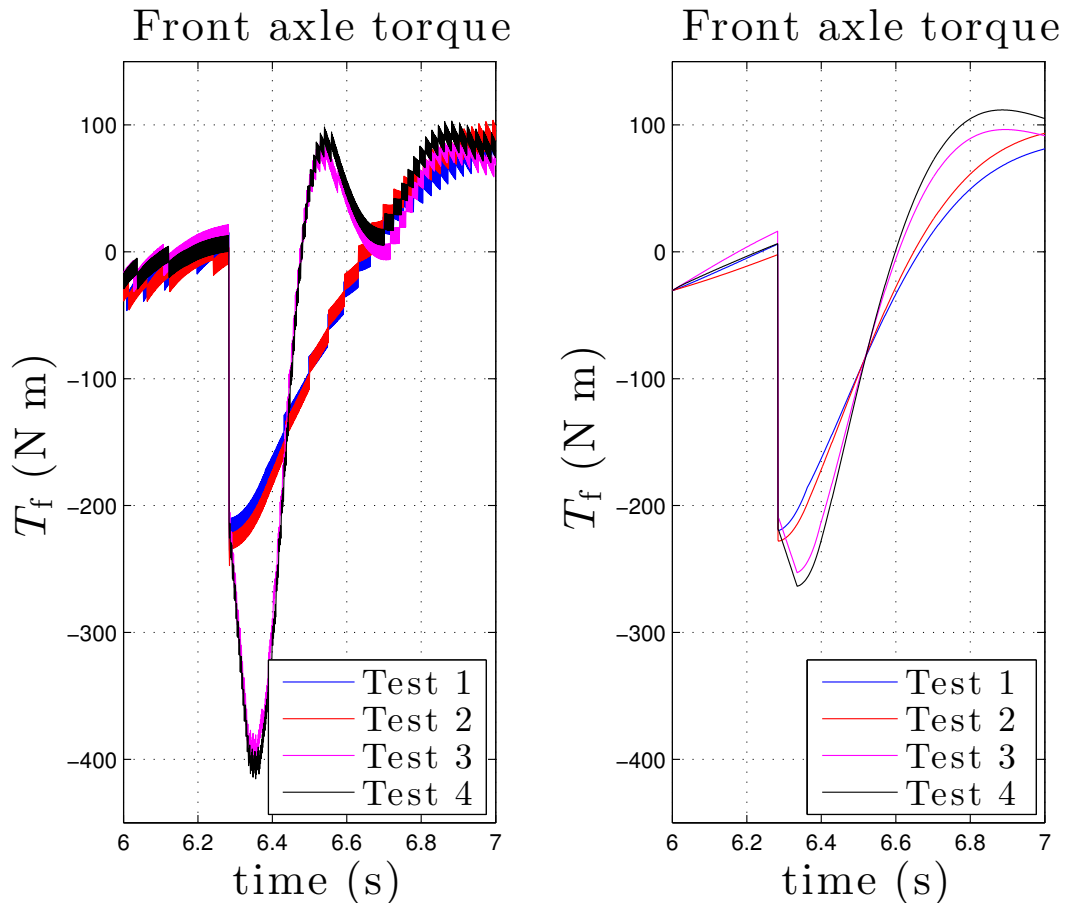


Figure 3.6: Detail of the control signals corresponding to controllers in Figure 3.5. Note that in the tests with delay, the increase of the control action is considerably stronger with the ISM controller

Table 3.1: RMS Error $e_{RMS,\nu}$, $\nu = \{f, r\}$

Test	FOSM	SSOSM	STSM	PI	ISSOSM	ISM
1	0.0217	0.0364	0.0320	0.0534	0.0384	0.0456
	0.0215	0.0359	0.0319	0.0540	0.0380	0.0464
2	0.0216	0.0365	0.0323	0.0553	0.0383	0.0477
	0.0221	0.0357	0.0322	0.0554	0.0382	0.0478
3	0.3562	1.3307	0.0740	0.0654	1.3496	0.0535
	0.3584	1.4793	0.0750	0.0665	1.4089	0.0544
4	0.3506	1.3731	0.0716	0.0680	1.3960	0.0554
	0.3520	1.4131	0.0726	0.0683	1.3748	0.0557

In Figure 3.4 the same controllers are evaluated against disturbances and delays, except for FOSM and ISSOSM, whose behavior was found to be unsatisfactory, even with no disturbances. SOSM and ISSOSM, although not unstable, show oscillations induced by the delays which cannot be accepted: the high gain in the SMC reduces the robustness to delays, the same way increasing the gain in a linear system reduces the phase margin. The STSM algorithm shows a better response, yet the chattering induced by the delay exceeds the 50% of the target wheel-slip value. The best performance is the one guaranteed by the PI and ISM controllers, which are shown in detail in the second graph of Figure 3.4. While the conventional controller, even with a strong integral action, struggles to bring the steady state error to zero, the ISM neutralizes the effect of the matched disturbances, thanks to its discontinuous control action, without increasing the overall system bandwidth. The ISM shows a better step response than the PI both in the transient and at steady state, with faster response, reduced overshoot and steady state convergence.

In Figure 3.5 the effect of the different disturbances and delays when the PI and ISM controllers are applied is shown. It can be seen that on both controllers parameter uncertainties have a minor impact compared to the matched uncertainties, as it is confirmed by the Root Mean Square (RMS) error values in Table 3.1 (e_{RMS}). Moreover, Table 3.2 reports the values of the control effort, E_c , for all controllers.

The delay, on the other hand, has a significant impact: in the PI controlled system it increases the overshoot, while in the ISM case the delay makes the response even faster, with no overshoot increase. This effect is due to the increased control action (see Figure 3.6) induced by the nonlinear control, which is up to the 68% of the original value, compared to the increment of only the 15% with the conventional controller.

A graphic rendering of the performance indices in case of STSM, PI and ISM controllers, which are the best ones in presence of delays, is reported in Figure 3.7.

3.4.3 Controllers Evaluation

The performance indices reported in Tables 3.1 and 3.2 help us assessing the different controllers considered in this thesis.

The FOSM control is the most aggressive solution: it ensures the minimum e_{RMS} in all the considered conditions, while at the same time it has a control signal RMS

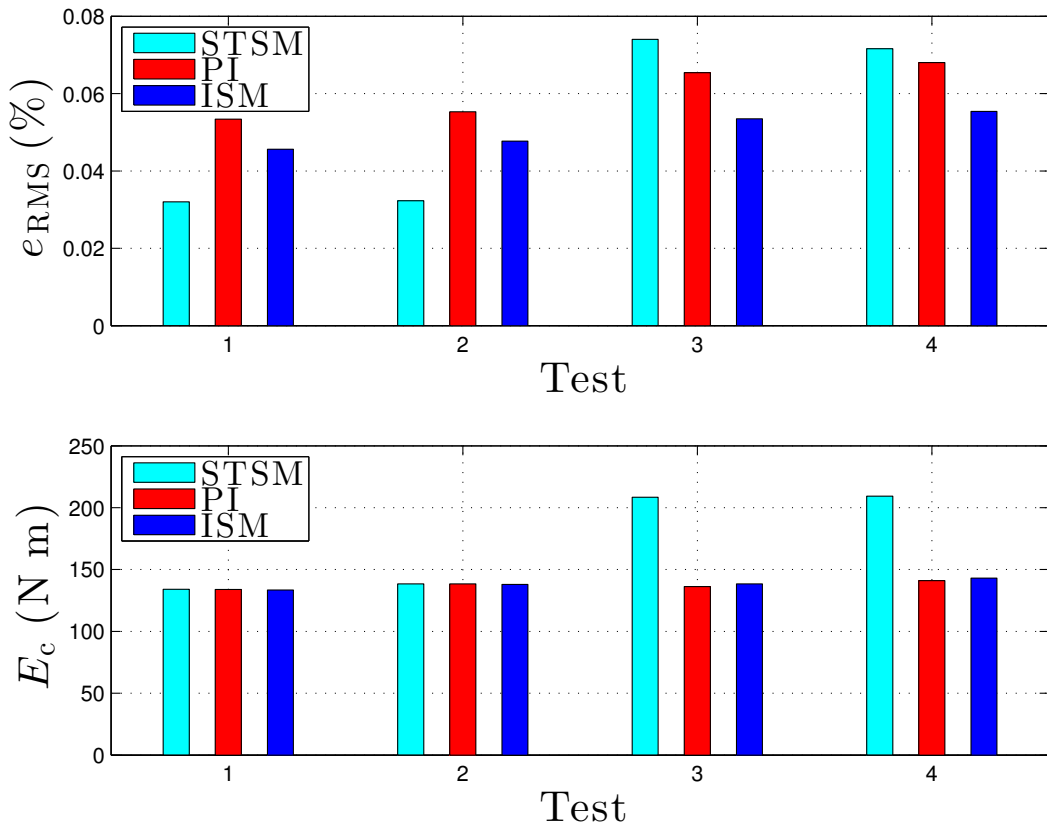


Figure 3.7: Perfomance indices representation for controllers STSM, PI and ISM

Table 3.2: RMS value of Control Signal $E_{c,\nu}$, $\nu = \{f, r\}$

Test	FOSM	SSOSM	STSM	PI	ISSOSM	ISM
1	1300	146.1	134.0	133.9	146.0	133.4
	1300	150.4	138.5	138.2	150.3	137.1
2	1300	150.8	138.4	138.4	150.8	138.0
	1300	153.4	141.0	140.9	153.5	140.0
3	1300	1070.9	208.5	136.2	1073.4	138.4
	1300	1123.4	211.8	140.7	1092.0	142.4
4	1300	1088.8	209.3	141.0	1095.1	143.1
	1300	1112.6	211.2	143.6	1094.5	145.1

E_c which is larger than those of all other controllers by one order of magnitude. This fact makes such a controller a non feasible solution, once the actuators limitations and dynamics are taken into account.

As verified in simulation, when delays are not present, the SMC controllers are able to reject the matched uncertainties affecting the system and they result sufficiently insensitive even to parameters variations (unmatched disturbances). More specifically, by construction, the ISSOSM and the ISM controllers are robust from the initial time instant. The second order algorithms have the smallest e_{RMS} of the remaining controllers, when considering tests with no delay. Their respective control signal RMS values E_c are comparable to the ones of the PI and ISM controllers.

When the delays are introduced, the SSOSM and the ISSOSM are no more acceptable. In fact, both the algorithms are based on the presence of a peak detector to find the extremal values of the sliding variable. This device is implemented in a discrete time way by comparing the signals in subsequent time instants. This implies that the extremal values in presence of delays are corrupted, causing an oscillatory behavior which can be critical for the considered system. The STSM does not include a peak detection, so that the deterioration of the performance is not as sharp.

The best performance in the presence of delays is guaranteed by the ISM controller. In this case, while the discontinuous component is able to reject the matched uncertainties affecting the system, the nominal component (see Figure 3.1, second scheme) is robust enough in front of delays, since it has the effect of reducing the bandwidth of the equivalent controlled system, thus increasing its phase margin. On top of this expected behavior, the discontinuous action appears to positively impact the system response in the presence of delays, which is particularly evident in Figure 3.6.

3.5 Conclusions

In this chapter, the assessment of sliding mode control algorithms for wheel slip control of road vehicles has been presented. In particular, this work focuses on the impact of uncertainties and delays on the different controllers. While the first order sliding mode algorithm has comparable results with and without delay, due to its aggressive nature it is not suited for being utilized in this context. The second order sliding mode algorithms are characterized by excellent performances in presence of disturbances, which deteriorate in presence of delays. The proposed ISM controller offers the most encouraging results, which allows us to conclude, at the best of our knowledge, that this kind of controller can be a good candidate for application to a real vehicle.

Chapter 4

Simulation results

In this chapter the obtained simulation results will be described. The vehicles taken into account in simulation are the same, and the parameters of each vehicle are shown in tables 4.1, 4.2, 4.3 and 4.4

Parameter	Value
g	9.81 m/s^2
m	1202 kg
J_f	1.07 kgm^2
J_r	1.07 kgm^2
C_x	0.4
f_{roll}	0.013
r_f	0.32 m
r_r	0.32 m
l_f	1.15 m
l_r	1.45 m
l_h	0.65 m
$v_x(0)$	30 m/s
$\lambda_f(0)$	0.01
$\lambda_r(0)$	0.01

Table 4.1: vehicle parameters

Parameter	Value
Longitudinal controll Gain	1
Front Slip controll Gain	2000
Rear Slip controll Gain	2000

Table 4.2: Control parameters for the first follower

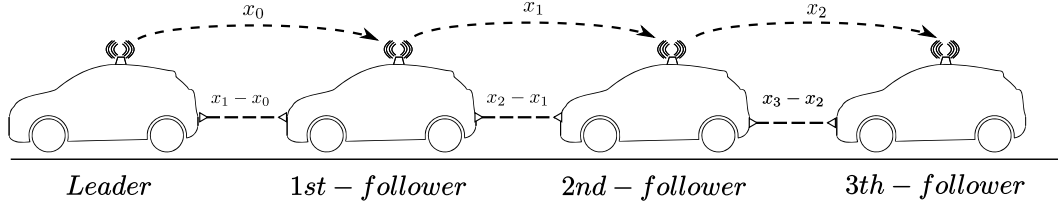


Figure 4.1: Vehicles Platooning

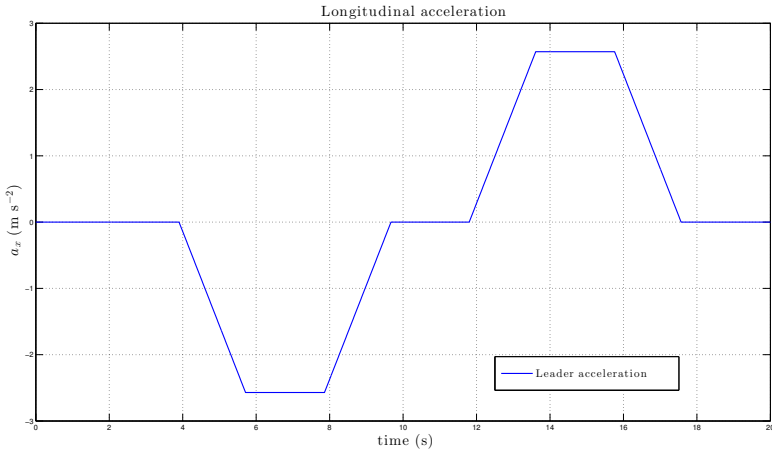


Figure 4.2: Leader acceleration

4.1 Discussion

All vehicles have an initial velocity of 30 m/s . The distances between the vehicles at the initial instant is 7m . As for the acceleration of the leader, the profile is the one shown in Figure 4.2. The parameter for the road condition μ_p is equal 0.85 (dry conditions). The parameters of the safety distance according to (2.19) are $S_{d_0} = 2\text{m}$ and $h = 0.3\text{s}$. In our study, we consider three follower vehicle and one leader (see the Figure 4.1). Under this assumption, the results are illustrated and discussed in the following.

From figure 4.3 we notice the action of the outer loop controller. In Figure 4.20, in agreement with the theory discussed in the previous chapter, the controller acts on derivative of the acceleration and this alleviates the so-called chattering phenomenon. Therefore, the acceleration is given by the integral of the control variable, obtaining a more smooth shape. This can be notice also in Figure 4.4, where the velocity is illustrated and the trends is similar for all the vehicles without oscillation due to the chattering. Moreover, from Figure 4.4, we can see that after a setting time, the speed profiles that vehicles follow are exactly equal to that of the leader. This allow the correct travel of the vehicle, avoiding possible collisions. From Figure 4.5, we can see the run distance that the vehicles have traveled during the simulation. Furthermore we note that vehicles never collide, in fact the distances traveled by individual vehicles never intersect. In Figure 4.6 the evolution of the distance between

Parameter	Value
Longitudinal controll Gain	4
Front Slip controll Gain	7000
Rear Slip controll Gain	7000

Table 4.3: Control parameters for the second follower

Parameter	Value
Longitudinal controll Gain	7
Front Slip controll Gain	10000
Rear Slip controll Gain	10000

Table 4.4: Control parameters for the third follower

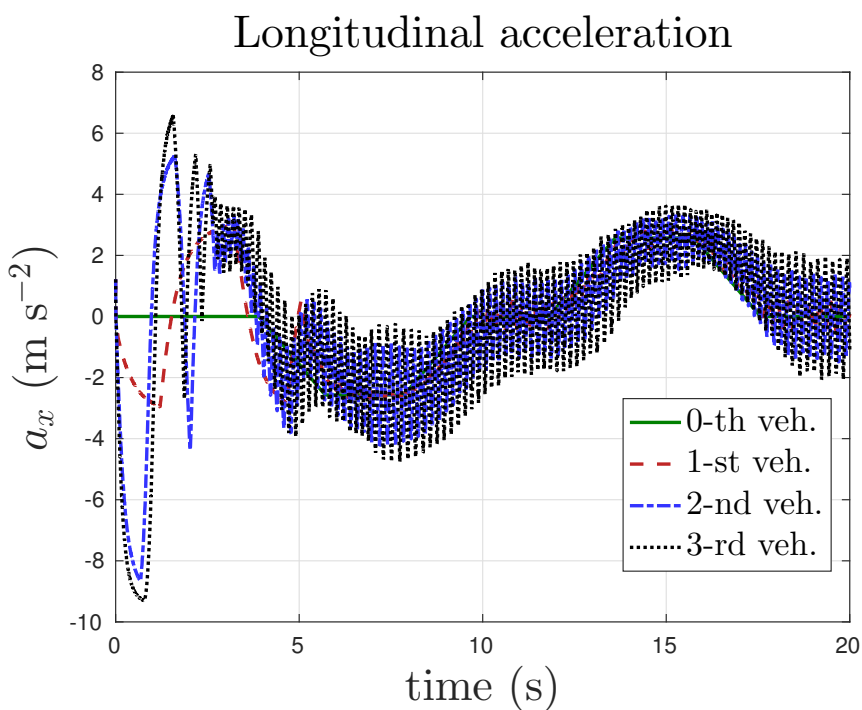


Figure 4.3: Longitudinal acceleration

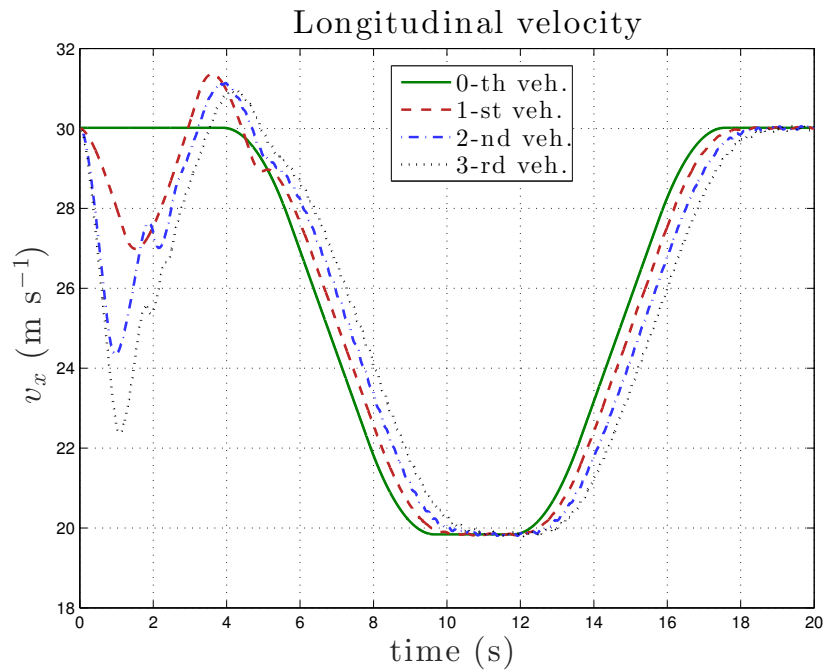


Figure 4.4: Longitudinal velocity

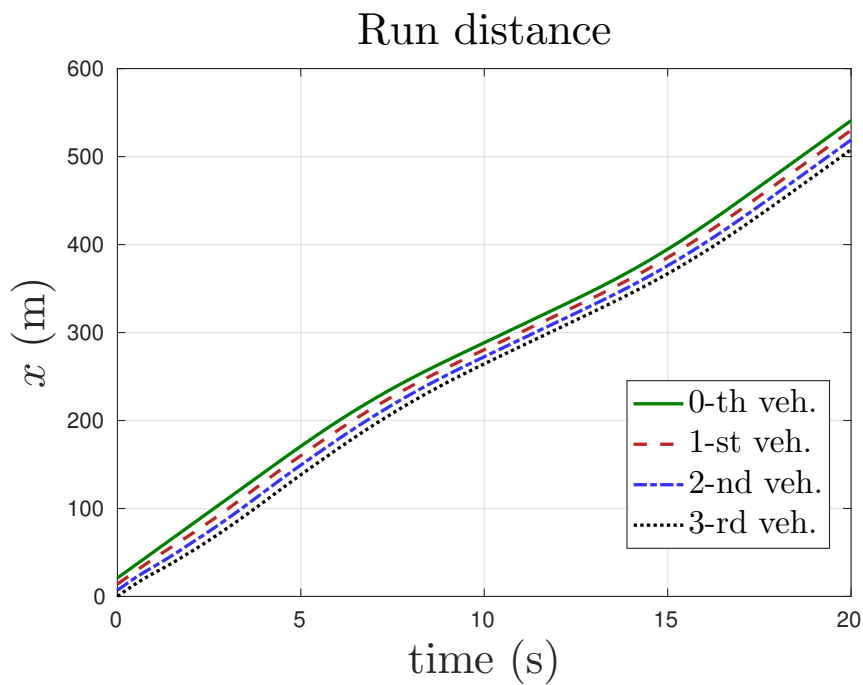


Figure 4.5: Run distance

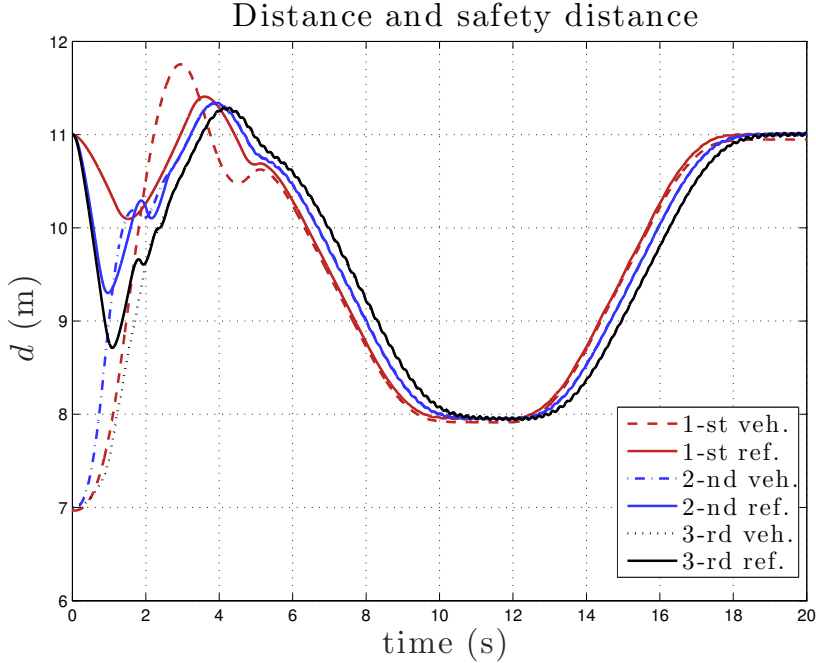


Figure 4.6: Distance and safety distance

vehicles is illustrated, and it is possible to see that the safety distance is reached in finite time and maintained for all simulation. In particular, the safety distance between the leader and the first vehicle is reached after 5 s, while the safety distance between the first and the second vehicle is reached after 3 s as well as the safety distance between the second and the third vehicle. This is due to the different gain values of the controllers set to cope with the error propagation. From figure 4.7, 4.8 we can see as the outer controller acts on the traction forces to follow the safety distance reference. According to the described control scheme, the forces generated by the integral action depend on the outer control variable. In Figures 4.9, 4.10 one can see that also for rear/front velocity, after a first moment the speed have the same shape.

The longitudinal dynamics is controlled by the slip ratio controller. From Figure 4.11 and 4.12, according to (1.7), we can see the evolutions over the time of the front/rear slip ratio. The outer loop, by acting on the acceleration derivative of the vehicles, generates the reference of slip ratio for the inner loop. In Figure 4.11, 4.12 we can see that the references of slip are reached and maintained in a finite time for all vehicles. The sliding variable for inner loop reaches the sliding manifold in finite time, i.e., $s_f = s_r = 0$. This shown in Figures 4.13 and 4.14. The front sliding variable of the first vehicle reaches the manifold in 0.2 s, while those of the second and third vehicle in 0.19 s. In Figure 4.16, 4.15 one can see the integral of the control variable of inner loop. In fact, according to (2.42) the inner controller acts on the derivative of the torque to follow the slip references. According to equations (1.34), one obtains the results shown in Figure 4.17, 4.18. As for the outer sliding variables, one can note that the sliding variables of the third and second vehicle

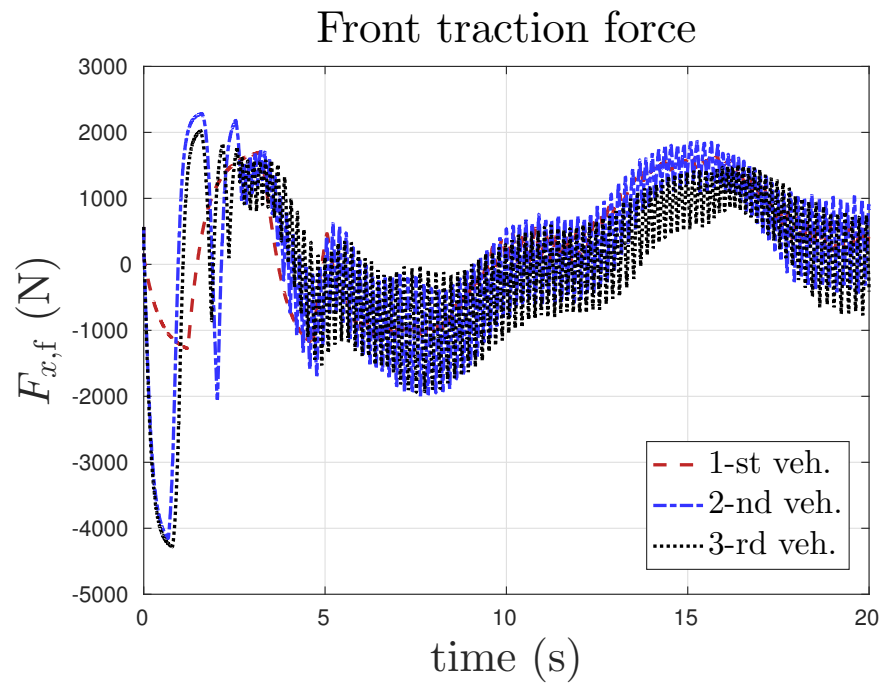


Figure 4.7: Front traction force

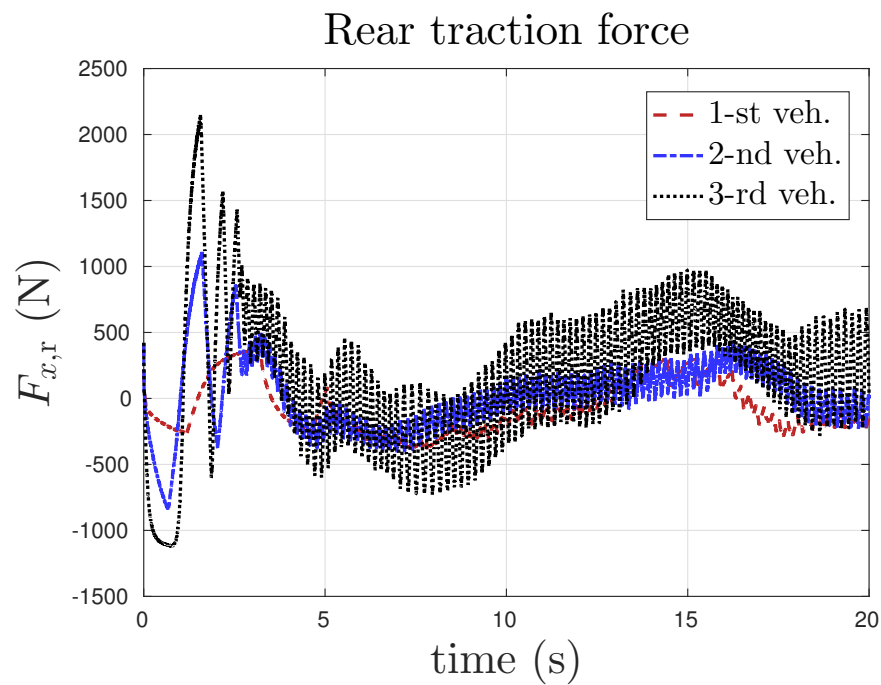


Figure 4.8: Rear traction force

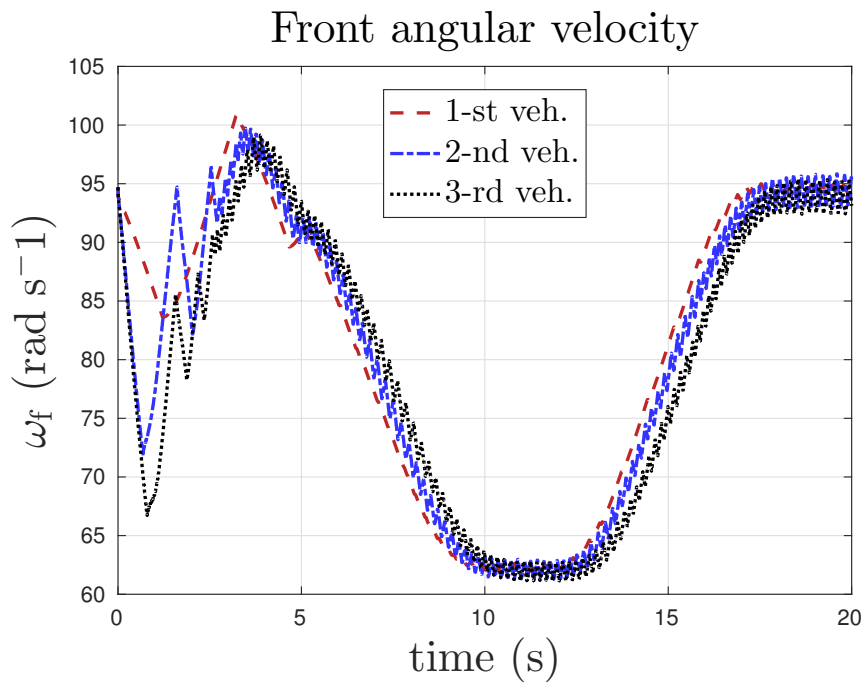


Figure 4.9: Front angular velocity

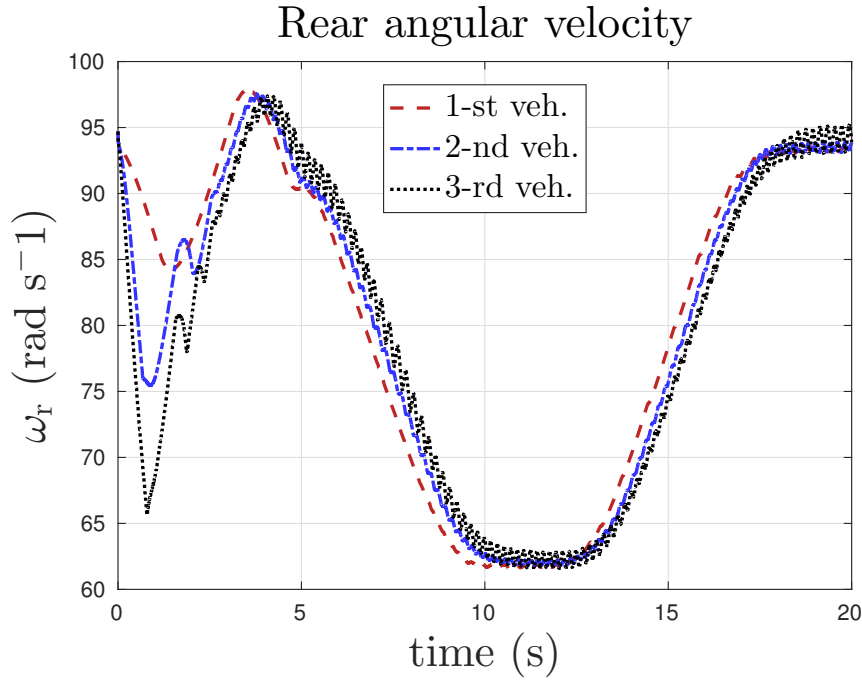


Figure 4.10: Rear angular velocity

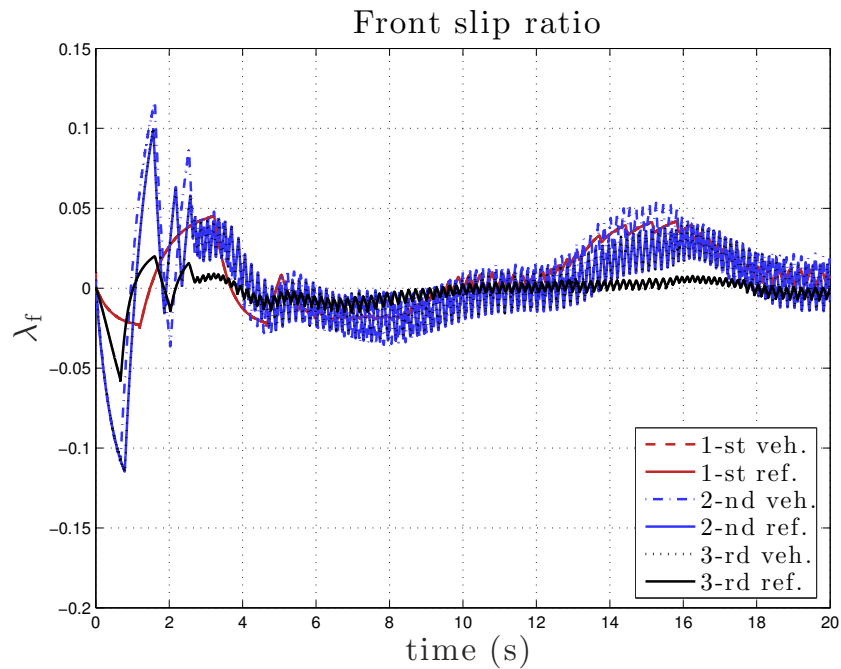


Figure 4.11: Front slip ratio

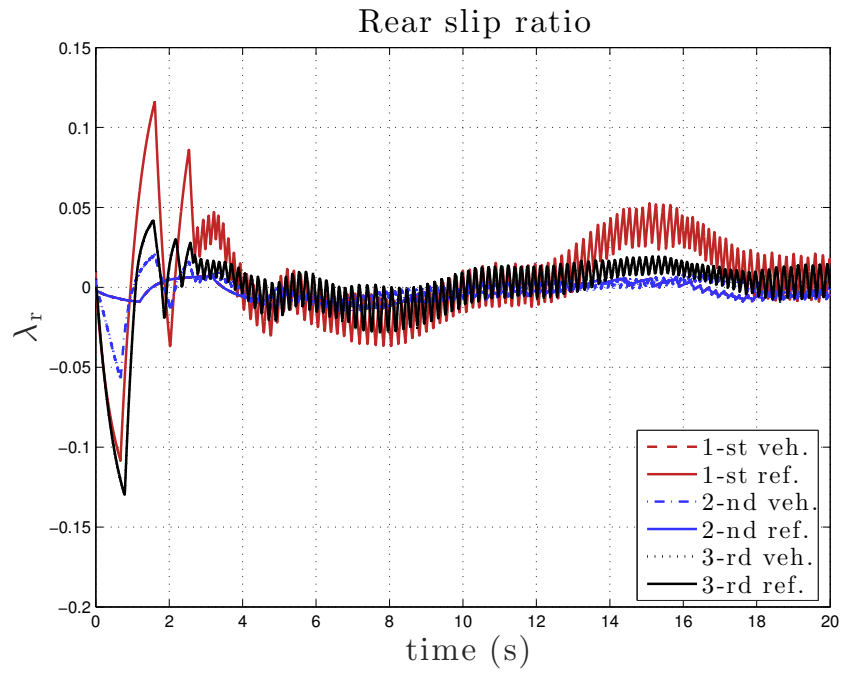


Figure 4.12: Rear slip ratio

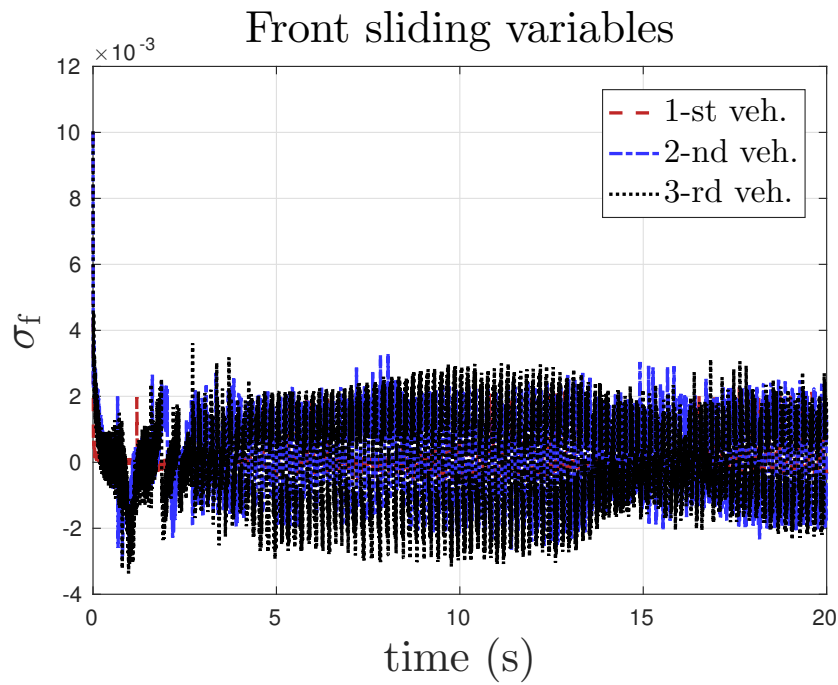


Figure 4.13: Front sliding variables

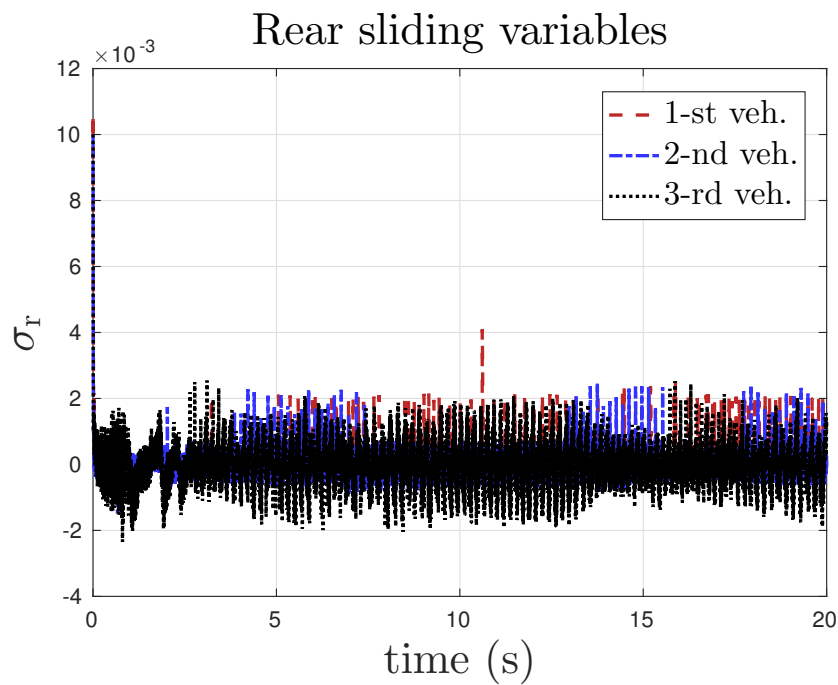


Figure 4.14: Rear sliding variables

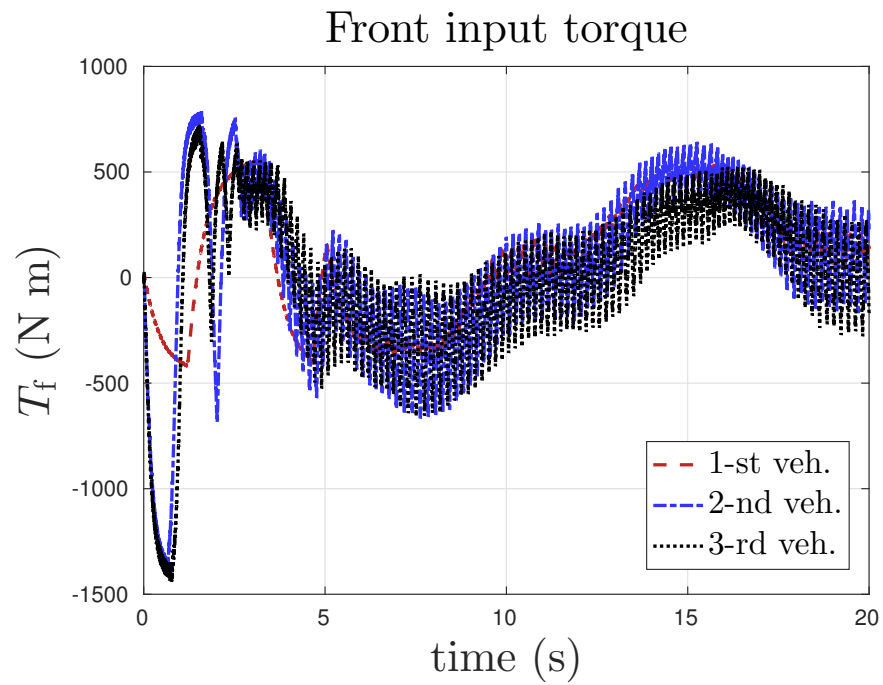


Figure 4.15: Front input torque

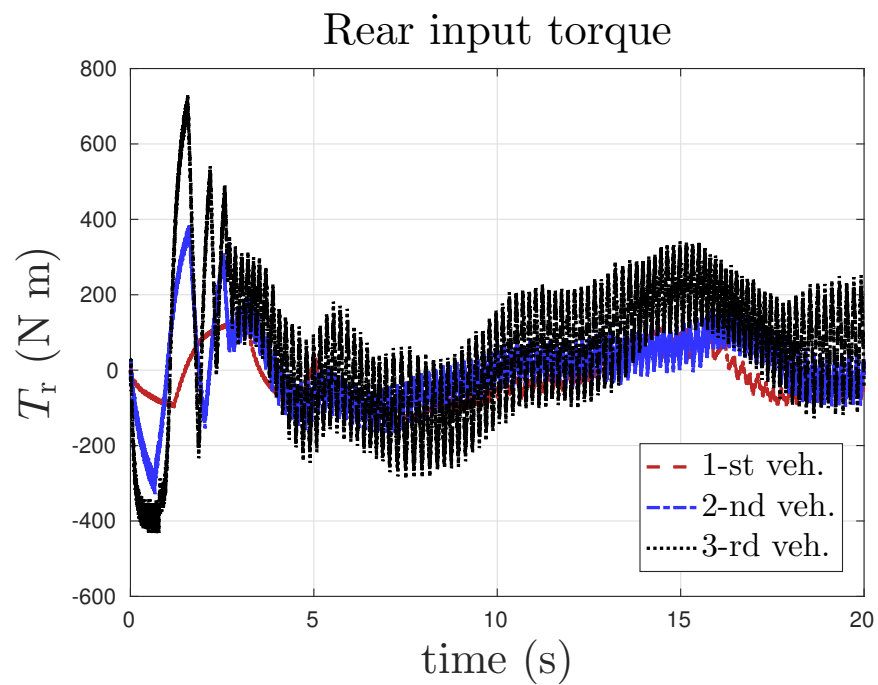


Figure 4.16: Rear input torque

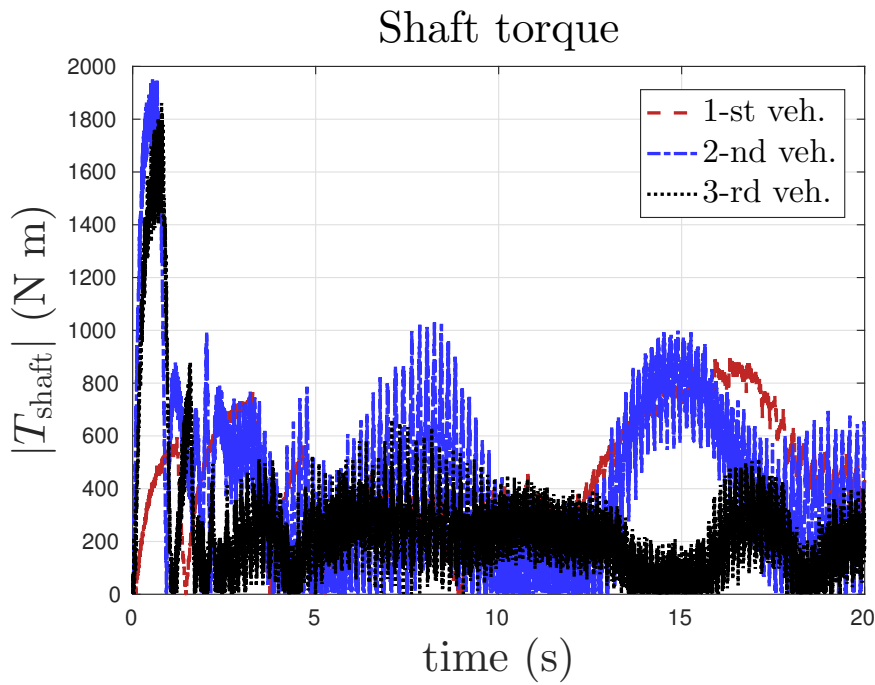


Figure 4.17: Shaft torque

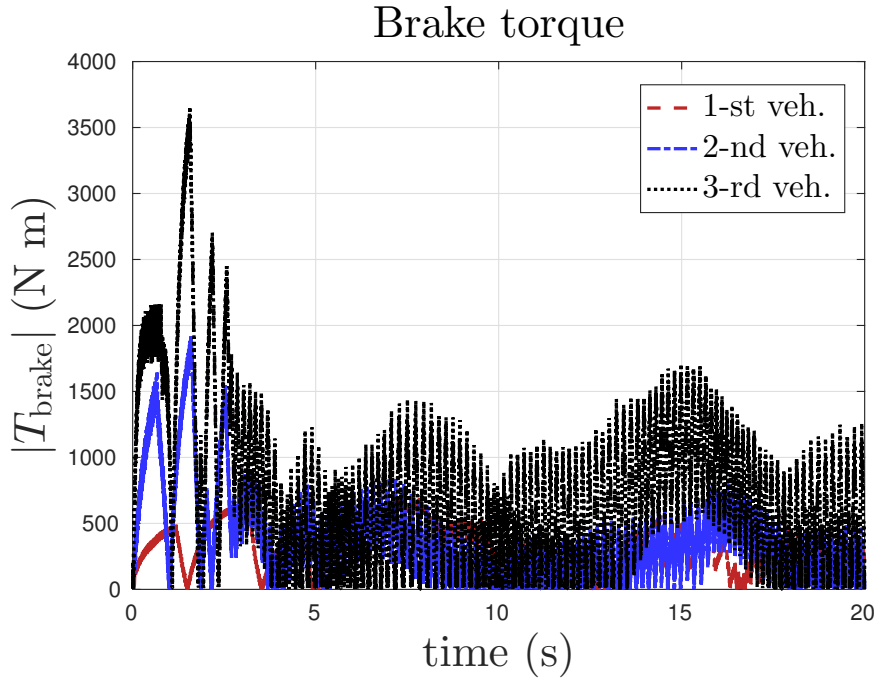


Figure 4.18: Brake torque

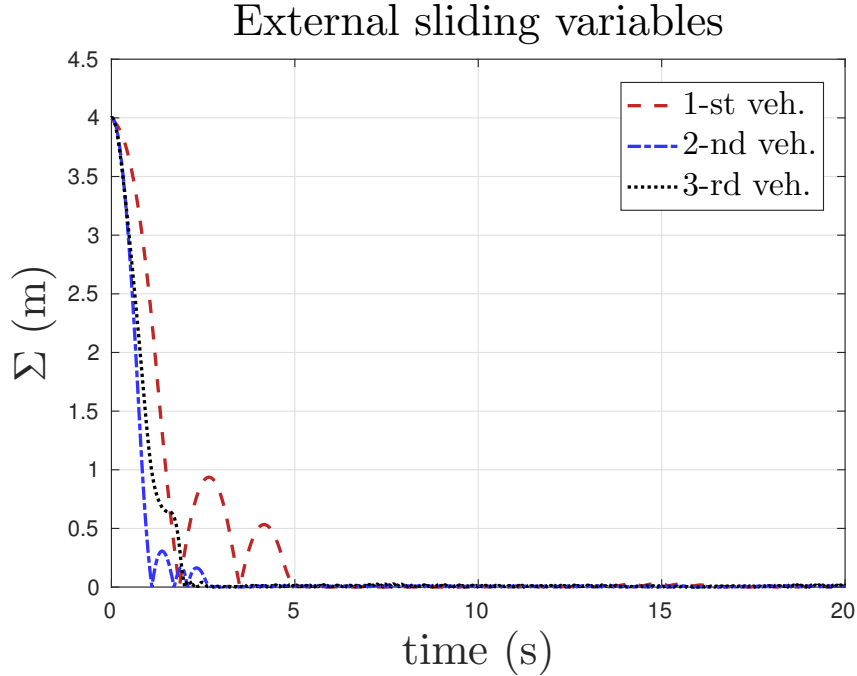


Figure 4.19: External sliding variables

reach the manifold in 3 s, while the sliding variable for the first vehicle is steered to zero in 5 s. As one can see the dynamics of the sliding variables are similar. The small differences are due to different values of gains for the controllers. In Figure 4.20 we can see the dynamics of the outer control variable. Furthermore one can note that the control variable is not perfectly smooth. In fact, we have used a low pass filter, with a bandwidth $\omega_{cut} = 0.0628[\text{rad}/\text{s}]$, instead of an integrator, because of non-modeled dynamics that can increase the effective relative degree of the system.

The fuel consumption of the vehicles is shown in Figure 4.21. We can notice that the shape depends by the value of T_{shaft} , ω_f . Thus, when the shaft torque (see Figure 4.17) and the front angular wheel velocity (see Figure 4.9) are biggest, consequently the fuel consumptions are biggest and viceversa. The evolution of the drag coefficient, according to [27], for follower vehicle is shown in Figure 4.22. One can see that it is variable according to the follower (Figure 1.5). In fact if the distance between the considered vehicles increase (see Figure 4.6), the coefficient of drag will increase because the vehicle less uses the wake effect of the previous vehicle.

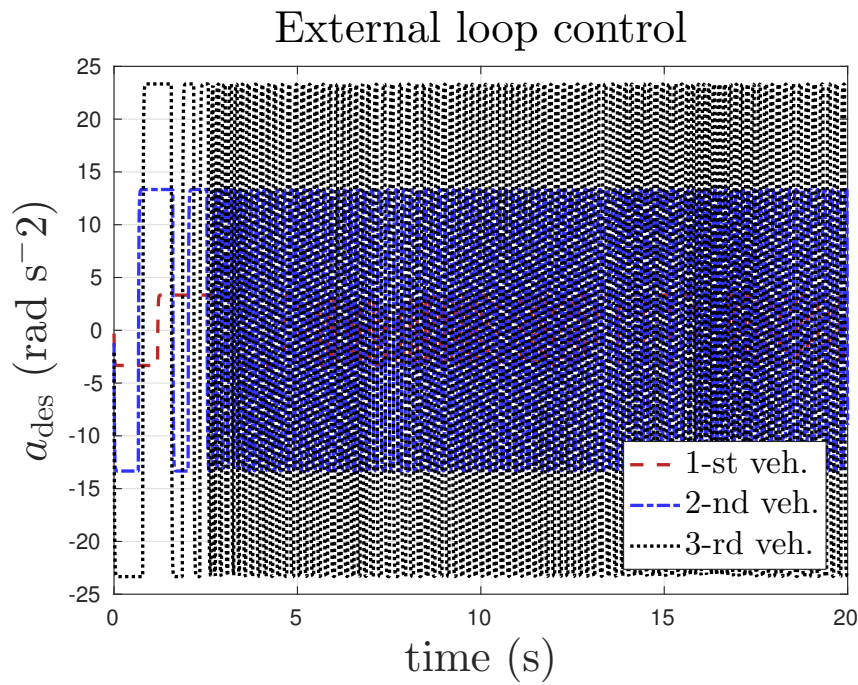


Figure 4.20: External loop control

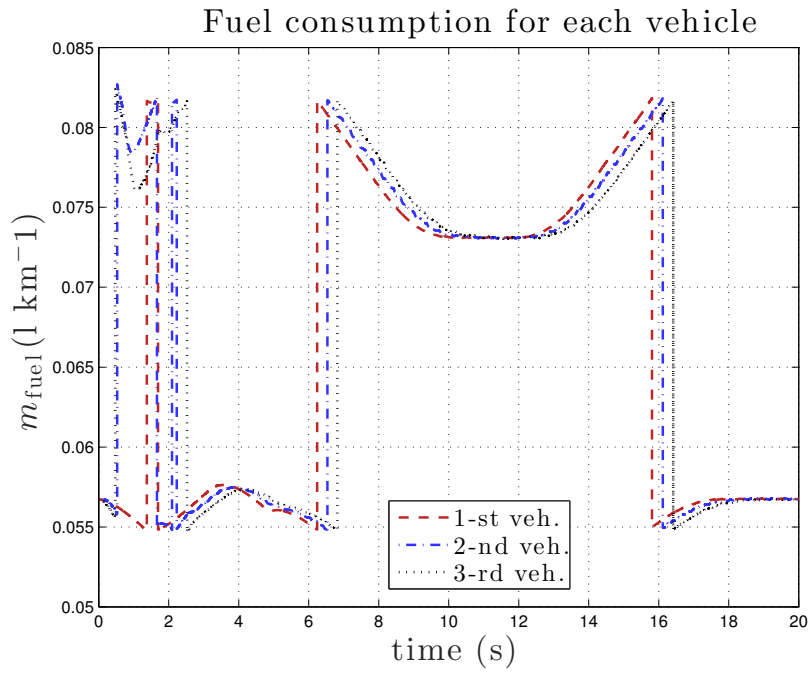


Figure 4.21: Fuel consumption vehicles

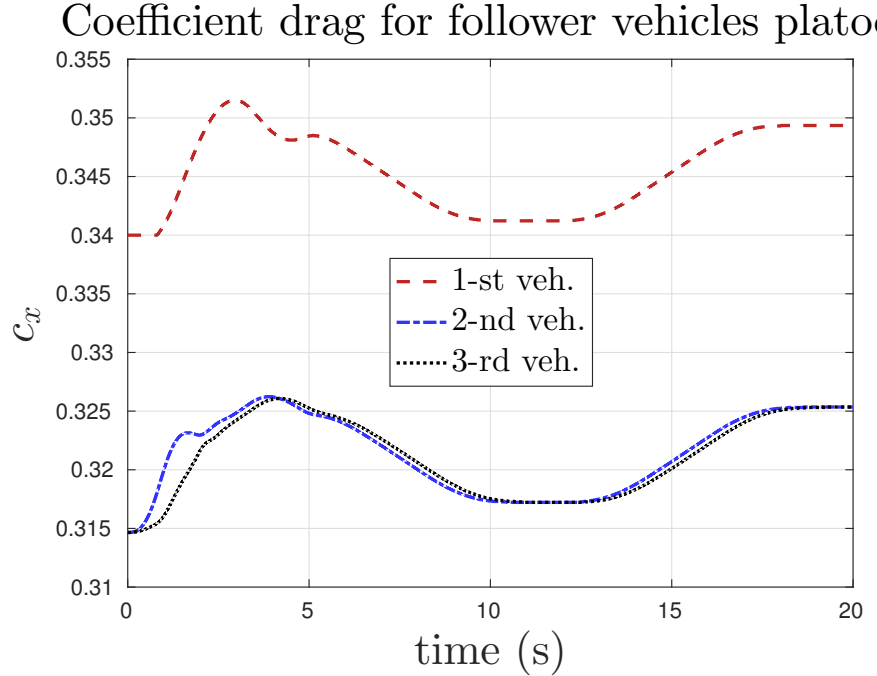


Figure 4.22: Drag coefficient for follower vehicles platoon

Variable	RMS Value
Outer sliding variable first vehicle	0.8720
Outer sliding variable second vehicle	0.6332
Outer sliding variable third vehicle	0.6835
Inner front sliding variable first vehicle	0.0004
Inner front sliding variable first vehicle	0.0013
Inner front sliding variable first vehicle	0.0014
Inner rear sliding variable first vehicle	0.0005
Inner rear sliding variable first vehicle	0.0004
Inner rear sliding variable first vehicle	0.0007
Front Torque first vehicle	311.5616
Front Torque first vehicle	405.1120
Front Torque first vehicle	384.7322
Rear Torque first vehicle	72.9965
Rear Torque first vehicle	97.8972
Rear Torque first vehicle	191.7245

From the last table we can see the root mean square (RMS) values for the action of the controller T_{f_i} T_{r_i} . The different values are due to different gains for the controllers. Therefore, we can see the RMS for the outer and inner loop, and one can note that for inner loop the value of the RMS increases. The cause is the error propagation that typically affects the control of a vehicles platoon.

Chapter 5

Conclusions

In my thesis I have dealt with the control of the longitudinal dynamic. After careful analysis of the state of art, the main activity has been to derive a model for the longitudinal dynamic control of the vehicle taking into account the typical parameter variations encountered under actual working conditions:

- variation of the vehicle mass m_i in order to simulate both the decrease of the fuel and the variation of the number of passengers;
- changes in the aerodynamic drag coefficient C_{drag} to simulate the conditions of platooning;
- variation of the tire/road adhesion coefficient μ_p to simulate the variation of the street conditions (as particular case we have considered the conditions of dry, wet and snow);
- introduced a delay to simulate the transmission of data and the execution of commands on the part of the actuators.

This model was joined with a model for the estimation of the vehicle's fuel consumption and the first objective was to design a first control loop for the regulation of the slip ratio. The longitudinal dynamic control of the vehicle is based on the wheel slip control because the traction forces are dependent from the wheel slip ratio and then by controlling the slip it is possible to obtain the desired traction force and thus control the vehicle dynamics. In particular, advanced algorithms have been studied, in particular of sliding mode type. The stability properties have been analyzed, and recently appeared control law have been applied for the first time in this context. After simulating the real working conditions, which may be all or only some of those previously listed. Sliding mode algorithms in general are quite efficient in case of systems affected by hard uncertainties. In particular it was noted that as long as the delay is not introduced, all the algorithms work well, but when we consider also the delay only ISM is able to follow the reference signal. Since we decided not to introduce the delay to study the problem of platoon, we decided, for the first control loop, to use a SOSM control methodology, because it is robustness against disturbances, model inaccuracies, and parameter variation in addition to the main advantage over FOSM that generates a continuous control action, that allows attenuating chattering phenomenon and thus limiting the stress on the actuator.

The second part of the thesis was devoted to the study of the problem of vehicle platooning. We have therefore extended our model to more vehicles (from 2 until 4 vehicles) in the platoon with the aim of regulating their mutual distance in accordance with the safety distance. Furthermore we have modeled the fuel consumption also in the case where the vehicles are traveling in platooning. In fact, the vehicles traveling in the platoon have lower aerodynamic resistance coefficient and therefore a lower fuel consumption. To do this it has been implemented an algorithm that provides the C_{drag} value as a function of the distance between the vehicles and of their number to evaluate the possible savings fuel. Even in this case, after evaluating the properties of the model it was applied a sliding mode algorithm with excellent results. The final control system designed is constituted by two rings, the outer one, made to solve the problem of platooning, while the inner one has the task of acting, through torques wheels T_f and T_r , to reach the references of slip ratio generated by outer loop.

5.1 Future Work

The results obtained with the control scheme for the platooning is nothing more than a starting point for possible future developments. In particular, it would be interesting reframe the model of the platooning found in a motorway context, and through the control of platoon, reduce fuel consumption / energy and improve the traffic conditions considering the recent results in this field for automatic control. Leverage platooning could increase the capacity of the road, and it would be interesting to understand how to reduce vehicle journey time avoiding any possible traffic jams. The reduction of fuel / energy and pollutant emissions and the possible reduction of travel time, with the growing capacity of the road, are important and very interesting topic in the recent research aim at improving the quality of life.

Appendix A

Simulink Control Scheme

Slip Control for Vehicles Platooning
Mosca, Incremona, Ferrara, Apr. 2016

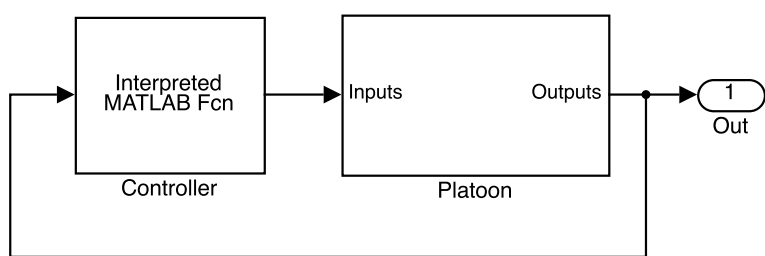


Figure A.1: Slip Control for Vehicles Platooning

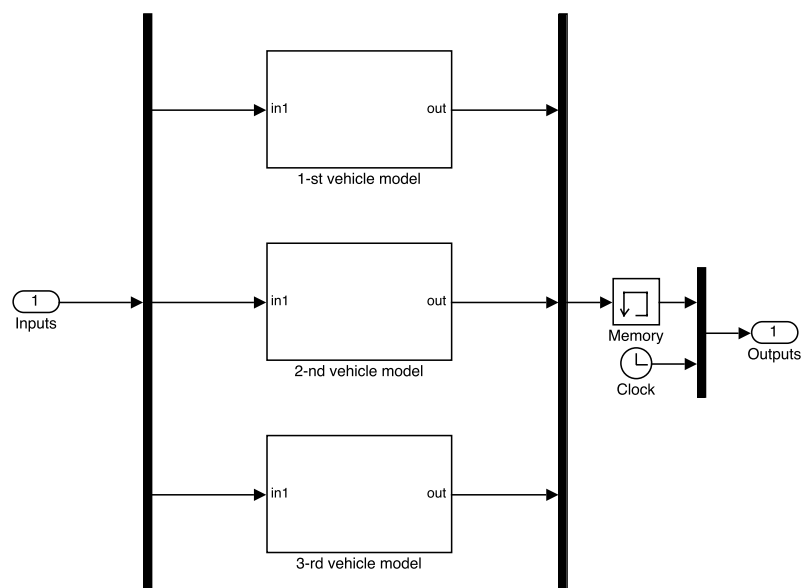
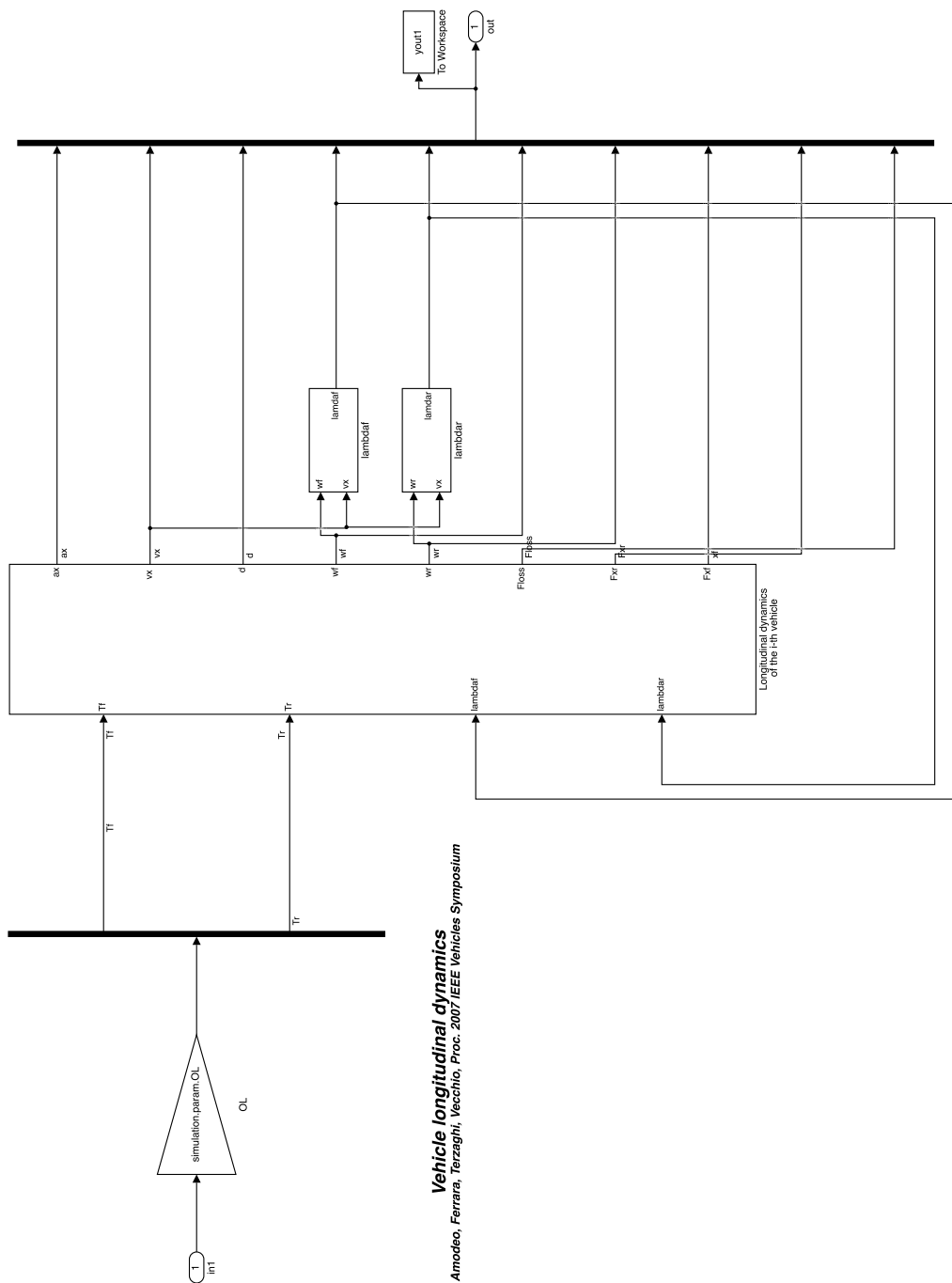


Figure A.2: Platoon



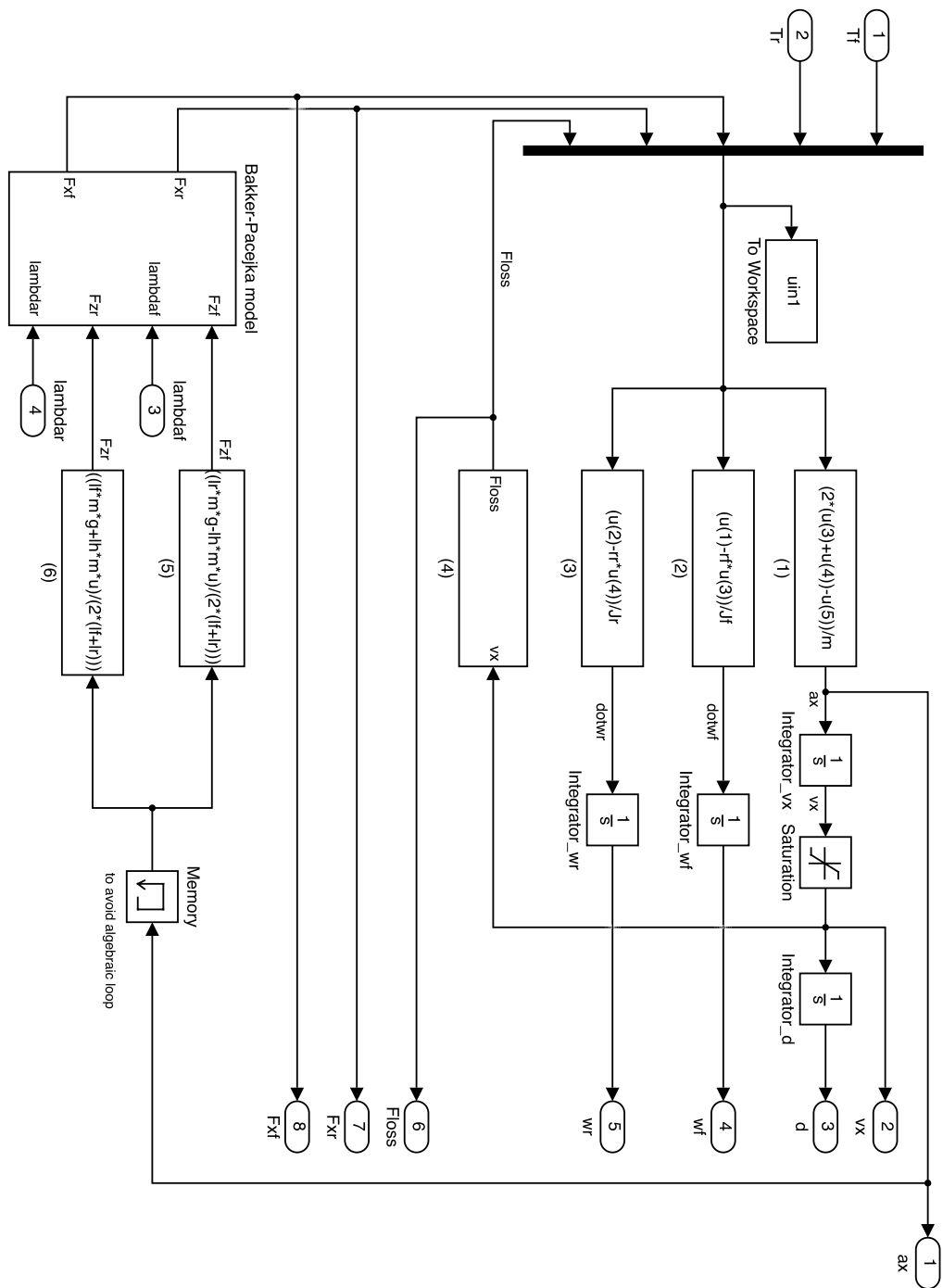


Figure A.4: Vehicle longitudinal dynamics

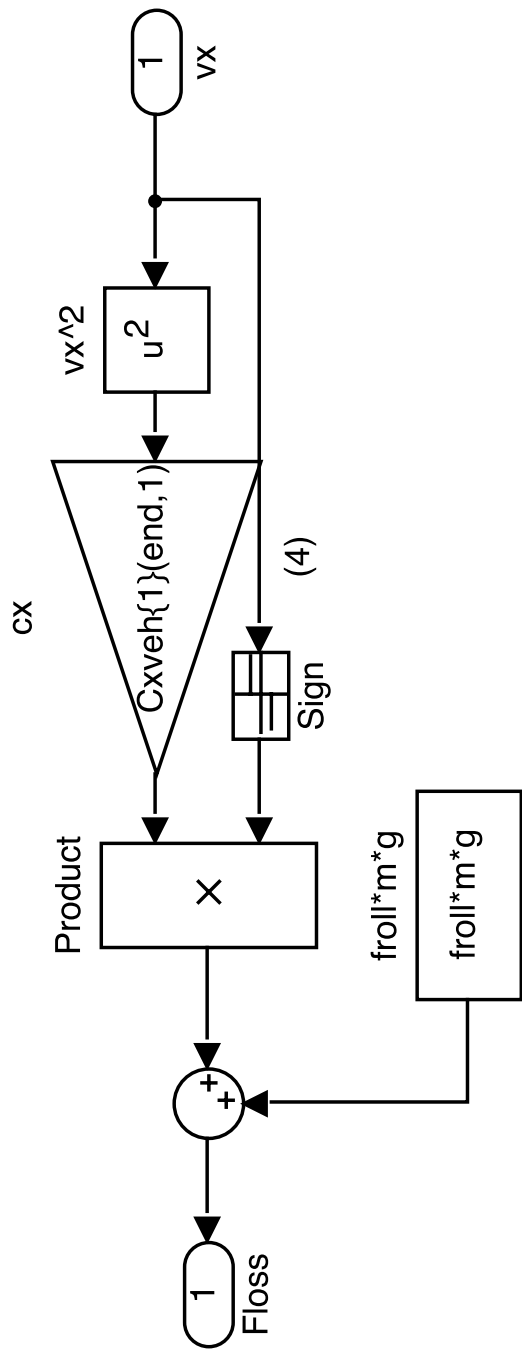


Figure A.5: Floss

Bakker-Pacejka Model
Genta pag 60

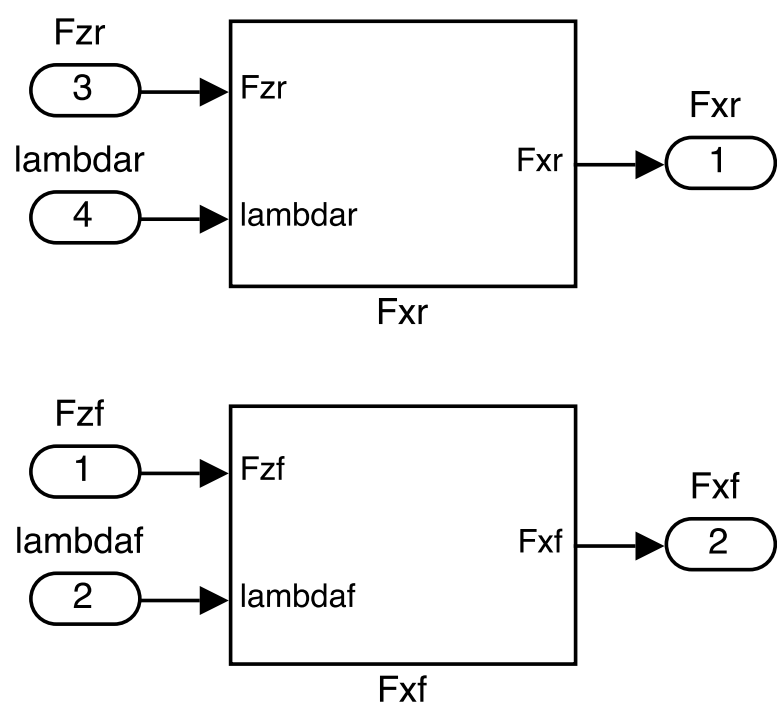


Figure A.6: Bakker-Pacejka models

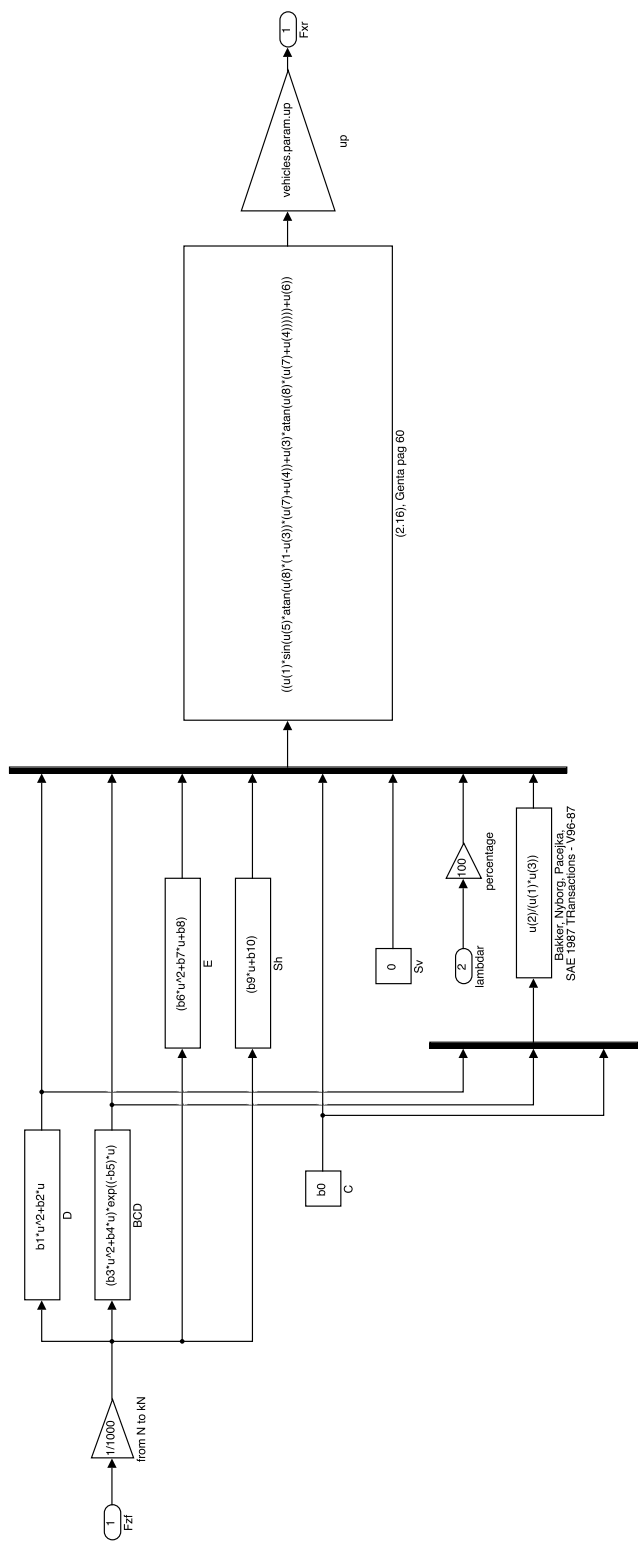


Figure A.7: Front wheel Bakker-Pacejka

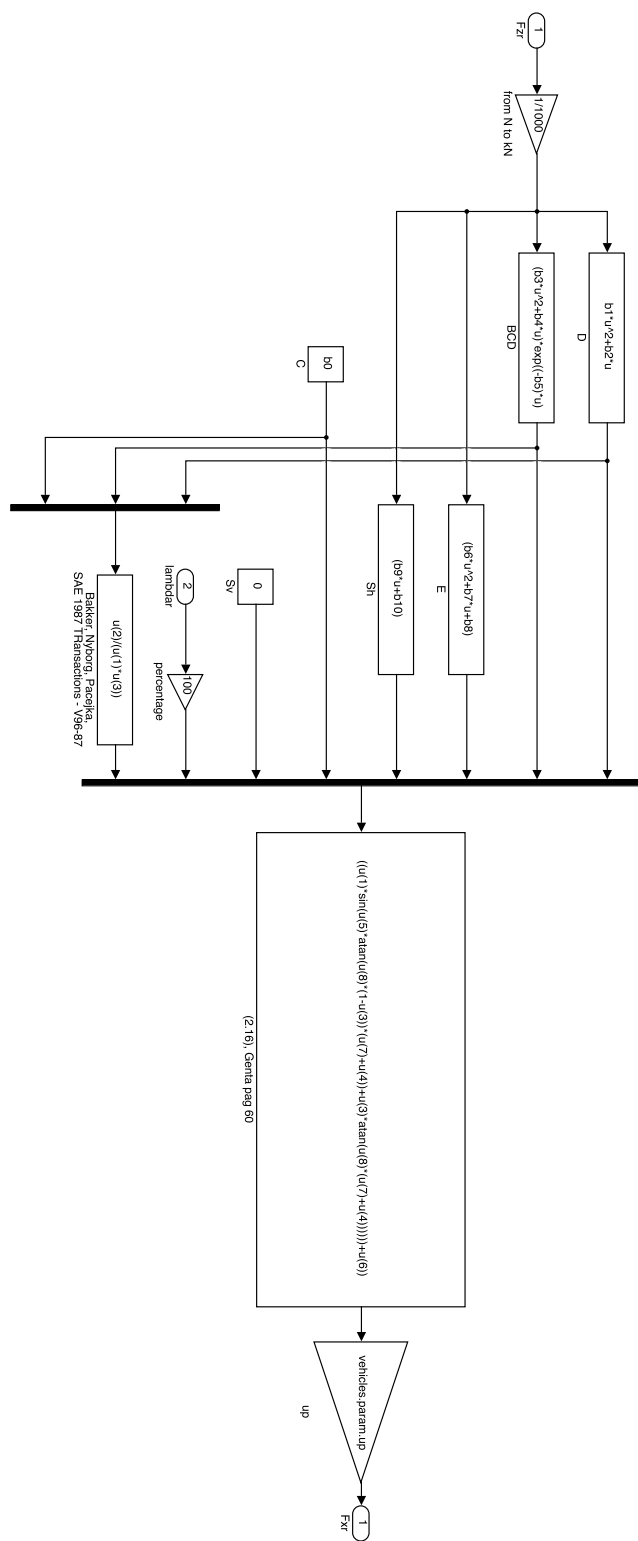


Figure A.8: Rear wheel Bakker-Pacejka model

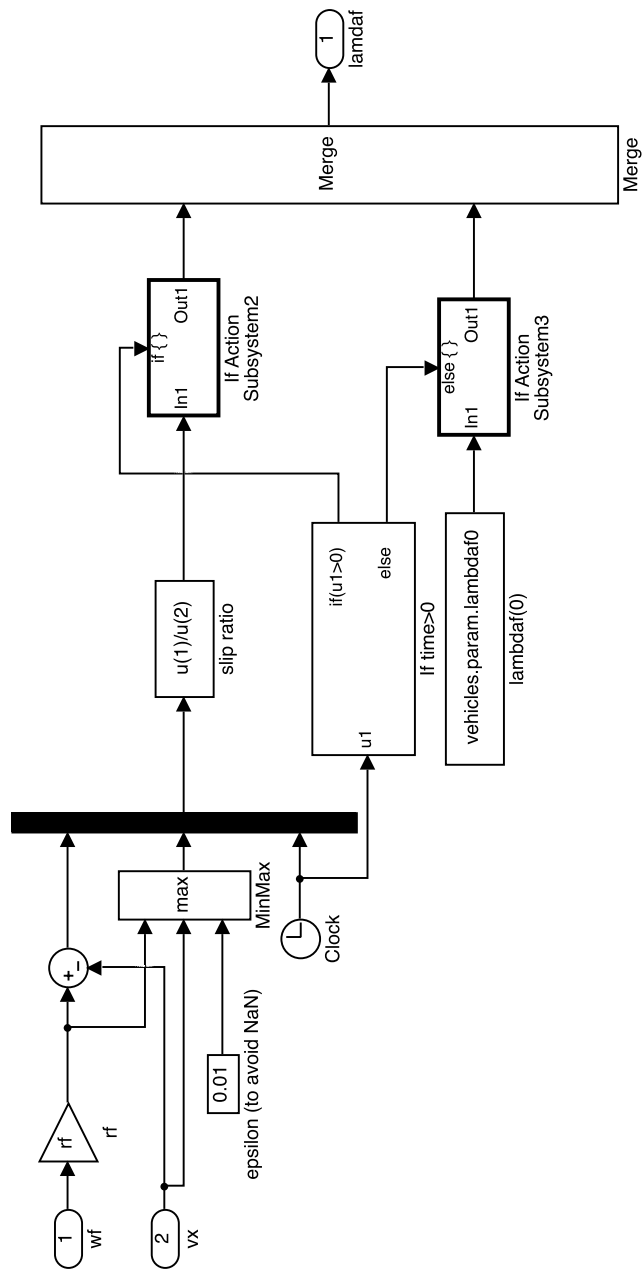


Figure A.9: Front wheel slip ratio

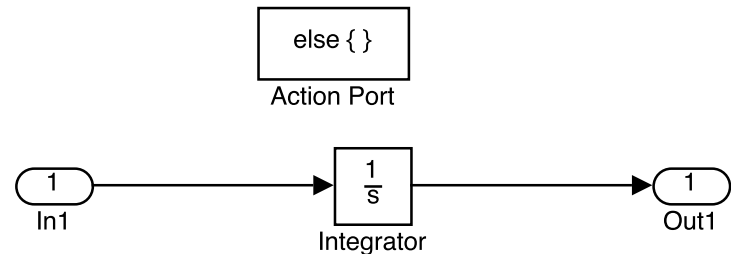


Figure A.10: Else front wheel slip ratio

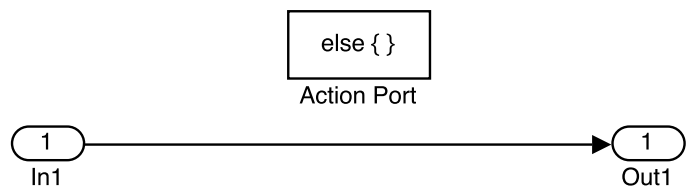


Figure A.11: If front wheel slip ratio

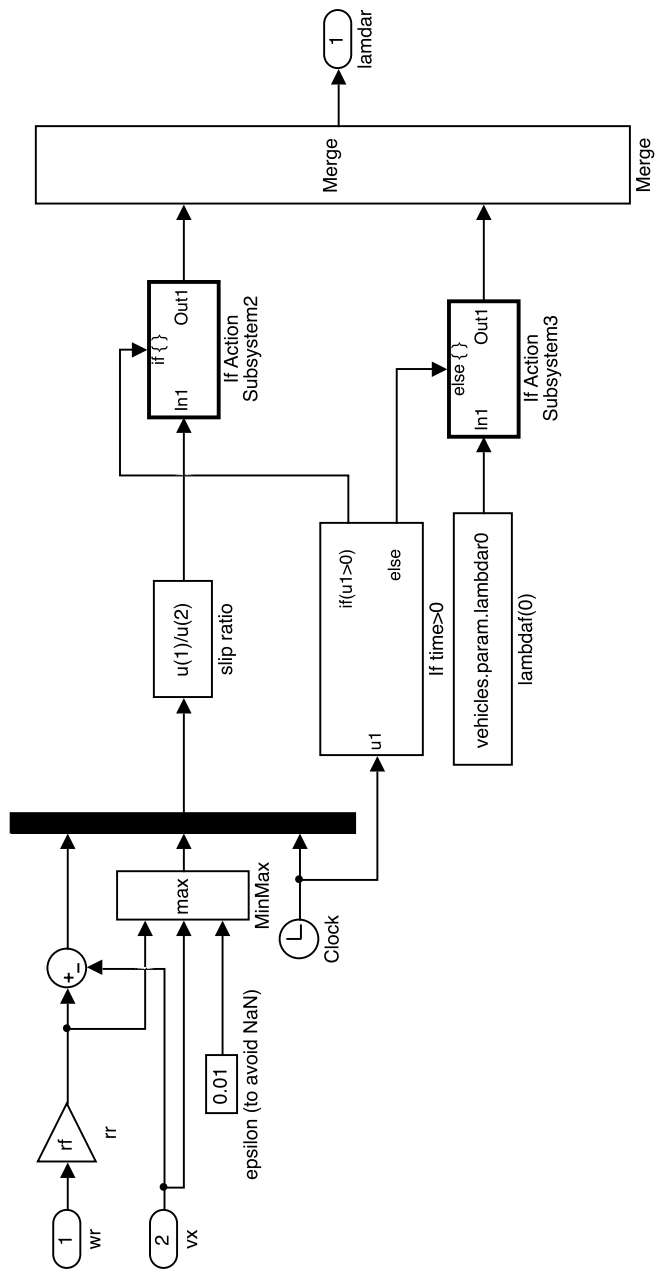


Figure A.12: Rear wheel slip ratio

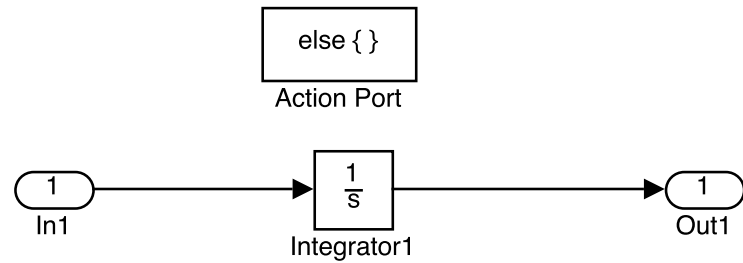


Figure A.13: Else rear wheel slip ratio

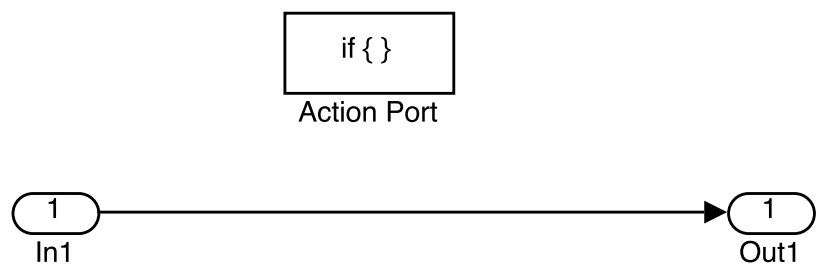


Figure A.14: If rear wheel slip ratio

Bibliography

- [1] S. Cheon, “An overview of automated highway systems (ahs) and the social and institutional challenges they face,” 2003.
- [2] P. I. C.C.Chien and M. C. Lai, “Entrainment and vehicle following controllers design for autonomous intelligent vehicles,” *American Control Conference Baltimore, Maryland*, June 1994.
- [3] A. Broggi, “Intelligent vehicle applications worldwide,” *IEEE INTELLIGENT SYSTEMS*, 2000.
- [4] M. O. J. Zhao and A. Kamel, “A safety spacing policy and its impact on highway traffic flow,” in *Intelligent Vehicles Symposium, 2009 IEEE*, 2009.
- [5] D. Swaroop and K. Rajagopal, “Intelligent cruise control systems and traffic flow stability,” *Transportation Research Part C: Emerging Technologies*, 1999.
- [6] S. E. Shladover, “Longitudinal control of automotive vehicles in close-formation platoons,” *Journal of Dynamic Systems, Measurement, and Control*, 1991.
- [7] Shiadover, “Operation of automated guideway transit vehicles in dynamically reconfigured trains and platoons,” *Automated Guidewuy Transit Technology Progmm*, 1979.
- [8] Y. Ohshima, “Control system of automatic car driving.” *Proc. IFAC Symposium on Tohyo Systems Engineeringfor Control systern Design,,* 1965.
- [9] S. E. Shladover, “Advanced vehicle control systems (avcs),” *SAE Technical Paper*, 1990.
- [10] S. Tsugawa, “An overview on control algorithms for automated highway system,” *IEEE*, 1999.
- [11] B. Bosacchi and I. Masaki, “Fuzzy logic technology & the intelligent higway system (ihs),” *IEEE*, 1993.
- [12] K. Padash, Tavassoli and Hadidi, “A sophisticated algorithm for using fuzzy logic controllers in adaptive cruise controller systems,” *Universal Journal of Electrical and Electronic Engineering*, 2013.
- [13] L. Magni and R. Scatolini, *Complementi di controlli automatici.* Pitagora editrice Bologna, 2006.

- [14] D. N. B. Kim and J. Sasiadek, "Model predictive control of an autonomous vehicle," *IEEE/ASME International Conference on Advanced Intelligent Mechatronics Proceedings*, 2001.
- [15] F. Flehmig, Sardari and Wagner, "Energy optimal adaptive cruise control during following of other vehicles," *IEEE Intelligent Vehicles Symposium (IV)*, 2015.
- [16] V. Utkin, "Variable structure systems with sliding modes." *IEEE Transactions on Automatic Control*, 1977.
- [17] V. U. KD Young and Ü. Özgüner, "A control engineer's guide to sliding mode control," *IEEE Transactions on Control Systems Technology*, 1999.
- [18] P. V. Suryawanshi, P. D. Shendge, and S. B. Phadke, "A boundary layer sliding mode control design for chatter reduction using uncertainty and disturbance estimator," *International Journal of Dynamics and Control*, pp. 1–10, 2015.
- [19] S. Drakunov, "Sliding mode observers based on equivalent control method," in *Conference on Decision and Control*, 1992.
- [20] G. Bartolini, A. Ferrara, and E. Usai, "Chattering avoidance by second-order sliding mode control," *IEEE Trans. Automat. Control*, vol. 43, no. 2, pp. 241–246, Feb. 1998.
- [21] A. Levant, "Chattering analysis," *IEEE Trans. Automat. Control*, vol. 55, no. 6, pp. 1380 –1389, Jun. 2010.
- [22] H. Lee and M. Tomizuka, "Adaptive vehicle traction force control for intelligent vehicle highway systems (ivhss)," *IEEE Trans. Ind. Electron.*, 2003.
- [23] R. T. Matteo Amodeo, Antonella Ferrara and C. Vecchio, "Slip control for vehicles platooning via second order sliding modes," *IEEE Intelligent Vehicles Symposium*, 2007.
- [24] H. Pacejka and E. Bakker, "The magic formula tyre model," *Vehicle Systems Dynamics*, vol. 21, pp. 1–18, 1993.
- [25] G. Genta, *Motor Vehicle Dynamics - Modeling and Simulation*. Singapore: World Scientific, 1993.
- [26] E. Bakker, L. Nyborg, and H. B. Pacejka, "Tyre modelling for use in vehicle dynamics studies," *SAE Technical Paper*, 1987.
- [27] S. F. M. Zabat, N. Stabile and F. Browand, "The aerodynamic performance of platoons: Final report," Institute of Transportation Studies, Tech. Rep., 1996.
- [28] Z. Asus, D. Chrenko, E. H. Aglizim, A. Kéromnès, and L. L. Moyne, "Simple method of estimating consumption of internal combustion engine for hybrid application," in *2012 IEEE Transportation Electrification Conference and Expo (ITEC)*, 2012.

- [29] H. Naunheimer, B. Bertsche, J. Ryborz, and W. Novak, *Automotive Transmissions*. Springer, 2011.
- [30] A. Filippov, *Differential Equations with Discontinuous Right-Hand Sides*. Kluwer, 1998.
- [31] V. I. Utkin, *Sliding Modes in Control and Optimization*. Springer, 1992.
- [32] W.-C. Su, S. V. Drakunov, U. Ozguner, and K. D. Young, “Sliding mode with chattering reduction in sampled data systems,” in *Decision and Control, 1993., Proceedings of the 32nd IEEE Conference on*, 1993.
- [33] F. Dinuzzo and A. Ferrara, “Higher order sliding mode controllers with optimal reaching,” *IEEE Trans. Automat. Control*, vol. 54, no. 9, pp. 2126 –2136, Sep. 2009.
- [34] D. V. F. L. Lewis and V. L. Syrmos, *Optimal Control*. John Wiley and Sons, 2012.
- [35] A. Levant, “Sliding order and sliding accuracy in sliding mode control,” *International Journal of Control*, 1993.
- [36] M. Amodeo, A. Ferrara, R. Terzaghi, and C. Vecchio, “Wheel slip control via second-order sliding-mode generation,” *IEEE Transactions on Intelligent Transportation Systems*, vol. 11, no. 1, pp. 122–131, Mar. 2010.
- [37] V. Ivanov, D. Savitski, and B. Shyrokau, “A survey of traction control and antilock braking systems of full electric vehicles with individually controlled electric motors,” *IEEE Transactions on Vehicular Technology*, vol. 64, no. 9, pp. 3878–3896, Sep. 2015.
- [38] H. Imine, L. Fridman, H. Shraim, and M. Djemai, *Sliding Mode Based Analysis and Identification of Vehicle Dynamics*, ser. Lecture Notes in Control and Information Sciences. Springer-Verlag Berlin Heidelberg, 2011, vol. 414.
- [39] M. Tanelli, A. Ferrara, and P. Giani, “Combined vehicle velocity and tire-road friction estimation via sliding mode observers,” in *Proc. IEEE International Conference on Control Applications*, Oct. 2012, pp. 130–135.
- [40] M. Reichhartinger, S. K. Spurgeon, and M. Weyrer, “Design of an unknown input observer to enhance driver experience of electric power steering systems,” in *European Control Conference*, Aalborg, Denmark, Jul. 2016. [Online]. Available: <http://kar.kent.ac.uk/56324/>
- [41] R. Tafner, M. Horn, and A. Ferrara, “Experimental evaluation of nonlinear unknown input observers applied to an eps system,” in *Proc. American Control Conference*, Boston, MA, Jul. 2016, pp. 2409–2414.
- [42] H. S. Tan and M. Tomizuka, “An adaptive sliding mode vehicle traction controller design,” in *Proc. American Control Conference*, San Diego, CA, May 1990, pp. 1856–1862.

- [43] S. Drakunov, U. Ozguner, P. Dix, and B. Ashrafi, "Abs control using optimum search via sliding modes," *IEEE Transactions on Control Systems Technology*, vol. 3, no. 1, pp. 79–85, Mar. 1995.
- [44] C. Unsal and P. Kachroo, "Sliding mode measurement feedback control for antilock braking systems," *IEEE Transactions on Control Systems Technology*, vol. 7, no. 2, pp. 271–281, Mar. 1999.
- [45] J. J. Moskwa and J. K. Hedrick, "Sliding mode control of automotive engines," in *Proc. American Control Conference*, Pittsburgh, PA, Jun. 1989, pp. 1040–1045.
- [46] C.-M. Lin and C. F. Hsu, "Neural-network hybrid control for antilock braking systems," *IEEE Transactions on Neural Networks*, vol. 14, no. 2, pp. 351–359, Mar. 2003.
- [47] M. Tanelli, C. Vecchio, M. Corno, A. Ferrara, and S. M. Savaresi, "Traction control for ride-by-wire sport motorcycles: A second-order sliding mode approach," *IEEE Transactions on Industrial Electronics*, vol. 56, no. 9, pp. 3347–3356, Sep. 2009.
- [48] S. Kuntanapreeda, "Super-twisting sliding-mode traction control of vehicles with tractive force observer," *Control Engineering Practice*, vol. 38, pp. 26–36, 2015.
- [49] R. de Castro, R. E. Araújo, and D. Freitas, "Wheel slip control of evs based on sliding mode technique with conditional integrators," *IEEE Transactions on Industrial Electronics*, vol. 60, no. 8, pp. 3256–3271, Aug. 2013.
- [50] V. I. Utkin, *Sliding Modes in Optimization and Control Problems*. New York: Springer Verlag, 1992.
- [51] A. Levant, "Higher-order sliding modes, differentiation and output-feedback control," *International Journal of Control*, vol. 76, no. 9–10, pp. 924–941, Jan. 2003.
- [52] V. I. Utkin and J. Shi, "Integral sliding mode in systems operating under uncertainty conditions," in *Proc. 35th IEEE Conference on Decision and Control*, vol. 4, Kobe, Japan, Dec. 1996, pp. 4591–4596.
- [53] A. Ferrara and G. P. Incremona, "Design of an integral suboptimal second order sliding mode controller for the robust motion control of robot manipulators," *IEEE Transactions on Control Systems Technology*, vol. 23, no. 6, pp. 2316–2325, May 2015.
- [54] G. Bartolini, A. Ferrara, A. Levant, and E. Usai, "On second order sliding mode controllers," in *Variable Structure Systems, Sliding Mode and Nonlinear Control*, ser. Lecture Notes in Control and Information, K. D. Young and Ü. Özgürner, Eds. London, UK: Springer-Verlag, 1999, pp. 329–350.
- [55] V. I. Utkin, "Sliding mode control design principles and applications to electric drives," *IEEE Transactions on Industrial Electronics*, 1993.

- [56] K. Santhanakrishnan and R. Rajamani, "On spacing policies for highway vehicle automation," *IEEE TRANSACTIONS ON INTELLIGENT TRANSPORTATION SYSTEMS*, 2003.
- [57] M. Dellnitz, J. Ecksteinc, K. Flaßkampb, P. Friedelc, C. Horenkampa, U. Köhlerc, S. Ober-Blöbauma, S. Peitza, and S. Tiemeyerc, "Development of an intelligent cruise control using optimal control methods," *Elsevier Ltd. 2nd International Conference on System-Integrated Intelligence: Challenges for Product and Production Engineering*, 2014.
- [58] D. Swaroop, "String stability of interconnected systems: An application to platooning in automated highway systems," *California PATH Research Report*, 1997.
- [59] M. Yoshimura and H. Fujimoto, "Slip ratio control of electric vehicle with single-rate pwm considering driving force," *The 11th IEEE International Workshop on Advanced Motion Control*, 2010.
- [60] C. C. de Wit and B. Brogliato, "Stability issuesforvehicle platooning in automatehdighway system," *International Conference on Control Applicalions Kohala Coast-Island of Hawai'i, Hawai'i, USA*, 1999.
- [61] M.-H. Hsiao and C.-H. Lin, "Antilock braking control of electric vehicles with electric brake," in *SAE Techology Paper Series*, 2005.
- [62] T. K. Bera, K. Bhattacharya, and A. K. Samantaray, "Bond graph model based evaluation of a sliding mode controller for a combined regenerative and antilock braking system," in *Proc. IMechE I, Journal Systems Control Engineering*, vol. 226, no. 8, 2012, pp. 1060–1076.
- [63] E. Mayhorn, K. Kalsi, J. Lian, and M. Elizondo, "Model predictive control-based optimal coordination of distributed energy resources," in *Proc. 46th Hawaii Int. Conf. System Sciences*. Wailea, Maui, HI USA: IEEE, Jan. 2013, pp. 2237–2244.
- [64] A. Ferrara, G. P. Incremona, and L. Magni, "Model-based event-triggered robust MPC/ISM," in *Proc. European Control Conf.*, Strasbourg, France, Jun. 2014, pp. 2931–2936.
- [65] G. P. Incremona, A. Ferrara, and L. Magni, "Hierarchical model predictive/sliding mode control of nonlinear constrained uncertain systems," in *Proc. 5th IFAC Nonlin. Model Predictive Control Conf.*, vol. 48, no. 23, Seville, Spain, Sep. 2015, pp. 102 – 109.
- [66] D. Q. Mayne, "Model predictive control: Recent developments and future promise," *Automatica*, vol. 50, no. 12, pp. 2967–2986, 2014.
- [67] D. Mayne, J. Rawlings, C. Rao, and P. Scokaert, "Constrained model predictive control: Stability and optimality," *Automatica*, vol. 36, no. 6, pp. 789–814, Jun. 2000.

- [68] J. Rawlings and D. Mayne, *Model Predictive Control: Theory and Design*. Nob Hill Pub, Llc, 2009.
- [69] E. Camacho and C. Bordons, *Model Predictive Control*, ser. Advanced Textbooks in Control and Signal Processing Series. Springer-Verlag GmbH, 2004.
- [70] J. M. Maciejowski, *Predictive control with constraints*. Essex, England: Prentice Hall, 2002.
- [71] M. Morari and J. Lee, “Model predictive control: Past, present and future,” *Computers & Chemical Engineering*, vol. 23, no. 4, pp. 667–682, May 1999.
- [72] A. Ferrara, G. P. Incremona, and L. Magni, “A robust mpc/ism hierarchical multi-loop control scheme for robot manipulators,” in *Proc. 52th IEEE Conf. Decision Control*, Florence, Italy, to appear, Dec. 2013.
- [73] M. Rubagotti, D. Raimondo, A. Ferrara, and L. Magni, “Robust model predictive control with integral sliding mode in continuous-time sampled-data nonlinear systems,” *IEEE Trans. Automat. Control*, vol. 56, no. 3, pp. 556–570, Mar. 2011.
- [74] L. Magni and R. Scattolini, “Model predictive control of continuous-time nonlinear systems with piecewise constant control,” *IEEE Trans. Automat. Control*, vol. 49, no. 6, pp. 900–906, Jun. 2004.
- [75] G. P. Incremona, M. Cucuzzella, and A. Ferrara, “Adaptive suboptimal second-order sliding mode control for microgrids,” *International Journal of Control*, pp. 1–19, Jan. 2016.
- [76] M. Cucuzzella, G. P. Incremona, and A. Ferrara, “Design of robust higher order sliding mode control for microgrids,” *IEEE J. Emerg. Sel. Topics Circuits Syst.*, vol. 5, no. 3, pp. 393–401, Sep. 2015.
- [77] F. Katiraei, R. Iravani, N. Hatziargyriou, and A. Dimeas, “Microgrids management,” *IEEE Power and Energy Magazine*, vol. 6, no. 3, pp. 54–65, 2008.
- [78] N. Rugthaicharoencheep and M. Boonthienthong, “Smart grid for energy management on distribution system with distributed generation,” in *Cyber Technology in Automation, Control, and Intelligent Systems (CYBER), 2012 IEEE International Conference on*. IEEE, 2012, pp. 165–169.
- [79] K. Tan, P. So, Y. Chu, and M. Z. Chen, “Coordinated control and energy management of distributed generation inverters in a microgrid,” *IEEE Trans. Power Delivery*, vol. 28, no. 2, pp. 704–713, 2013.
- [80] D. S. Palasamudram, R. K. Sitaraman, B. Urgaonkar, and R. Urgaonkar, “Using batteries to reduce the power costs of internet-scale distributed networks,” in *Proc. of the Third ACM Symposium on Cloud Computing*. San Jose, CA, USA: ACM, Oct. 2012, p. 11.

- [81] H. Rahimi-Eichi, U. Ojha, F. Baronti, and M.-Y. Chow, "Battery management system: An overview of its application in the smart grid and electric vehicles," *Industrial Electronics Magazine, IEEE*, vol. 7, no. 2, pp. 4–16, 2013.
- [82] T. Hornik and Q.-C. Zhong, "A current-control strategy for voltage-source inverters in microgrids based on h^∞ and repetitive control," *IEEE Trans. Power Electronics*, vol. 26, no. 3, pp. 943–952, Mar. 2011.
- [83] A. Bidram, A. Davoudi, F. Lewis, and S. S. Ge, "Distributed adaptive voltage control of inverter-based microgrids," *IEEE Trans. Energy Conversion*, vol. 29, no. 4, pp. 862–872, Dec. 2014.
- [84] D. Salomonsson, L. Soder, and A. Sannino, "An adaptive control system for a dc microgrid for data centers," *IEEE Trans. Industry Applications*, vol. 44, no. 6, pp. 1910–1917, Nov. 2008.
- [85] C.-T. Lee, C.-C. Chu, and P.-T. Cheng, "A new droop control method for the autonomous operation of distributed energy resource interface converters," *IEEE Trans. Power Electronics*, vol. 28, no. 4, pp. 1980–1993, Apr. 2013.
- [86] K. De Brabandere, B. Bolsens, J. Van den Keybus, A. Woyte, J. Driesen, and R. Belmans, "A voltage and frequency droop control method for parallel inverters," *IEEE Trans. Power Electronics*, vol. 22, no. 4, pp. 1107–1115, Jul. 2007.
- [87] A. Parisio, E. Rikos, and L. Glielmo, "A Model Predictive Control Approach to Microgrid Operation Optimization," *IEEE Trans. Control Syst. Techn.*, vol. 22, no. 5, pp. 1813–1827, 2014.
- [88] R. Palma-Behnke, C. Benavides, F. Lanas, B. Severino, L. Reyes, J. Llanos, and D. Saez, "A microgrid energy management system based on the rolling horizon strategy," *IEEE Trans. Smart Grid*, vol. 4, no. 2, pp. 996–1006, Jun. 2013.
- [89] M. Cucuzzella, G. P. Incremona, and A. Ferrara, "Master-slave second order sliding mode control for microgrids," in *Proc. IEEE American Control Conf.*, Chicago, IL, USA, Jul. 2015.
- [90] ———, "Third order sliding mode voltage control in microgrids," in *Proc. IEEE European Control Conf.*, Linz, Austria, Jul. 2015.
- [91] M. Rubagotti, A. Estrada, F. Castanos, A. Ferrara, and L. Fridman, "Integral sliding mode control for nonlinear systems with matched and unmatched perturbations," *IEEE Trans. Automat. Control*, vol. 56, no. 11, pp. 2699–2704, Nov. 2011.
- [92] E. Planas, A. G. de Muro, J. Andreu, I. Kortabarria, and I. M. de Alegría, "General aspects, hierarchical controls and droop methods in microgrids: A review," *Renewable and Sustainable Energy Reviews*, vol. 17, no. 0, pp. 147–159, 2013.

- [93] R. H. Park, "Two-reaction theory of synchronous machines - generalized method of analysis - part i," *Trans. American Instit. Electr. Eng.*, vol. 48, no. 3, pp. 716 – 727, 1929.
- [94] O. Palizban, K. Kauhaniemi, and J. M. Guerrero, "Microgrids in active network management–part i: Hierarchical control, energy storage, virtual power plants, and market participation," *Renewable and Sustainable Energy Reviews*, vol. 36, no. 0, pp. 428–439, 2014.
- [95] C. Edwards and S. K. Spurgen, *Sliding Mode Control: Theory and Applications*. London, UK: Taylor and Francis, 1998.
- [96] G. Bartolini, A. Ferrara, and E. Usai, "Output tracking control of uncertain nonlinear second-order systems," *Automatica*, vol. 33, no. 12, pp. 2203 – 2212, Dec. 1997.
- [97] M. Babazadeh and H. Karimi, "A robust two-degree-of-freedom control strategy for an islanded microgrid," *IEEE Trans. Power Del.*, vol. 28, no. 3, pp. 1339–1347, Jul. 2013.
- [98] J. Guerrero, P. C. Loh, T.-L. Lee, and M. Chandorkar, "Advanced control architectures for intelligent microgrids - part ii: Power quality, energy storage, and ac/dc microgrids," *IEEE Trans. Ind. Electron.*, vol. 60, no. 4, pp. 1263–1270, Apr. 2013.
- [99] H. Karimi, E. Davison, and R. Iravani, "Multivariable servomechanism controller for autonomous operation of a distributed generation unit: Design and performance evaluation," *IEEE Trans. Power Syst.*, vol. 25, no. 2, pp. 853–865, May 2010.
- [100] H. Karimi, H. Nikkhajoei, and R. Iravani, "Control of an electronically-coupled distributed resource unit subsequent to an islanding event," *IEEE Trans. Power Del.*, vol. 23, no. 1, pp. 493–501, Jan. 2008.
- [101] I. Boiko, L. Fridman, A. Pisano, and E. Usai, "Analysis of chattering in systems with second-order sliding modes," *IEEE Trans. Automat. Control*, vol. 52, no. 11, pp. 2085–2102, Nov. 2007.
- [102] P. Piagi and R. Lasseter, "Autonomous control of microgrids," in *Power Eng. Society General Meeting*, Montreal, Que., May 2006, p. 8.
- [103] S. Amin and B. Wollenberg, "Toward a smart grid: power delivery for the 21st century," *IEEE Power Energy Mag.*, vol. 3, no. 5, pp. 34–41, Sep. 2005.
- [104] F. Katiraei, M. Iravani, and P. Lehn, "Micro-grid autonomous operation during and subsequent to islanding process," *IEEE Trans. Power Del.*, vol. 20, no. 1, pp. 248–257, Jan. 2005.
- [105] R. Lasseter and P. Paigi, "Microgrid: a conceptual solution," in *Proc. 35th IEEE Power Electron. Specialists Conf.*, vol. 6, Aachen, Germany, Jun. 2004, pp. 4285–4290.

- [106] H. B. Puttgen, P. MacGregor, and F. Lambert, “Distributed generation: Semantic hype or the dawn of a new era?” *Power and Energy Magazine, IEEE*, vol. 1, no. 1, pp. 22–29, Jan. 2003.
- [107] L. Fridman, “Singularly perturbed analysis of chattering in relay control systems,” *IEEE Trans. Automat. Control*, vol. 47, no. 12, pp. 2079 – 2084, Dec. 2002.
- [108] R. Lasseter, “Microgrids,” in *IEEE Power Engineering Society Winter Meeting*, vol. 1, 2002, pp. 305–308.
- [109] G. Bartolini, A. Ferrara, E. Usai, and V. Utkin, “On multi-input chattering-free second-order sliding mode control,” *IEEE Trans. Automat. Control*, vol. 45, no. 9, pp. 1711–1717, Sep. 2000.

